N-1817

NCEL
Technical Note

October 1990

By R.L. Jones

Sponsored By Office of the Chief
of Naval Research

A CONSTITUTIVE RELATIONSHIP BETWEEN CRACK PROPAGATION AND SPECIFIC DAMPING CAPACITY IN STEEL

ABSTRACT An expression stating crack propagation as a function of specific damping capacity was developed. Development was based on the premise that fatigue damage is due to plastic work. Plastic work is calculated from small changes in damping between fatigue cycles where the damping changes are assumed to result from an increase in size of the plastic zone at the tip of the crack. A series of fatigue tests, using 4340 and 1018 steel specimens, were monitored for damping changes during fatigue crack growth. Each notched and uncracked beam specimen was mounted in a knife-edge fixture and fatigued by a four-point load. The fatigue load had a stress ratio of zero. Between fatigue load cycles, a vibration generator would resonate the specimen mounted in the knife-edge fixture. Strain measurements from the specimen, and force measurements from the vibration generator, were used to calculate internal damping. Test results were compared to a dynamic mathematical model of the cracked specimen to verify the crack growth-specific damping relationship. Two types of damping were noted in the region of the fatigue crack. First, dislocation damping at the crack tip was observed in 1018 steel for large plastic zones. Second, damping proportional to the beam slope at the crack was observed in 4340 steel for small plastic zones and attributed to rubbing of the crack faces. Experimental results of both types of damping are duplicated by a computer program of the mathematical model.

NAVAL CIVIL ENGINEERING LABORATORY PORT HUENEME CALIFORNIA 93043-5003

METRIC CONVERSION FACTORS

Approximate Conversions to Metric Measures

Symbol	When You Know	Multiply by	To Find	Symbol
		LENGTH		
in	inches	*2.5	centimeters	cm
ft	feet	30	centimeters	cm
yd	yards	0.9	meters	m
mi	miles	1.6	kilometers	km
		AREA		
in^2	square inches	6.5	square centimeters	cm^2
ft^2	square feet	0.09	square meters	m^2
yd^2	square yards	0.8	square meters	m^2
mi^2	square miles	2.6	square kilometers	km^2
	acres	0.4	hectares	ha
		MASS (weight)		
oz	ounces	28	grams	g
lb	pounds	0.45	kilograms	kg
	short tons (2,000 lb)	0.9	tonnes	t
		VOLUME		
tsp	teaspoons	5	milliliters	ml
Tbsp	tablespoons	15	milliliters	ml
fl oz	fluid ounces	30	milliliters	ml
c	cups	0.24	liters	l
pt	pints	0.47	liters	l
qt	quarts	0.95	liters	l
gal	gallons	3.8	liters	l
ft^3	cubic feet	0.03	cubic meters	m^3
yd^3	cubic yards	0.76	cubic meters	m^3
		TEMPERATURE (exact)		
°F	Fahrenheit temperature	5/9 (after subtracting 32)	Celsius temperature	°C

*1 in = 2.54 (exactly). For other exact conversions and more detailed tables, see NBS Misc. Publ. 286, Units of Weights and Measures, Price $2.25, SD Catalog No. C13.10:286.

Approximate Conversions from Metric Measures

Symbol	When You Know	Multiply by	To Find	Symbol
		LENGTH		
mm	millimeters	0.04	inches	in
cm	centimeters	0.4	inches	in
m	meters	3.3	feet	ft
m	meters	1.1	yards	yd
km	kilometers	0.6	miles	mi
		AREA		
cm^2	square centimeters	0.16	square inches	in^2
m^2	square meters	1.2	square yards	yd^2
km^2	square kilometers	0.4	square miles	mi^2
ha	hectares (10,000 m^2)	2.5	acres	
		MASS (weight)		
g	grams	0.035	ounces	oz
kg	kilograms	2.2	pounds	lb
t	tonnes (1,000 kg)	1.1	short tons	
		VOLUME		
ml	milliliters	0.03	fluid ounces	fl oz
l	liters	2.1	pints	pt
l	liters	1.06	quarts	qt
l	liters	0.26	gallons	gal
m^3	cubic meters	35	cubic feet	ft^3
m^3	cubic meters	1.3	cubic yards	yd^3
		TEMPERATURE (exact)		
°C	Celsius temperature	9/5 (then add 32)	Fahrenheit temperature	°F

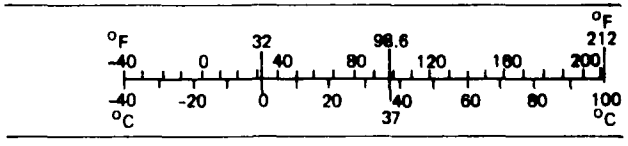

REPORT DOCUMENTATION PAGE

Form Approved
OMB No. 0704-018

1. AGENCY USE ONLY *(Leave blank)*	2. REPORT DATE	3. REPORT TYPE AND DATES COVERED
	October 1990	Final: Oct 84 through Apr 88

4. TITLE AND SUBTITLE
A CONSTITUTIVE RELATIONSHIP BETWEEN CRACK PROPAGATION AND SPECIFIC DAMPING CAPACITY IN STEEL

5. FUNDING NUMBERS
PE - 61152N
PR - ZR000-01-191
WU - DN665020

6. AUTHOR(S)
R. L. JONES

7. PERFORMING ORGANIZATION NAME(S) AND ADDRESSE(S)
Naval Civil Engineering Laboratory
Port Hueneme, CA 93043-5003

8. PERFORMING ORGANIZATION REPORT NUMBER
TN - 1817

9. SPONSORING/MONITORING AGENCY NAME(S) AND ADDRESSE(S)
Office of the Chief of Naval Research
Office of Naval Research
Arlington, VA 22217-5000

10. SPONSORING/MONITORING AGENCY REPORT NUMBER

11. SUPPLEMENTARY NOTES

12a. DISTRIBUTION/AVAILABILITY STATEMENT
Approved for public release; distribution unlimited.

12b. DISTRIBUTION CODE

13. ABSTRACT *(Maximum 200 words)*

An expression stating crack propagation as a function of specific damping capacity was developed. Development was based on the premise that fatigue damage is due to plastic work. Plastic work is calculated from small changes in damping between fatigue cycles where the damping changes are assumed to result from an increase in size of the plastic zone at the tip of the crack. A series of fatigue tests, using 4340 and 1018 steel specimens, were monitored for damping changes during fatigue crack growth. Each notched and uncracked beam specimen was mounted in a knife-edge fixture and fatigued by a four-point load. The fatigue load had a stress ratio of zero. Between fatigue load cycles, a vibration generator would resonate the specimen mounted in the knife-edge fixture. Strain measurements from the specimen, and force measurements from the vibration generator, were used to calculate internal damping. Test results were compared to a dynamic mathematical model of the cracked specimen to verify the crack growth-specific damping relationship. Two types of damping were noted in the region of the fatigue crack. First, dislocation damping at the crack tip was observed in 1018 steel for large plastic zones. Second, damping proportional to the beam slope at the crack was observed in 4340 steel for small plastic zones and attributed to rubbing of the crack faces. Experimental results of both types of damping are duplicated by a computer program of the mathematical model.

14. SUBJECT TERMS	15. NUMBER OF PAGES
Crack propagation, fatigue, damping, internal friction, dislocations, specific damping capacity	185
	16. PRICE CODE

17. SECURITY CLASSIFICATION OF REPORT	18. SECURITY CLASSIFICATION OF THIS PAGE	19. SECURITY CLASSIFICATION OF ABSTRACT	20. LIMITATION OF ABSTRACT
Unclassified	Unclassified	Unclassified	UL

CONTENTS

APPENDIXES

INTRODUCTION

The major objective of this report is to establish a relationship between fatigue crack growth and internal damping. In defining this relationship, a basis for monitoring the structural integrity of systems subject to fatigue will be demonstrated. Thus, the value of this relationship is in nondestructive diagnostics, where the detection of crack initiation and propagation are of great interest.

A secondary objective is the mathematical modeling of the crack growth-internal damping relationship. To understand the relationship, and apply it in the analysis of complex structures, a model is essential. Without a model, extension of the relationship to allow monitoring of structural integrity would be awkward and prone to failure. The model provides a foundation to begin observations of fatigue failure, in complex structures, using damping.

Previous work that categorized and analyzed damping mechanisms and explored their relation with fatigue is described. Also, a detailed description of subgoals required to establish a crack growth-internal damping relationship is provided.

BACKGROUND

The purpose of this background section is to review existing literature about internal damping and crack propagation and give the reader an introduction to the research topic. Aspects of damping or fatigue that relate to the research objective and are crucial to its accomplishment are explored.

Damping Mechanisms

When a solid is subjected to vibration, several processes may occur to dissipate energy, even at low amplitudes of vibration. The ratio of energy dissipated to peak elastic energy is usually quite small; the main significance being that information is provided as to the nature of the processes involved. At large amplitudes, the proportion of energy dissipated may be much larger as permanent damage accumulates within the material.

The most important material damping process is the vibration of dislocations. A dislocation is defined as a stable arrangement of atoms such that, in the region of a few atomic distances, (n + 1) atoms in the slip plane face (n) atoms across the slip plane (Figure 1). Movement of dislocations produce an incremental strain that diminishes the effective elastic modulus, while the energy dislocations dissipate during vibration manifesting itself as "internal friction." There are also several relaxation processes contributing to internal friction that do not involve dislocations. They are called relaxation processes because they change the shape of the solid under load and because each has a certain characteristic "relaxation time." Such processes are grain boundary sliding, thermal diffusion, atomic diffusion, and magnetostriction.

The relaxation processes were named anelastic by Zener, who first interpreted them in toto (Ref 1). They create a peak in the curve of internal friction versus frequency of vibration at a frequency approximately equal to $(\text{relaxation time})^{-1}$. The magnitude of the internal friction is independent of the amplitude of vibration in a first approximation. The more significant dislocation process is different in that no peak exists until megacycle frequencies are reached, and the magnitudes of the associated internal friction are not so independent of the amplitude of vibration. To differentiate it from the relaxation processes it has been called a process of static hysteresis (Ref 2).

Internal friction typically varies with the amplitude of vibration (Ref 3) (Figure 2). Up to a strain amplitude of about 10^{-5} (Figure 2) internal friction is independent of amplitude ("amplitude-independent" range), then commences to increase with amplitude ("amplitude-dependent"

range). For very large amplitudes, material enters the fatigue range and damping increases still faster, ultimately resulting in a fatigue fracture. In addition to the amplitude of vibration, temperature and frequency may affect the internal friction.

Considerable evidence indicates that most of this internal friction is connected with the movement of dislocations (Ref 4 through 8). Provided the selected conditions do not excite a relaxation peak, dislocation movement is the process responsible for most of the internal friction in metals.

Having established the basics of internal damping and its primary mechanisms, the next step is to examine previous attempts to relate damping and fatigue.

Damping and Fatigue

Various researchers have sought a relation between damping and fatigue. For many years, damping was believed to be the first indication of damage to material subjected to cyclic stress. It was further believed that each metal was capable of dissipating only a certain quantity of energy by internal damping, and that when this quantity was exceeded, fracture by fatigue must follow. In fact, every experiment made for the purpose of verifying this hypothesis has given negative results.

Experimentally, Föppl (Ref 9) has shown that the capacity for dissipation of energy in the form of heat by internal damping is unlimited. He conducted an alternating torsion test continuously for a period of 3 years without the test piece breaking or showing any sign of deterioration after 1,100 million cycles of stress. The rate of dissipation of energy was sufficient to maintain the test piece at about 100°C above the ambient temperature.

Damping, then, is not directly related with fracture by fatigue. It depends principally on the strain energy of the cycles, on the temperature and certain other conditions of the test, and also, to a smaller extent, on the number of stress cycles which have previously been applied. For many metals, the damping capacity increases

noticeably up to a certain number of cycles (about 2 to 10 million), and then remains stationary as long as the conditions of the endurance test are maintained unchanged.

From previous tests, it is possible to advance the following theory: a fatigue crack results from the accumulation of damping effects (i.e., from the fact that under a variable stress higher than the fatigue limit, constantly applied, damping continually increases up to fracture). For a cyclic stress below the fatigue limit, the damping moves toward a fixed value, or else diminishes continuously.

The origination of fatigue cracks is marked by an increase in damping. This increase is associated with the accumulation of dislocations. Since cyclic input of strain energy alters the thermal and internal surface energies, dislocations tend to collect on the planes already containing one or more dislocations (Figure 3). Eventually, (n) atoms face (n + 2), (n + 3), or more atoms, resulting in relative motion of one plane to the other. For aluminum alloys, Hanstock and Murray (Ref 10) were able to predict the endurance, in tests under alternating torsion, by observing the stage at which this increase in damping occurred.

The change in damping with the number of stress cycles applied is related to the process of accumulative damage that results in fatigue fracture, although it does not directly express the effect of damage, but rather the effect of localized inelastic deformations accompanying damage. It is, therefore, not the absolute value of damping capacity, but its change with the number of cycles that indicates the process of progressive damage. As a further complication to the interpretation of damping, above a certain value of stress, the damping capacity is reduced by work hardening, and is increased by the repetition of stress cycles.

The work-hardening process in a material seems to be due to the long-range elastic interactions of its dislocations. Additional input of strain energy may help to overcome these long-range stresses to accumulate more dislocations on the slip planes, until the crystal separates into two or more fragments, with interference and distortion of the adjacent crystals. Continued cycling would eventually cause the cracks to grow and coalesce into an open area (resulting in an insufficient area to support the load) and finally fracture.

With the lack of success in previous attempts to directly relate crack growth and internal damping, a different approach was sought. Prerequisites to defining a new approach are the examination of fatigue processes and an understanding of how these processes are modeled.

Fatigue Processes

In examining the crack tip on a microscopic scale, it is convenient to regard the fatigue life as consisting of a number of stages (Ref 11, 12). The total number of cycles to fracture is divided into four parts. The first stage occupies an average period of N_1^* cycles and represents the completion of work hardening. A plastic zone forms under load and the crack tip blunts. An average period N_2^* is required for the formation of the first submicrocracks, created by the accumulation of dislocations at slip planes. Further N_3^* cycles delineate the third stage, during which the submicrocracks grow and coalesce to form a crack of detectable size. Finally, these cracks propagate across grains until fracture or rupture occurs, and an additional number of N_4^* cycles elapse denoting the fourth stage.

Damage occurs in the second stage and can be attributed to submicrocracks that are formed in regions where stresses are concentrated because of the piling up of dislocations, or the presence of inclusions. In succeeding stages two possible developments can occur. Either the cracks grow quickly to a detectable size (the observable cracks at the end of the third stage) or plastic flow occurs at the crack ends which are stress concentration sites, so that the crack growth is temporarily stayed. Stresses subsequently increase because of work hardening, and new submicrocracks are formed at the ends of old submicrocracks. This would suggest that cracks grow iteratively.

The general and most significant features of fatigue failure are the initiation of surface microcracks and their subsequent extension across and penetration into the body of the metal. The increased life resulting from the removal of a surface layer at frequent intervals throughout a test, irrespective of whether the life is many millions or only a few thousand cycles (Ref 13), demonstrates that crack initiation is confined to the surface grains. Dislocation models leading to surface

cracking have been proposed (Ref 14, 15, and 16) that lead to a geometric cause of damage or damage on the slip plane. In general, surface cracking can occur in any of three ways; specifically, as a continuation of surface roughening in broad slip bands, as a result of severe strain incompatibilities across grain boundaries, or because of the presence of inclusions or inhomogeneities in the surface.

Theories of crack growth based on a dislocation model begin with a crack loaded in antiplane strain (Mode III). The plastic zone at its tip can be conveniently represented by a continuously distributed array of infinitesimal dislocations on the crack plane. Crack growth is assumed to start when the accumulated plastic strain distribution at a crack tip exceeds a critical value (stage 3), and continues as this value is exceeded at successive points ahead of the original crack tip. It is then assumed that the behavior in Mode I is similar to behavior in Mode III. In general, such theories (Ref 17) predict that the rate of crack growth is proportional to K_I^4 (or ΔK, depending on the load cycle considered, where $\Delta K = (K_{max} - K_{min})$ and K_{max} and K_{min} are the maximum and minimum values of K_I during the fatigue cycle). As an example, Weertman's theory (Ref 18) started with a model (Ref 19) of a freely slipping crack subjected to an applied shear. In the model, a crack of length 2a, having plastic zones at either end, was considered and the dislocation theory was used to calculate the displacement in the vicinity of the crack tips due to this shear stress. It was then shown that, under certain conditions, a crack lying normal to a tensile stress, σ, can be considered in a similar manner.

The energy associated with the plastic zone at a crack tip is proportional to K_I^4. Theories based on the energy required to operate the fracture mechanism, in general, will predict that the rate of crack growth is proportional to K_I^4, which is in agreement with dislocation theories.

The modeling of fatigue processes has found some success in estimating fracture based on energy or work at the crack tip. In particular, equations relating plastic work and fracture are common in the literature. Relating crack growth to internal damping through plastic work dictates a study of the role of plastic work in fatigue.

Plastic Work in Fatigue

Coffin and others (Ref 20) found that data obtained from reversed direct constant plastic strain amplitude tests, designed to give failures in up to about 10^5 cycles, conformed to the relationship:

$$N^{1/2} \varepsilon_p = C \qquad (1)$$

where N is the number of fatigue cycles, ε_p is the plastic strain amplitude, and C is a material constant. In the case of annealed low-carbon steels exhibiting a marked yield point, the relation does not apply in the immediate region of discontinuous yielding, but becomes applicable for the balance of the stress-strain curve. Manson (Ref 21 through 24) presented an analysis of direct loading constant plastic strain amplitude tests for 30 materials of widely differing static properties (Ref 25) showing that in all cases the endurance up to about 5×10^4 cycles was related to the plastic strain range by the relationship.

$$N^{0.6} \varepsilon_p = C$$

He suggested that the results conformed to this relationship, and not Equation 1, because N had been taken as the number of cycles to complete the fracture of the specimen. Equation 1 was based on endurances where cracks were first visible on the specimen surface. It is now accepted that the value of the exponent in Equation 1 is not a universal constant; it varies with material, environment, and the criterion adopted for failure (Ref 26, 27).

The relationship between stress, plastic strain, and plastic strain energy during a low-endurance fatigue test was studied by Morrow (Ref 26). He related fatigue life to the total plastic strain energy generated; that is, C is made a function of the integrated areas of the hysteresis loop up to the point of failure. Radhakishnan (Ref 28) modeled fatigue failure on the basis of total energy absorbed and proposed that the total hysteresis energy to failure, W_f, can be given by:

$$W_f = \int_0^{N_f} dw(N)\, dN \qquad (2)$$

where dw is the plastic energy absorbed per cycle at any given time and N_f is the number of fatigue cycles to failure. For most materials, the hysteresis loop is relatively stable after a certain initial life. Taking $\bar{\varepsilon}_p$ as the average value of the plastic-strain range during the lifetime, the energy absorbed per cycle can be approximately given as:

$$dw = A_2 \sigma_a \bar{\varepsilon}_p \qquad (3)$$

and the total energy absorbed, W_f, up to fracture will be:

$$W_f = A_2 \sigma_a \bar{\varepsilon}_p N_f \qquad (4)$$

where A_2 is a material-dependent constant and σ_a is the maximum cyclic stress.

Experimental data supporting the $(\Delta K)^4$ dependency of growth rate predicted by both dislocation and energy theories can be found in the literature. For example, tests (Ref 29) on steel, aluminum alloy, titanium, and magnesium sheet have shown that:

$$\frac{da}{dN} = D(\Delta K)^4$$

where D is a material constant. Similar results were obtained for 70/30 brass specimens (Ref 30). On the other hand, data can be found in the literature that do not conform to this relationship (Ref 31).

Attempts to correlate plastic work directly with crack growth (Ref 32) have resulted in:

$$\frac{da}{dN} = A \frac{(\Delta K)^4}{G\psi^2 U}$$

where A is a dimensionless constant, G is the shear modulus, ψ is a strength parameter, and U is the integrated plastic work expended in the plastic zone. Izumi and Fine (Ref 32) conclude that the plastic work per unit area of fatigue crack propagation is an important parameter that establishes the rate of fatigue crack growth. This report will assume that Izumi and Fine are accurate in their conclusion, and will attempt to use plastic work as a basis for measuring structural damage and coupling internal damping with crack propagation.

OBJECTIVES

This research has two objectives. The first objective is to experimentally develop a relationship between low cycle fatigue crack growth and internal damping. The second objective is the mathematical modeling of specimens to interpret and extrapolate the internal damping-crack growth relationship and apply it to other geometries and load conditions.

Accomplishment of these two objectives will establish a foundation upon which nondestructive evaluation techniques may be constructed. The first objective, the relationship, provides a basis for monitoring structural integrity. The second objective, the mathematical model, provides a process for expanding the relationship to meet the demands of monitoring complex structures.

Relationship of Crack Growth and Damping

Various researchers have shown that crack propagation and internal damping are closely linked: fatigue damage is accompanied by changes in specific damping capacity. This relationship, however, is not a direct one. The failure of many experiments to prove a direct relationship has made that point clear. To determine how damping is related to crack growth, an investigation must look for an indirect linkage between the two phenomenon. An indirect linkage suggests that the establishment of this relationship requires the merger of two previously developed theories rather than the creation of a new theory; two theories, an internal damping

mechanism and a fatigue damage mechanism, that have a common element. In merging the two mechanisms to form a single theory of fatigue damage accompanied by internal damping, care must be taken to assure that both mechanisms are used within the context of their assumptions.

The relationship must be expressed in a manner that facilitates experimental verification. Thus, an analytical expression of crack growth or fatigue damage as a function of changes in specific damping capacity is required. To verify this expression and the associated relationship, a series of fatigue tests must be planned. In general, testing would begin with fatigue specimens that minimize effects of complex parameters such as specimen geometry, variable loading and stress fields. After these initial experiments provided satisfactory results, more complex parameters could be included for testing and verification.

Mathematical Model

To incorporate increasing complexity into the testing, the specimens must be mathematically modeled. The modeling provides two significant functions:

1. A model allows more complex specimens to be fatigue tested by revealing the interaction of the additional parameters. Changes to specimen geometry or loading will affect both crack growth and internal damping, the effects of these changes must be known in advance in order to verify the test results.

2. A model will provide a solid foundation for a diagnostic tool for detecting crack growth in structures. The model must be simple to act as a tool, but it must be comprehensive to provide accuracy.

Verification of the model requires simple fatigue specimens that can be vibrated at low amplitudes during the fatigue process for data collection. The data from the series of tests will be analyzed using the model for comparison with the actual test results.

The model will have to include elements to express a continuous structure (the specimen) undergoing both dynamic (data collection cycles) and static (fatigue cycle) loading. In addition, the model must adequately handle a growing crack (or cracks) in the specimen as well as the changing internal damping capacity. The internal damping is not only changing at a global level, but on a local level as well. Damping is a localized phenomenon, and areas close to a propagating crack will dissipate heat at higher rates than areas remote from the crack (Ref 33).

TECHNICAL APPROACH

An analytical approach to develop a relationship between crack growth and internal damping is presented to provide the theoretical foundation for the relationship; a foundation integrating internal damping, crack growth, plastic strain, and dislocations.

Internal Damping Mechanism

The goals of this section are to define an analytical expression for internal damping and to accommodate, within that expression, the strain distribution experienced by a structure or system. The phrase "analytical expression" is used, rather than "mathematical model," because the product of this section represents a single mathematical term or expression of the final model.

Analytical Expression. In 1956, Granato and Lücke (Ref 34) presented a theory of internal damping due to dislocations. Granato and Lücke examined two types of losses: frequency-dependent loss (Δ_I) and strain-amplitude dependent hysteresis loss (Δ_H). Their theory provides a quantitative interpretation of these losses. The two losses are given by (Ref 35):

$$\Delta_H = \frac{\Omega \Delta_0 \Lambda L_N^3}{\pi L_c} \frac{K\varepsilon' A}{L_c} \frac{1}{\varepsilon_0} \exp\left(-\frac{K\varepsilon' a}{L_c} \frac{1}{\varepsilon_0}\right) \quad (5)$$

and

$$\Delta_I = \frac{\Omega \Delta_0 \Lambda L_c^4 B\omega}{p2C}$$

where Δ = mechanical energy lost per cycle divided by twice the total vibrational energy

Λ = total length of movable dislocation line per unit volume (dislocation density)

a = lattice parameter

ε_0 = strain amplitude

ω = circular frequency

ν = Poisson's ratio

$\Delta_0 = 4(1-\nu)/\pi^2$

$A = \pi\rho b^2$

$C = 2Gb^2/\pi(1-\nu)$

ρ = density

b = Burger's vector

L_N = network loop length

L_c = impurities loop length

L_e = effective length of dislocation loop

K = orientation and anisotropy parameter

Ω = orientation factor

Assuming that all parameters in Equation 5 can be held constant for a given material under cyclic stress, with the exception of Λ and ε_0, the equation may be rewritten as:

$$\Delta_H = \Lambda C_1 C_2/\varepsilon_0 \exp(-C_2/\varepsilon_0) \quad (6)$$

where $C_1 = \Omega\Delta_0 L_N^3/\pi L_c$ and $C_2 = K\varepsilon' a/L_c$. As modeled by Equation 6, all of the strain amplitude data may be described in terms of a single function and when plotted in the form:

$$\log(\varepsilon_0\Delta_H) \text{ versus } 1/\varepsilon_0$$

should lie on a straight line. The slope of this straight line is given by C_2 and the intercept by $\Lambda C_1 C_2$. Figure 4 shows a Granato-Lücke plot of strain amplitude times decrement versus (strain amplitude)$^{-1}$.

Bauer and Gordon (Ref 36) expressed the amplitude-independent decrement, Δ_I, resulting from dislocation vibration in the kilocycle range of frequencies as:

$$\Delta_I = C_3\Lambda \quad (7)$$

where $C_3 = \Omega\Delta_0 L_c^4 B\omega/\pi^2 C$. The total decrement, Δ, equal to $\Delta_I + \Delta_H$ is now presented in terms of Equation 6 and 7.

$$\Delta = \Lambda[C_3 + C_1 C_2/\varepsilon_0 \exp(C_2/\varepsilon_0)] \quad (8)$$

Equation 8 provides a relation between internal damping, Δ, and dislocation density, Λ.

The Granato-Lücke (G-L) theory does not always reflect experimental results and its accuracy is unclear. At times, experimental data plots of $\log(\varepsilon_0\Delta_H)$ versus $1/\varepsilon_0$ are not straight but somewhat curved (see Figure 4). The decrement measured at low strain amplitudes appears to be greater than that predicted by the theory. Some have argued that the model is essentially correct but the calculations are not yet sufficiently refined. Other authors have recommended modifications to correct the model (Ref 37 through 40). Unfortunately, all these detailed discussions

are inconclusive because of the difficulty of specifying all the various significant factors. In particular, the dependence of the decrement on strain amplitude (Equation 5) is largely determined by the distribution function for the lengths of the dislocation loops, L_N. Granato and Lücke assume an exponential function, but there is little substantiation of this approximation for any given material or geometry.

The theoretical treatment that researchers have used to explain internal damping, as illustrated in Figure 2, is broken into three regions. These regions are labeled in Figure 2. The first two regions, elastic and anelastic, are a function of dislocation damping. For the elastic region, the dislocations are assumed pinned by point defects, and vibrating as stretched strings, subject to viscous damping. In the anelastic region, the stress level is sufficient to bow out the dislocation and pull it away from pinning point defects. Lowering the stress repins the dislocation, but the motion is different on the outward and return paths, producing a hysteresis loop. The third region, fatigue-plastic, is believed to result from the formation of microcracks that can fuse together to form fatigue cracks. For pure aluminum, shown in Figure 2, dislocation damping is the dominate form of damping up to 2×10^{-4} microstrain.

A second treatment, evolving from McKavangh and Stacey (Ref 41) and Jackson and Anderson (Ref 42), is that the dominate cause of energy dissipation, in the anelastic region, is grain boundary relaxation or slippage. It is difficult to apply the conclusions of Jackson and Anderson to this research, however, since their study investigated attenuation in the earth's mantle, an environment of high temperature where dislocations are likely to be annealed out. The work of McKavangh and Stacey, on the other hand, raises doubt as to the nature of the hysteresis in the anelastic region. Their observations support non-linear internal friction due to cracks or grain boundaries. Further examination into the nature of anelastic internal damping is needed, but given the two theoretical treatments available, this research effort will rely upon the extensive experimentation and analysis that are embodied in the Granato and Lücke model.

Application of the G-L theory in the form of Equation 8 is complicated by the pattern of strain amplitude distribution within a specimen. Longitudinal, flexural, and torsional forced vibrations produce different strain distributions. The different strain distributions necessitate the derivation of mathematical expressions of the decrement on the basis of each type of vibration.

Strain Distribution. According to Equation 4 of Reference 43, the strain amplitude-dependent decrement distribution is given by:

$$\bar{\Delta}_H = \int \varepsilon^2 \Delta_H(\varepsilon) dV / \int \varepsilon^2 dV \qquad (9)$$

where V is the volume of the specimen. Povolo (Ref 44) showed that an expression for Δ_H can be obtained directly in terms of exponential integral functions and that Equation 6 oversimplifies the results for the valid range of strains as given by Granato and Lücke, that is, $\varepsilon_0/C_2 \leq 0.25$. From Povolo:

$$\Delta_H^c = AC_1(C_2/\varepsilon_0)^2 E_1(C_2/\varepsilon_0) \qquad (10)$$

where E_1 is the exponential integral of order n = 1 and:

$$E_n(x) = \int_1^\infty \frac{e^{-xt}}{t^n} \, dt$$

is the exponential integral function. From Equation 9, using Povolo's corrected strain amplitude-dependent decrement of Equation 10, the distribution peculiar to the type of vibration can be derived.

A slight modification to Equation 9 (required for specimens that have developed interior plastic zones at a location of stress concentration) is separate integrals for the plastic and elastic regions.

Given a small amplitude of vibration, ε_0, it is assumed that the only parameter that changes in Equation 9 between the two regions is the dislocation density, A. This assumption is based on small amplitude vibration of the specimen when internal damping data is collected. Burdett and Queen (Ref 45) noted that internal damping developed during plastic strain may be expressed in the form:

$$\Delta_p = A \exp [B(\varepsilon_0 - \varepsilon_p)]$$

where ε_p is the critical strain above which plastic strain occurs, and A and B are temperature-dependent terms. Burdett and Queen concluded that the G-L model is valid in cases where the movement of the dislocations is not affected by obstacles outside their equilibrium position. This is the case when the specimen experiences low strain vibration; therefore, it is valid to assume that only the dislocation density has changed when comparing internal damping between the elastic region and plastic zone. The distinction between the Δ_H and Δ_p contributions appears to involve the degree of pinning of dislocations. For lightly pinned dislocations the contributions are well separated. In the case of heavily pinned dislocations, the Δ_H is suppressed completely and the dislocations contribute immediately to Δ_p at relatively high strain amplitudes.

The plastic zone size and shape depends on the plastic flow properties (Ref 46), but the dimensions are proportional to $(K_I/\sigma_Y)^2$. The nominal plastic zone radius, r_p, is approximately:

$$r_p = \frac{1}{2\pi}\left(\frac{K_I}{\sigma_Y}\right)^2 \quad \text{for plane stress} \qquad (11)$$

and

$$r_p = \frac{1}{6\pi}\left(\frac{K_I}{\sigma_Y}\right)^2 \quad \text{for plane strain} \qquad (12)$$

where σ_Y is yield stress. The plastic zone radius is about half the extent of the plastic zone and is applicable when the zone size is small compared to the specimen dimensions in the plane of the plate.

Breaking Equation 9 into two separate integrals (the first for the elastic region and the second for the plastic zone) produces:

$$\bar{\Delta}_H^c = [\Lambda_e \int_e \varepsilon^2 \theta_H^c(\varepsilon) dV + \Lambda_p \int_p \varepsilon^2 \theta_H^c(\varepsilon) dV] / \int \varepsilon^2 dV \qquad (13)$$

where the parameters with subscripts e and p correspond to the elastic region and plastic zone, respectively; the strain-dependent function, θ_H^c, is given by:

$$\theta_H^c = C_1 (C_2/\varepsilon_0)^2 E_1 (C_2/\varepsilon_0) \qquad (14)$$

that is, $\theta_H^c = \Delta_H^c / \Lambda$. In a similar manner, the strain-independent decrement may be expressed as $\bar{\Delta}_I^c = C_3 (\Lambda_e V_e + \Lambda_p V_p)/V$, where V_e and V_p are the volumes of the elastic region and plastic zone, respectively.

Equation 13 expresses material dislocation damping as a function of elastic and plastic strain distributions given by Equation 14. Having obtained an analytical expression for dislocation damping, the second step is to develop a fracture failure criterion.

Crack Growth

Monitoring structural integrity requires a procedure for quantifying fatigue damage and estimating crack growth. A fracture criterion based on plastic work is proposed for accomplishing this task and providing an interface to amplitude-dependent damping.

Failure Criterion. In selecting Equation 3 as a fracture criterion, Feltner and Morrow used the empirical equation $\sigma_a = k_p \varepsilon_p^n$ (see Figure 5) to relate the true plastic strain to true stress as shown in Figure 6 (Ref 47). With their empirical stress-strain relation, Feltner and Morrow were able to express Equation 3 as:

$$W_f = A_2 k_p \bar{\varepsilon}_p^{n+1} N_f \qquad (15)$$

so that the total energy absorbed to fracture is a function of the true plastic strain average, $\bar{\varepsilon}_p$. For the purposes of this investigation, the definitions of true stress and true strain are taken from Davis, Troxell, and Wiskocil (Ref 48). In postulating that the plastic-strain energy portion of the hysteresis energy accounts for the damaging effects of cyclic stress, Feltner and Morrow made three assumptions: (1) a logarithmic plot of static true stress versus true plastic strain is valid when extrapolated back into the fatigue stress region; (2) the damaging energy per cycle for a given stress amplitude is constant and is equal to the area under the static stress plastic-strain curve; and (3) the total damaging energy required to cause fatigue fracture is constant and as a first approximation is equal to the area under the static true stress - true strain curve.

A correction made to assumption 3 is that the total damaging energy required for fatigue fracture is not constant but related to the strain amplitude per cycle as follows:

$$\frac{W_2}{W_1} = \left(\frac{\varepsilon_2}{\varepsilon_1}\right)^{-m} \qquad (16)$$

where m is the hysteresis energy exponent which Halford and Morrow (Ref 49) derived from Griffith's crack theory. Halford and Morrow's value, $m = 4n$, is accurate for 4340 steel, but not necessarily for other metals. There does not appear to be a relationship between strain amplitude and hysteresis energy to failure that is independent of material properties. The lack of a relationship between strain amplitude and hysteresis energy does not invalidate Equation 16 or assumption 3, it simply requires experimental determination of m for each material investigated. Combining Equations 15 and 16 results in a relationship between plastic strain and fatigue life:

$$\frac{N_2}{N_1} = \left(\frac{\varepsilon_2}{\varepsilon_1}\right)^{-k}$$

where k = 1/C and C, the fatigue-ductility exponent introduced in the Manson-Coffin law, is shown to be 1/(5n+1). Again, this value is accurate only for 4340 steel. From Radhakishnan (Ref 28), m is not equal to 4n, but is given by the formula:

$$m = k - (n + 1)$$

Both n and C (and thus k) must be determined experimentally. Substituting ε_{pu}, $\bar{\varepsilon}_p$, 1/2, and N_f for ε_1, ε_2, N_1, and N_2, respectively, and rearranging Equation 15:

$$N_f = 1/2\ (\bar{\varepsilon}_p/\varepsilon_{pu})^{-k} \qquad (17)$$

produces a power law relation between fatigue life and the average plastic strain per cycle. In Equation 17, ε_{pu} is the static plastic strain fracture value at 1/2 cycle. Figure 7 demonstrates the relationship between fatigue life and average plastic strain per cycle as modeled by Equation 17.

Criticism has been levied against the use of hysteresis energy as a criterion for fatigue failure. The first criticism is that attempts to correlate fatigue life with tensile properties have been unsuccessful. However, there are investigations that indicate a relationship between the fatigue strength and parameters of the true stress-true strain curve (Ref 50 and 51). The second source of criticism is due to the difference between monotonic and cyclic stress-strain curves. This is a minor argument, since the difference is small enough to neglect when the two curves are compared in the fatigue stress range (Ref 28).

Material Properties. Crack growth is a material-dependent phenomenon. The total hysteresis energy to failure, W_f, and plastic energy absorbed per cycle, dw, were presented in Equation 2. For most materials, the hysteresis loop is relatively stable after a certain initial life. This

stability is dependent on the stress level. There is more stability at low stress levels than at high stress levels. In some cases, like carbon steels, no stable loop is obtained throughout the life of the specimen, especially when the stress level is near the yield strength. A considerable amount of softening is observed during the initial stages, followed by a hardening process, which is rapid when the stress level is high and slow when the stress level is low. Hence, the value of dw per cycle changes with stress cycles depending on the hardening and softening of the material.

The empirical relationships and mathematical models developed to correlate fatigue life with mechanical properties of metal have been criticized for depending too greatly on the idealization of the properties of metals. At the microscopic level where fatigue damage initiates, all metals are heterogeneous. The fatigue resistance of a small volume of material will differ from that of another because of inclusions, differences in grain size, anisotropy, orientation, micro-residual stress, etc. The fatigue behavior of a real material is the integrated phenomenon of these various microscopic factors. The distribution of these factors, and thus the metal's mechanical properties, are random throughout the material. Because of this probabilistic distribution, the fatigue limit and fatigue life at a given stress will vary from specimen to specimen.

Plastic Strain and Dislocation Density

An empirical relationship between plastic strain and dislocation density is presented. This section couples together fracture criterion, based on plastic work, with internal damping, based on dislocation density.

Dislocation Model for Stress-Strain Behavior. A number of authors have expressed stress-strain behavior via a dislocation model. For alpha iron (α-Fe), during constant strain-rate tensile experiments, modeling the yield-point behavior has produced a variety of theories. Cottrell (Ref 52) explained the upper yield point by introducing the pinned dislocation concept A relatively high initial stress was required to unpin

dislocations, but once unpinned they could move at a lower stress level. In his approach, Hahn (Ref 53) explained the yield-point phenomenon as a result of the rapid increase of mobile dislocations when yielding begins. A model developed somewhat later by Bergström (Ref 54), emphasizes the Λ-ε relationship and is based on dislocation behavior during deformation.

Bergström has five assumptions for his model:

1. The true flow stress-dislocation density relation is given by:

$$\sigma = \sigma_{io} + \alpha G b \Lambda^{1/2} \tag{18}$$

where α and σ_{io} are constants. A review of experimental data in support of Equation 17 is provided by Otte and Hren (Ref 55).

2. Both mobile and immobile dislocations are present at any true strain, ε.

3. The mobile density, L, is strain independent and much smaller than the immobile density, Λ_i.

4. The variation of Λ with ε is determined by the creation, the immobilization, the remobilization, and the annihilation of dislocations.

5. Those effects that arise from changes to the scale or arrangement of the dislocation structure and that do not affect assumption 4 above, are negligible.

Bergström derived the following differential equation, giving the dislocation density, Λ, as a function of plastic strain, ε_p:

$$\frac{d\Lambda}{d\varepsilon_p} = U_i - \chi\Lambda \tag{19}$$

where U is the rate of immobilization of mobile dislocations and χ is the strain-independent probability for the remobilization of immobile dislocations, and:

$$U_i = 1/\Phi bs$$

where Φ is an orientation factor (0.5 and 0.32 for b.c.c. and f.c.c., respectively) and s is the dislocation mean free path. Bergström (Ref 54) contends that a strain-independent s is a good approximation for b.c.c. metals if χ is small enough for the product $\chi\Lambda$ to be negligible at small strains. With a strain-independent U_i, the integration of Equation 19 results in:

$$\Lambda = \frac{U_i}{\chi} [1 - \exp(-\chi\varepsilon_p)] + \Lambda_0 \exp(-\chi\varepsilon_p)$$

with $\Lambda = \Lambda_0$ at $\varepsilon_p = 0$.

As a modification to the Bergström theory, Vetter and van den Beukel (Ref 56) assume the dislocation mean free path is of the order of and proportional to the dislocation cell size, d. The cell size decreases with increasing strain, and has been shown to depend on the dislocation density according to:

$$d = \frac{K}{\Lambda^{1/2}}$$

where K = 20 for iron. Therefore:

$$s = f \frac{K}{\Lambda^{1/2}} \qquad (20)$$

where f is a constant of order 1. Inserting Equation 20 into Equation 19 and integrating

$$\Lambda^{1/2} = \frac{A'}{\chi} [1 - \exp(-1/2\chi\varepsilon_p)] + \Lambda_0^{1/2} \exp(-1/2\chi\varepsilon_p) \qquad (21)$$

where $A' = 1/\Phi bKf$.

Damping Mechanism-Fatigue Criterion. Equation 21 provides a relationship between plastic strain amplitude and dislocation density and is the link to combining the damping mechanism (Equation 13) with the fatigue criterion (Equation 17). Rearranging Equation 21 so as to express ε_p as a function of Λ,

$$\varepsilon_p = \frac{2}{\chi} \ln \left(\frac{\Lambda^{1/2} \chi - A'}{\Lambda_0^{1/2} \chi - A'} \right) \tag{22}$$

For the fatigue criterion, as described by Equation 17, the average plastic strain, $\bar{\varepsilon}_p$, is the sum of the plastic strain per cycle, ε_{pi}, divided by the number of elapsed stress cycles. In equation form:

$$\bar{\varepsilon}_p = \frac{1}{N} \sum_{i=1}^{N} \varepsilon_{pi} \tag{23}$$

where N is the number of elapsed cycles. The right-hand side of Equation 22 is then substituted for ε_{pi} in Equation 23 and the fatigue criterion becomes a function of dislocation density:

$$\bar{\varepsilon}_p = \frac{2}{N\chi} \sum_{i=1}^{N} \ln \left(\frac{\Lambda_i^{1/2} \chi - A'}{\Lambda_0^{1/2} \chi - A'} \right) \tag{24}$$

Damping was previously shown to be dependent on dislocation density (see Equation 13); however, this dependency consists of two dislocation density terms: Λ_e and Λ_p. It is now assumed that the plastic zone dislocation density, Λ_p, is responsible for all plastic strain directly related to crack growth, so that no crack growth exists in the elastic region. That is to say, Equation 22 may be rewritten as:

$$\varepsilon_p = \frac{2}{\chi} \ln \left(\frac{\Lambda_p^{1/2} \chi - A'}{\Lambda_0^{1/2} \chi - A'} \right) \tag{25}$$

Equation 25 is consistent with the fatigue process N_2^* stage (Ref 11, 12) where voids form in the plastic zone and coalesce into microcracks. This situation is illustrated in Figure 8 and is modeled by Ishikawa (Ref 57) as a slow crack extension within the plastic zone, where the plastic zone is a uniform distribution of dislocations. Ishikawa derives the plastic strain in the plastic zone from the crack extension force as:

$$\varepsilon_p = \alpha(s/r_p) \tag{26}$$

where α is approximate unity.

Rearranging Equation 13 into:

$$\Lambda_p = \frac{\Delta^c V \int \varepsilon^2 dV - \Lambda_e [V \int_e \varepsilon^2 \theta_H^c(\varepsilon) dV + C_3 V_e \int \varepsilon^2 dV]}{V \int_p \varepsilon^2 \theta_H^c(\varepsilon) dV + C_3 V_p \int \varepsilon^2 dV} \tag{27}$$

solves for the plastic zone dislocation density Λ_p in terms of the corrected total decrement, $\bar{\Delta}^c$; the elastic region dislocation density, Λ_e; the plastic zone radius, r_p; and the strain amplitude, ε. Dislocation density increases for some metals at stresses below the macroscopic yield (Ref 58) and under these conditions it is not possible to eliminate Λ_e as a variable. However, for metals whose dislocation density does not increase appreciably until yield, Λ_0 may be used in place of Λ_ε (Ref 56).

Equation 17 presents fatigue life as a function of average plastic strain. Equation 24 determines average plastic strain from dislocation density in the crack tip plastic zone. Equation 27 gives plastic zone dislocation density from internal damping. With Equations 17, 24, and 27, the objective of developing a theoretical relation between fatigue and damping has been accomplished. The next requirement is to test the validity of Equations 17, 24 and 27.

EXPERIMENTAL APPROACH

Experimental verification of the theoretical development of a relationship between crack growth and internal damping begins with the determination of material properties, including damping, and concludes with fatigue testing of 1018 and 4340 steel beam specimens.

Purpose

The main purpose of experiments is to test hypotheses. The fatigue tests used in this research will determine whether internal damping changes with crack growth as suggested by Equations 17, 24, and 27.

Damping Mechanism-Fatigue Criterion Relationship. Successful verification of Equations 17, 24, and 27 in a test series of one material and specimen type is no assurance that the proposed constitutive relationship between crack propagation and internal damping is valid for all material and specimen types. It merely states that the relationship between fatigue and damping is valid for the material and strain distribution tested. A measure of validity, rather than complete verification, is required at this point. Determining whether or not the relationship can be established for a particular material and specimen type is the first step. This relationship was built through a process of steps culminating in Equations 24, 25, and 27. As many of these steps as possible must be independently verified to assist in determining the problem areas if discrepancies arise. Therefore, the primary purpose of testing is to determine:

1. Is plastic work related to fracture as suggested by Equation 15?

2. Is plastic strain related to fracture by Equation 17?

3. Does Equation 13 accurately model internal damping as a function of strain and plastic zone and elastic region dislocation densities?

4. Will the Bergström model relate plastic strain and dislocation density as expressed in Equation 22?

5. Do all the previous steps combine to relate crack propagation to internal damping?

The five questions listed above interrelate internal damping, crack propagation, plastic strain, and dislocation density. These four parameters must all be evaluated during testing in order to verify the internal damping-fatigue criterion relationship.

Fatigue Life, Damage Assessment, and Fracture Prediction. A step beyond verifying the internal damping-crack growth relationship is to predict fatigue specimen life and the subsequent specimen failure. The fracture prediction process entails extrapolating the average plastic strain calculated from the damping data to arrive at the predicted total number of fatigue cycles to fracture, N_{fp}, as presented in Equation 17. A simple approach to damage assessment is to use the ratio of fatigue cycles completed, N_c, to fatigue cycles to fracture, N_{fp}, as predicted by the fatigue life estimate of Equation 17. In equation form:

$$D\% = 100\% \ (N_c/N_{fp}) \tag{28}$$

where D% is the damage assessment in percent. A comparison of this estimate with the actual crack growth will suffice as verification. This linear approach to damage assessment should prove satisfactory for low cycle fatigue using constant crack growth rates.

The linear prediction of fatigue damage represented by Equation 28 is adequate for loads of a constant stress intensity factor; however, it is inaccurate for other types of loads. The life of a structure undergoing fatigue, when based on plastic work, is given by Equation 17. Specifically, for a varying plastic strain per j^{th} fatigue cycle, ε_{pj}, the fraction of fatigue life expended for a structure is given by:

$$LF = 2 \sum_j \left(\frac{\varepsilon_{pj}}{\varepsilon_{pu}} \right) \tag{29}$$

where ε_{pu} is the static plastic strain fracture value at 1/2 cycle. As the crack growth to failure, a_f, divided by the crack growth in one cycle, Δa_j, results in fatigue cycles to failure, N_f, substitution in Equation 17 produces the following relation:

$$\varepsilon_{pj} = \varepsilon_{pu} \left(\frac{\Delta a_j}{a_f} \right)^{1/k} \tag{30}$$

Substitution of ε_{pj} into Equation 21 determines the plastic zone dislocation density for the j^{th} fatigue cycle. Combined with an estimate of the plastic zone radius from Equation 11 or 12, an approximation of the internal damping can be made from Equation 13.

Equation 29 is presented as a more accurate and reliable estimation of fatigue damage than Equation 28. Successful verification of Equation 29 will meet the objective of establishing nondestructive evaluation techniques based on internal damping.

Test Arrangements

The two test arrangements described here are designed to answer the questions raised above. In so doing, these experiments will verify the proposed relationship between fatigue and damping for 1018 and 4340 steel.

Fatigue Test. To accomplish the desired goals of relating damping to crack growth and predicting fatigue life, a series of fatigue tests is required. These tests monitor crack growth, damping, load, strain, and number of fatigue cycles.

The fatigue test schematic is shown in Figure 9, the fatigue beam specimen in Figure 10, and the test procedure is described in detail in Appendix A. The following description briefly summarizes the fatigue test procedure.

An MTS test machine applies a cyclic load to a 4340 beam specimen (100 pounds for damping datum and up to 1,400 pounds for fatigue). The beam specimen is initially notched and uncracked. The fatigue load has

a stress ratio of zero and is continuously adjusted to maintain a constant stress intensity factor during the fatigue process. Crack length data is collected during data collection cycles from crack propagation gages on either side of the specimen. The crack length measurement is used to update the fatigue load setting. The stress intensity factor is calculated from (Ref 59):

$$K_I = \sigma\sqrt{\pi a}\, F(a/b) \tag{31}$$

where $\sigma = 6M/b^2$

M = moment

b = specimen thickness

and

$$F(a/b) = 1.122 - 1.4(a/b) + 7.33(a/b)^2 - 13.08(a/b)^3 + 14.0(a/b)^4 \tag{32}$$

is an empirical formula accurate to 0.2 percent for $a/b \leq 0.6$. In the case of a four-point beam, the moment is given by $M = 1/2Pl_a$, where P is the total applied load and l_a is the distance from a knife edge to the nearest load point. Substituting for σ in Equation 31 and solving for P:

$$P = \frac{b^2 K_I}{3l_a \sqrt{\pi a}\, F(a/b)} \tag{33}$$

P of Equation 33 is calculated after every data cycle and a new fatigue load setting is communicated to the MTS test machine.

A vibration generator attached to the specimen excites the beam in a range of 5 to 20 Hz around the fundamental frequency, ω_{n1}. For example, if the specimen resonates at 320 Hz, a frequency range from 310 to 330 Hz is swept by the vibration generator. While the beam is being excited, strain gage data are input to a spectrum analyzer that converts the data

from the time domain to the frequency domain and then transfers it to the Lab-Datax computer for damping calculations. The same data also provide the fundamental frequency of the beam. For each damping data cycle the following data are collected:

1. Fatigue cycle number, N
2. Fatigue load, P
3. Maximum strain, ε_a
4. Minimum strain, ε_{min}
5. Crack length, a
6. Stress intensity factor, K_I
7. Damping decrement, Δ
8. Transfer function amplitude ratio at ω_{n1}, TF

The data are saved in a file on disk to be transferred at a later time to a mainframe for processing and plotting.

All fatigue tests will begin with a 2000 load cycle damping datum phase. During this phase, approximately 50 damping data cycles will be performed and the resultant average damping value will be interpreted as the normal damping state of the uncracked specimen as configured and mounted in the fixture. The load during this phase will be approximately 100 pounds. The light loading is sufficient to detect minor slippage at the knife edges and make appropriate adjustments to the clamping bolts.

Fatigue tests of 1018 steel beam specimens are similar to those described for the 4340 steel specimens. The major difference is in the fatigue load. For the 1018 steel specimens, the fatigue load is approximately 800 pounds. Also, the load is held constant. Therefore, the stress intensity factor increases as the crack grows. The stress intensity factor is held constant for the 4340 steel specimens.

Microcracks initiate in the vicinity of a stress concentration as a consequence of high load stress. High load stress forces dislocations to pile up on a slip plane. A microcrack is nucleated as a result of the short-range interactions of a few dislocations at the head of the

pile. The remaining dislocations are presumed to produce the high stress concentration needed to force the leading dislocations to form a microcrack (Ref 11, 60, 61, 62). In ductile metals, where dislocations are easily generated, crack nuclei continue to form with increasing amounts of strain, and these nuclei grow slowly into microcracks that eventually join to form a macroscopic crack. Elasto-plastic analysis of cracks often ignore the microcrack phase and directly model crack propagation with dislocation strips or arrays (Ref 57, 63, 64).

For a cyclic load having a compressive mean stress, microcracks are prevented from opening, retarding development, and impeding the coalescence of microcracks into macrocracks. On the other hand, a tensile mean stress tends to open a microcrack and spur crack development (Ref 60). The fatigue tests of 4340 steel beams are designed to generate a tensile mean stress. The microcracks developed in these specimens remain open, under a zero stress condition, due to residual plastic stress.

Within the plastic region, elliptical microcracks have displacement in two modes: opening and shear. Opening displacement spreads and then closes the microcrack. This mode creates internal damping through energy loss when the surfaces are in contact. Shear displacement moves one microcrack surface parallel to the other. Damping is incurred through the dissipation of heat as the two surfaces rub past one another.

The following assumptions were set forth by Budiansky and O'Connell (Ref 65), in their analysis of randomly distributed cracks:

1. Microcrack closure effects are ignored.

2. Microcracks have small openings between their opposite faces.

3. Microcrack edges are considered blunt.

4. Small stresses do not produce contact between microcrack faces.

5. Macroscopic incremental stress-strain relationship is linear.

6. General elliptic planform.

Having a mean tension fatigue stress, microcracks in the 4340 beam specimens meet the condition of assumption 2. Given the small damping data cyclic stress (on the order of 500 psi) applied to the specimen (described in Appendix A), it is reasonable to presume that condition 4 is also met. Meeting conditions 2 and 4 suggest that the microcrack surfaces do not touch and thereby dissipate energy. Without dissipation of energy, the microcracks cannot contribute to internal damping.

Two alterations to the fatigue test arrangement of Appendix A could result in microcracks contributing to internal damping. First, the mean fatigue stress would have to be in a range that would allow the microcrack surfaces to move relative to one another under a small data collection cyclic loading. The motion could be shear mode, opening mode, or a combination of the two. Second, the data collection cyclic loading would have to be large enough to overcome the residual plastic strain holding the microcracks open and cause the microcrack surfaces to rub against one another.

Internal Damping Test. Material parameters, required to calculate dislocation damping in the plastic zone from Equation 27, are determined experimentally by internal damping tests. This section summarizes the test arrangement for determining internal damping material parameters.

Physical properties of materials are determined by repeatable experimental testing. Internal damping, being a physical property, must be determined by a series of tests for each material of interest. To answer the question whether Equation 13 accurately models internal damping as a function of strain and plastic zone and elastic region dislocation densities, testing of 4340 steel at various levels of strain is required.

Figure 11 is a schematic of the damping test arrangement and Figure 12 shows the damping specimen. Appendix B contains a description of the test procedure. The following description summarizes this procedure. A sine load function is applied to the symmetric cantilever beam specimen furnishing a stress ratio of negative one. An accelerometer measures the load function while strain gages on the specimen measure the beam response. The ratio of strain to acceleration at the resonant frequency of the beam provides a transfer function ratio. From this ratio, internal

damping for the material may be plotted against strain levels, thus obtaining plots similar to Figures 2 and 4. The data collected from these tests will include decrement, Δ, and strain, ε. From data reduction, the parameters C_1, C_2, and C_3 of Equations 14 and 26 are estimated for later application in refining the fatigue test data reduction.

Material Properties

Prior to performing fatigue and damping tests, testing was done to determine the mechanical properties of 4340 steel. The chemical composition, heat treatment, and engineering tensile properties of the SAE 4340 steel used in this investigation are presented in Table 1. The SAE 4340 steel was selected as the test material for several reasons: (1) a significant amount of crack growth data had been previously collected, (2) a small plastic zone on the order of 0.01 to 0.03 inch developed at the notch, and (3) there was continued usage of the material in applications with conditions leading to cyclic fatigue. The large amount of crack growth data available for 4340 steel allows quick verification of fatigue test results. Conversely, 1018 steel produces a large plastic zone that sharply contrasts with 4340 steel.

Testing and subsequent calculations (Ref 66 and 48) were done to determine the true stress-true strain relationship of the materials. Figure 13 depicts this relationship and has a strong resemblance to Figure 6, the true stress-strain curve of 4340 steel used by Feltner and Morrow (Ref 47). The true stress-plastic strain curve representative of Figure 13 may be expressed as:

$$\sigma_a = k_p \varepsilon_p^{\,n} \qquad (34)$$

where the strength coefficient $k_p = 230.3 \times 10^3$ psi, and the strain hardening exponent $n = 0.0902$. Coefficients k_p and n were computed using a least squares technique (Ref 67).

Inserting Equation 21 into Equation 18 produces a second equation relating stress, σ and plastic strain, ε_p,

$$\sigma = \sigma(0) + \frac{A'}{\chi} \alpha G b [1 - \exp(-1/2\chi\varepsilon_p)] \quad (35)$$

where $\sigma(0)$ is the stress at zero plastic strain. A simplex algorithm (Ref 68) was used to fit the data to a curve which resulted in $A' = 6.128 \times 10^6$ in.$^{-1}$, $\sigma(0) = 162.8 \times 10^3$ psi, and $\chi = 8.613$ assuming $\alpha = 0.8$ and the Burger's vector, $b = 10^{-8}$. The shear modulus is calculated from (Ref 69):

$$G = \frac{E}{2(1+\nu)} \quad (36)$$

where the elastic modulus has been experimentally determined as $E = 28.0 \times 10^6$ psi and Poisson's ratio is $\nu = 0.29$ (Ref 66). Equation 36 produces $G = 10.9 \times 10^6$ psi. From Feltner and Morrow (Ref 47) the total hysteresis energy for static fracture, based on Equation 34, is given by:

$$W_u = \frac{k_p \varepsilon_{pu}^{n+1}}{n+1} \quad (37)$$

or based on Equation 35,

$$W_u = [\sigma(0) + \frac{A'}{\chi} \alpha G b] \varepsilon_{pu} + \frac{2A'}{\chi^2} \alpha G b [\exp(-1/2\chi\varepsilon_{pu}) - 1] \quad (38)$$

The static test results are summarized in Table 2.

The final preliminary tests determined the critical stress intensity factor of 4340 steel, K_{Ic}. Three compact tension specimens (Ref 70) were tested, producing a $K_{Ic} = 76.5 \times 10^3$ psi-in.$^{1/2}$. From Equation 12 and the yield stress given in Table 1, the plastic zone r_p would be expected to reach a maximum of 0.016 inches for a specimen experiencing plane strain conditions. Equation 27 integrates the dislocation density and strain functions over volumes of the plastic and

elastic beam material. With an elastic volume of about 5.6 $in.^3$ versus a plastic volume of about 800 x 10^{-6} $in.^3$, the ratio of plastic to elastic material is on the order of 150 x 10^{-6}. This ratio suggests a large plastic zone dislocation density or strain level is required to produce a measurable internal damping change.

These values, together with the results from the internal damping tests, will be used in the mathematical model to verify Equations 17, 24, and 27.

TEST RESULTS

The results of the four-point beam fatigue tests, and brief results of the internal damping tests, are presented here. Detailed results of the internal damping tests are in Appendix E.

In addition to the dislocation damping discussed previously, an additional damping mechanism is analyzed for the 4340 steel beam specimens. This mechanism dominates the damping response observed in these specimens.

Internal Damping Tests

To validate the fatigue test results and mathematical model, internal damping tests were conducted. This section summarizes the results described in detail in Appendix E, and is based on the test procedure presented in Appendix B.

The coefficients associated with dislocation damping, C_1 and C_2, are used in Equations 13 and 14, and subsequently in Equation 27. Modeling of these equations is established in Appendix C, step 3.8. Appendix C is an algorithm for simulating internal damping in preparation for the mathematical model.

Estimates of material constants are C_1 = 54 x 10^{-3} and C_2 = 144 x 10^{-6}. Based on restrictions of the Granato-Lücke equation (Equation 5), the maximum beam strain during damping data collection is limited to 36 x 10^{-6}, that is, one fourth of C_2. From Figure 14, for a simple-supported

beam vibrating in the fundamental mode, the damping ratio for the maximum strain is 172 x 10^{-6}. This small amount of damping is difficult to measure accurately, a point that becomes more apparent in the next section, which documents the analysis of the four-point beam fatigue tests.

Fatigue Tests

The two materials used in the fatigue tests were 1018 and 4340 steel. The 1018 steel beam specimens were fatigued under a constant load and an increasing stress intensity factor. The 4340 steel beam specimens were fatigued under a decreasing load and a constant stress intensity factor.

4340 Steel Beam Fatigue Plots. Four beam specimens were fatigue tested in a four-point load arrangement. Figures 15 through 18 show the plotted crack extension, resonant frequency, and damping ratio data for each of the specimens. The figures share common peaks in damping and fluctuations of resonant frequency at approximately 300, 270, and 245 Hz. Since the tests were automated, no observations are available to explain these phenomena in the data. Due to differences in the initial tightness of the clamping bolts at the knife edges, the beams began their tests at different resonant frequencies. The specimen crack lengths also varied from beam to beam at these frequencies. Because of this, it does not appear that the fluctuations were due to the specimens themselves. One possible explanation is that some part of the test equipment or fixture on the MTS test machine resonates at these frequencies.

All four plots indicate a definite increase in damping as the crack grows. This upward trend in damping is consistent with the increase in energy losses in metals with propagating cracks as measured by Charles, Appl, and Francis (Ref 33). Freudenthal (Ref 71), noting the sharp increase in damping and fracture that ensued, offered the explanation that the increase is an expression of the formation and spreading of macroscopic cracks under considerable local deformation.

Specimen A. Crack extension, resonant frequency, and damping ratio data are presented in Figure 15 for this first specimen tested. Fatigue loading was set at 1250 pounds with a resulting K_{ave} = 26.1 and SD = 2.16 ksi-in.$^{1/2}$, where SD is the standard deviation. Due to a programming error in the calculation of Equation 32, the stress intensity factor was not held constant. A decision was made to fail the specimen while the crack growth was still being tracked by the crack propagation gages in order to assess their accuracy. Table 3 summarizes the data at failure. The crack propagation gage recorded a crack depth of approximately 0.25 inch at failure, indicating an error on the order of 10 percent. This error is probably associated with the error in measuring the location of the crack gages on the specimen prior to the start of the test.

Specimen B. The damping datum was established at a damping ratio of 460 x 10^{-6} and the load was initialized at 1250 pounds. Fatigue test data are shown in Figure 16. The average stress intensity factor was 34.4 with SD = 1.37 ksi-in.$^{1/2}$. The average crack growth rate, (da/dN), over the width of the crack propagation gage was 14.9 x 10^{-6}.

Specimen C. Figure 17 contains the crack extension, resonant frequency, and damping ratio data. The damping datum was established at a damping ratio of 460 x 10^{-6} over 50 data cycles. The fatigue load was initialized at 1250 pounds. K_{ave} = 30.5 and SD = 1.91 ksi-in.$^{1/2}$ with the crack growth rate, (da/dN), at 11.9 x 10^{-6}.

Specimen D. The data from the last test are presented in Figure 18. The damping was established at a damping ratio of 460 x 10^{-6} and the load was initialized at 1400 pounds. An average stress intensity factor of 36.3 with a standard deviation of 1.48 ksi-in.$^{1/2}$ was produced. Over the width of the crack gage the crack propagation rate was 17.0 x 10^{-6}.

Past experience with crack propagation gages had produced inconsistent results. The adhesive selected to glue the gages to a specimen often failed, resulting in erratic crack length data. The adhesive used on the 4340 steel beam specimens proved very reliable and secured crack length data within 100^{th} of an inch.

Analysis of Damping Results in 4340 Fatigue Specimens. Results from the damping tests are applied to the fatigue tests through the estimates of the material-dependent constants of Equation E-3 in Appendix E and usage of the frequency-dependent damping equation.

The plastic strain in the plastic zone at the fatigue crack tip was estimated at 400×10^{-6} in./in. for specimens B and C and 500×10^{-6} for specimen D. This estimate is based on Equation 17 and assumes a constant plastic zone size. For fatigue specimens B, C, and D the assumption of a constant plastic zone size is valid for the period of testing when the crack length was within the crack propagation gage range. Once outside of this range, erroneous crack length data were received by the control program and the applied fatigue load did not preserve a constant stress intensity factor. This small plastic strain, together with the small plastic zone radius (on the order of 0.003 inch) suggests a small contribution (on the order of 10^{-6}) to the overall internal damping by the dislocations in the plastic zone.

Figures 15 through 18 clearly indicate a significant increase in the internal damping as each test progressed. However, the cause of this increase cannot be associated with the dislocation density of the plastic zone at the fatigue crack as hypothesized. Another mechanism must be found to explain this phenomenon.

Alternate Damping Mechanism. The damping behavior observed in Figures 15 through 18 is not consistent with phenomenon associated with dislocation density in a plastic zone. For a constant plastic zone radius, this damping should be relatively constant. Damping in all specimens increased with increasing crack length, suggesting that damping is related to the crack length itself. Plots of damping versus maximum beam slope at the crack (Figures 19 through 21) reveal a straight line. Although

the slope is different for the three figures, it does suggest that the cause of the damping is related to the crack length or rotation of the cracked surface. A relation based on rotation of the beam at the crack surface has the form:

$$\zeta_1 \propto \phi'_{max}(1/2)$$

An initial conjecture is that the crack surfaces rub together when the beam vibrates. Figure 22 models the damping versus beam slope relation. This model suggests the following boundary equation using a constant, c_{ck}, multiplying the beam slope velocity to represent the crack surface dissipation function:

$$EIw''(1/2) = c_{ck}(a)\,\dot{w}'(1/2) + k_c(a)\,w'(1/2) \qquad (39)$$

This is an empirical relation, adequate for the model in this report, but requiring additional analysis at some later date.

1018 Steel Beam Fatigue Test Results. Figure 23 is a plot of data collected from a 1018 steel beam subjected to fatigue loading. The beam specimen has a shallow increase in damping between 17,500 to 20,000 cycles; however, it is not clear if this change in damping can be attributed to the fatigue phenomenon or if it is caused by an external effect. One possibility is that this additional damping is due to the crack motion, as reflected in Equation 39 and the coefficient c_{ck}. A scenario for this would be that the plastic zone is initially small and the crack surfaces rub as the beam is vibrated to collect damping data. As the crack grows and the stress intensity factor increases, the beam forms a plastic hinge at its midpoint. The plastic hinge permanently opens the crack, not allowing the surfaces to rub and effectively lowers the damping ratio. Excluding the damping increase mentioned above, the overall damping ratio remains roughly constant up to 25,000 cycles, whereupon it increases sharply.

Test results of 1018 and 4340 steel specimens demonstrate two different damping phenomenon. Results from the 1018 steel fatigue tests are consistent with the analytical approach presented previously in this report. That is, the damping is relatively stable for a small plastic zone, and increases rapidly with an expanding plastic zone. To validate the 1018 steel results and analyze the 4340 steel results, the specimens must be modeled and crack growth and damping phenomena included in the model. The questions raised in the Experimental Approach section of this report will be answered after comparing the fatigue test results with the model output. Completion of the research objectives are dependent on these answers.

DYNAMIC MATHEMATICAL MODEL

The purpose of the dynamic mathematical model is to answer the questions posed in the Experimental Approach section of this report. The model will be used to validate the technical approach through analysis of the 1018 and 4340 steel fatigue test results. Analysis of the 4340 steel results will explain, through the model, the steady increase in damping that cannot be represented by dislocation phenomena.

Beam Models

The two dynamic mathematical models developed to analyze damping are based on the Euler-Bernoulli beam equation (Ref 72). These models are viscously damped with the damping based on a dislocation damping expression, including both strain/amplitude-dependent and frequency-dependent damping. In addition, the fatigue specimen model simulates crack growth with a torsional spring, $k_c(a)$, that is a function of crack length, a.

Figures 24 and 25 illustrate models of the four-point beam fatigue and symmetric cantilever beam damping specimens, respectively. In both figures, m is the mass of the beam per unit length, E is Young's modulus, h is the beam height, b is the beam thickness, l is the beam length, and x and z are the beam coordinates. In Figure 24, k_{ke} is the torsional

stiffness of the knife-edge support, $k_c(a)$ is the torsional stiffness of the fatigue crack (as described above), m_{ex} is the mass of the exciter, l_{ex} is the distance from the knife-edge support to the exciter, and $F_{ex}(x,t)$ is the time-dependent forcing function of the exciter. In Figure 25, $\ddot{w}_b(t)$ is the time-dependent acceleration of the base support for the symmetric cantilever beam.

Symmetric Cantilever Beam Damping Specimen. Appendix F derives the equation of motion and mass, stiffness, and damping terms for the symmetric cantilever beam model. Results from the internal damping tests are analyzed using Equation F-13 from Appendix F. This equation determines the damping ratio, at resonant frequency, from the beam acceleration and strain.

Four-Point Beam Fatigue Specimen. Appendix G derives the boundary conditions, equation of motion and mass, stiffness, and damping terms for the four-point beam fatigue model. Damping data calculations for the fatigue tests are programmed into the test control computer. These calculations are based upon Equations F-13 and G-8 in the appendixes.

The following section develops an expression for the frequency-dependent decrement that must be determined to isolate the fatigue-induced damping.

Frequency-Dependent Decrement

A simple expression for frequency-dependent decrement, Δ_I, is provided by Zener (Ref 1, 73) for a beam vibrating in simple harmonic flexure at a frequency ω. According to the Zener thermoelastic theory, the frequency-dependent decrement for a beam is:

$$\Delta_I = \frac{2\pi\alpha^2 ET}{c} \frac{\omega\tau}{1 + \omega^2\tau^2} \tag{40}$$

where τ, the relaxation time for heat flow across a rectangular beam, is given by:

$$\tau = \frac{h^2 c}{\pi^2 k}$$

and α is the linear expansion coefficient, T is absolute temperature, c is the specific heat per unit volume, and k is the thermal conductivity. The decrement given by Equation 40 is maximum at a frequency $\omega = 1/\tau$ and falls off gradually to zero for very high and very low frequencies. Based on data presented in Table 4 (Ref 74), Figure 26 reflects the relaxation damping decrement of a beam modeled by Equation 40. The curve of Figure 26 describes a single relaxation mechanism. There are a number of such mechanisms, each with its own relaxation time, τ. Through linearity, these mechanisms can be superimposed to provide the total damping decrement (Ref 71).

Comparison of Fatigue Test and Mathematical Model

In summary, the steps used to compute the estimated internal damping for a four-point beam model undergoing fatigue crack growth are presented in Table 5. In applying these steps to 1018 steel, the following assumptions were made concerning material constants (refer to Table 6 for a listing of material-dependent constants): (1) use data previously collected to estimate constants, (2) if immediate data are unavailable, use data from literature, and (3) if literature data are unavailable, estimate from similar materials. Refer to Appendixes C and D for an application of the steps presented in Table 5.

True stress-strain for 1018 steel is modeled by Equation 34 (Figure 27) with $k_p = 84.2 \times 10^3$ psi and n = 0.110. Figure 28 is a plot of the output from a computer model depicting a 1018 steel beam subjected to fatigue loading. The model, outlined in Appendix C with data from Table 6, matches the damping characteristics of the fatigue specimen as the crack grows. The sharp increase in damping, demonstrated by the specimen for a large plastic zone, is also exhibited in the computer generated model.

Figure 29 is a plot of the results of a computer model depicting a 4340 steel beam subjected to fatigue loading. Data for the computer are shown in Table 6. This plot is compared with Figure 16. The model has

a nonzero value for the constant c_{ck}. This damping effect allows the model to accurately reflect the damping conditions of the steel specimen. Differences are observed at 12,000 and 23,000 cycles where sharp damping peaks exist in the beam specimen output. An initial impression of these peaks is that they are due to external causes, as they appear in all the 4340 steel specimens at consistent frequencies.

The mathematical model has many simplifications. The plastic zone is treated as a square area, where each side is twice the plastic zone radius in length. This is a simple treatment with room for refinement. Strain at the crack tip, during damping data collection (Equation 13), is assumed to be a function of the reduced cross section at the crack,

$$\varepsilon_0 = \frac{6M_c}{Et(h - a)^2} \tag{41}$$

This assumption discounts a large stress concentration that occurs at the crack tip for elastic behavior (Ref 60). The disregard for stress concentration is deemed acceptable in this instance because the plastic yielding that occurs within the plastic zone greatly mitigates stress concentration. To completely ignore the stress concentration is not realistic, but justifiable for an initial modeling attempt. The ratio of maximum stress to nominal stress is less than the elastic stress concentration factor, and can be interpreted as an elastic-plastic stress concentration factor, which must be determined experimentally.

CONCLUSIONS

Conclusions about the main objective, that is, the crack growth/internal damping relationship, and conclusions about the mathematical model used in the analysis of the damping and fatigue test results are presented.

Damping and Fatigue Tests

The major objective to develop a relationship between crack propagation and internal damping was accomplished. Fatigue tests were conducted for validation of the relationship. Conclusions based on the test results are presented and the reliability of the damping measurements made during the fatigue tests is addressed in the following.

Damping Mechanisms. Observations of fatigue specimens isolated two distinct damping mechanisms. The first was classified as a dislocation damping mechanism and was observable in 1018 steel specimens only after extensive fatigue crack growth under constant load produced a large plastic region. Dislocation damping is well documented (Ref 33 through 43), and the results of the 1018 steel beam fatigue tests reflect that mechanism. Observation of this mechanism was an objective of the 4340 steel beam fatigue tests. However, for the 4340 specimens, fatigued under a constant stress intensity factor, the plastic zone radius was too small (on the order of 0.003 inch) to furnish a measurable damping increase. Indeed, any damping increase generated by a plastic zone was obscured by a second damping mechanism that was observable within a few cycles of crack initiation. The damping ratio produced by this mechanism is directly proportional to the maximum beam rotation at the crack location. The second damping mechanism was classified as viscous damping expressed by Equation 39 and was attributed to the rubbing together of the two crack surfaces as the specimen vibrated.

No explanation is immediately available for the cause of the sharp peaks appearing in the damping plots of the 4340 steel beam specimens. Nevertheless, the occurrence of the peaks at consistent frequencies suggests the source is external to the specimens. This conclusion is based on the knowledge that each specimen had a different initial resonant frequency. Knife-edge stiffness is calculated from resonant frequency, thus all the 4340 beam specimens had different knife-edge stiffnesses. The crack length and general beam mode shapes are thus different for each beam at the frequencies where the damping peak occurs.

Test Procedures. Results from the symmetric beam damping tests indicate that the strain gage lead wire contribution to damping is stable and produces repeatable results that may be treated as an external damping source. For this reason, lead wire damping is assumed to be part of the damping datum established for each fatigue test.

Mathematical Model

The mathematical computer model developed to express damping in materials subject to crack growth is a combination of analytical and empirical relations. The empirical relations are primarily associated with the viscous damping observed in the 4340 steel beam specimens. Deduced as friction between the two crack surfaces, this viscous damping is repeatable in 4340 steel beam specimens. Another empirical relation, expressed in Equation 30, is assumed to exist between the torsional stiffness at the crack and the crack length. This relationship closely resembles a moment of inertia expression and gave consistent results for all four 4340 beam specimens.

The analytical expressions used to model dislocation damping and plastic strain, that is, Equations 13 and 21, accurately modeled large damping changes in the 1018 steel specimens. This conclusion reflects the difficulty in accurately measuring small changes in damping caused by dislocation damping, while acknowledging the model's credibility for simulating large damping changes which occurred after many thousands of fatigue cycles.

RECOMMENDATIONS

Additional testing is required to confirm the mathematical model and the viscous damping observed in the 4340 beam specimen. Other materials must be fatigued using both constant load and stress intensity factor. Greater accuracy is required in the measurement of damping.

Damping ratios in the 4340 steel beam specimens could be measured to 50 x 10^{-6}. Damping changes on the order of 3 x 10^{-6} are suggested by the mathematical model for simulating dislocation multiplication in the plastic zone.

The mathematical model should be refined to better represent the plastic zone in a beam. The plastic zone shape, as handled by the model, is shown in Figure 30. Using a square shape for the plastic zone is a gross approximation, particularly for the 1018 steel specimens. Under fatigue loading, the 1018 steel specimens displayed plastic hinges at the notch location. Figure 31 illustrates a plastic hinge, as observed in the 1018 steel specimens. The simple simulation used in the mathematical model does not accurately depict the plastic material opposite the cracked surface. A refinement that accounts for the plastic hinge effect would directly influence the calculated damping with the plastic zone and improve the model's accuracy. Along with shape is the question of strain within the plastic zone during damping data collection. Dislocation damping is a function of strain, and when the beam is vibrated to collect damping data, strain within the plastic zone is affected by both a reduced cross section and plastic flow. The model ignores stress concentrations at the crack tip on the basis that the concentration is greatly diminished by the presence of a plastic region (Ref 11). Further work is required in this area to ascertain what effect each phenomenon has upon the strain within the plastic zone.

Experimental data should also be collected to determine the elastic-plastic strain distribution around the notch tip. Equation 41 could then be refined to include an elastic-plastic stress concentration factor, reflecting plastic flow at the tip and accurately estimating the plastic strain in the plastic zone.

Damping has potential as a crack growth monitoring tool where external damping can be tightly controlled. Isolation from external effects is possible in a laboratory where conditions are rigidly controlled. Outside a laboratory, changes in external damping will often overwhelm smaller crack growth induced damping. A technique is needed to localize or "zoom-in" on crack-induced damping. Examination of

localized displacements (on the order of 0.5 microns) is possible with the Sharpe technique (Ref 75). This technique also has the advantage of eliminating strain gages and their affiliated wires and damping affects.

REFERENCES

1. C. Zener. Elasticity and anelasticity of metals. University of Chicago Press, Chicago, IL, 1948.

2. N.S. Nowick. Progress in metal physics. Pergamon Press, London and New York, vol 4, 1953, p 1.

3. W.P. Mason. "Physical acoustics and the properties of solids," The Journal of the Acoustical Society of America, vol 28, no. 6, 1956, p 1204.

4. T.A. Read. "Internal friction of single crystals of copper and zinc," Trans AIME, vol 143, 1941, p 30.

5. D.O. Thompson and D.K. Holmes. "Effects of neutron irradiation upon Young's modulus and internal friction of copper single crystals," Journal of Applied Physics, vol 27, 1956, p 713.

6. R.S. Barnes, N.H. Hancock, and E.C.H. Silk. Philosophical Magazine, vol 3, 1958, pp 519; ibid., 527.

7. K. Lücke. "Ultrasonic attenuation caused by thermoelastic heat flow," Journal of Applied Physics, vol 27, 1956, p 1433.

8. P.D. Southgate. "Temperature dependence of internal friction in germanium," Physics Review, vol 110, 1958, p 855.

9. O Föppl. "The practical importance of the damping capacity of metals, especially steels," Journal of the Iron and Steel Institute, vol 134, 1936, p 393.

10. R.F. Hanstock and A. Murray. "Damping capacity and the fatigue of metals," in Proceedings of the Royal Physics Society of London, England, vol 59, 1947, p 275.

11. T. Yokobori. Strength, fracture and fatigue of materials. P. Noordhoff, The Netherlands, 1965, pp 218-219.

12. J.G. Blauel. "Experimental techniques for the determination of the initiation of failure," Advances in Elasto-Plastic Fracture Mechanics, Applied Science Publishers, London, England, 1979, p 66.

13. M.H. Raymond and L.F. Coffin. "Geometrical effects in strain cycled aluminum," Transactions of the American Society of Mechanical Engineers, Journal of Basic Engineering, vol 85, 1963, p 548.

14. A.H. Cottrell and D. Hull. Proceedings of the Royal Society, vol A242, 1957, p 211.

15. A.J. Kennedy. Processes of creep and fatigue in metals. Edinburgh, Scotland, Oliver and Boyd, 1962.

16. F.R. Shanley. Colloquim on fatigue. Berlin, Germany, Springer-Verlag, 1955, p 251.

17. P.T. Heald and B.A. Bilby. "Fracture toughness of high-strength materials: theory and practice," ISI Publication No. 120, Iron and Steel Institute, 1970, p 63.

18. J. Weertman. International conference on fracture, Sendai, Japan. Vol 1, 1965, p 154.

19. B.A. Bilby, A.H. Cottrell, and K.H. Swinden. "Spread of plastic yield from notch," in Proceedings of the Royal Society, vol A272, 1963, p 304.

20. L.F. Coffin. "Design aspects of high-temperature fatigue with particular reference to thermal stresses," Transactions of the American Society of Mechanical Engineers, vol 78, 1956, p 527; Internal Stresses and Fatigue of Metals, Elsevier, NY, 1959, p 363.

21. National Aeronautics and Space Administration. NASA Technical Note D-1574: Fatigue behavior of materials under strain cycling in low and intermediate life range, by R.W. Smith, M.H. Hirschberg, and S.S. Manson. Washington, DC, 1963.

22. S.S. Manson. "Thermal stresses in design, Part 19 - Cyclic life of ductile materials," Machine Design, vol 32, 1960, p 139.

23. S.S. Manson. Machine Design, vol 33, 1960, p 165.

24. S.S. Manson. Transactions of the American Society of Mechanical Engineers, Journal of Basic Engineering, vol 84, 1962, p 537.

25. S.S. Manson. "Fatigue: a complex subject - some simple approximations," William M. Murray Lecture, Experimental Mechanics, vol 5, 1965, p 193.

26. J. Morrow. "Internal friction, damping and cyclic plasticity," American Society for Testing Materials, Special Technical Publication No. 378, 1965, p 45.

27. M. Kawamoto and T. Tanaka. Proceedings of the 10th Japanese National Congress of applied mechanics, 1960, p 151.

28. V.M. Radhakrishnan. "Inelastic response and energy criterion for fatigue failure," Engineering Mechanics, vol 17, 1977, p 219.

29. P.C. Paris and F. Erdogan. "Critical analysis of crack propagation laws," Transactions of the American Society of Mechanical Engineers, Journal of Basic Engineering, vol 85, 1963, p 528.

30. A.J. McEvily, R.C. Boettner, and A.P. Bond. "On cold work and fatigue-crack propagation in α-brass," Journal of the Institute on Metals, vol 93, 1965, p 481.

31. Royal Aircraft Establishment. Technical Report No. 64025: Min. of Aviation, by D.P. Rooke, N.J.F. Gunn, J.T. Ballet, and F.J. Bradshaw. Great Britain, 1964.

32. Y. Izumi and M.E. Fine. "Role of plastic work in fatigue crack propagation in metals," Engineering Fracture Mechanics, vol 11, 1979, p 791.

33. J.A. Charles, F.J. Appl, and J.E. Francis. "Thermographic determination of fatigue damage," Journal of Engineering Materials and Technology, vol 100, Apr 1978, p 200.

34. A. Granato and K. Lücke. "Theory of mechanical damping due to dislocations," Journal of Applied Physics, vol 27, no. 6, 1956, pp 583-593.

35. A. Granato and K. Lücke. "Application of dislocation theory to internal friction phenomena at high frequencies," Journal of Applied Physics, vol 27, no. 7, 1956, p 790.

36. C.L. Bauer and R.B. Gordon. "Dislocation damping effects in rock salt," Journal of Applied Physics, vol 31, no. 6, 1960, p 946.

37. J.C. Swartz and J. Weertman. "Modification of the Koehler-Granato-Lücke dislocation damping theory," Journal of Applied Physics, vol 32, no. 10, 1961, p 1864.

38. D.H. Rodgers. "An extension of a theory of mechanical damping due to dislocations," Journal of Applied Physics, vol 33, no. 3, 1962, pp 781-792.

39. D. Gelli. "A qualitative model for amplitude dependent dislocation damping," Journal of Applied Physics, vol 33, no. 4, 1962, p 1549.

40. R.R. Hasiguti, N. Igata, and K. Tanaka. "Amplitude dependent internal friction of an aluminum single crystal," letter to the editor, Acta Metallurgica, vol 13, 1965, pp 1083-1084.

41. B. McKavangh and F.D. Stacey. "Mechanical hysteresis in rocks at low strain amplitudes and seismic frequencies," Physics of the Earth and Planetary Interiors, vol 8, no. 1, 1974, pp 246-250.

42. D.D. Jackson and D.L. Anderson. "Physical mechanisms of seismic-wave attenuation," Reviews of Geophysics and Space Physics, vol 8, no. 1, Feb 1970, pp 1-63.

43. Y. Shimanuki and H. Doi. "Influence of a strain amplitude distribution in a crystal on the hysteretic breakaway loss," Journal of Applied Physics, vol 41, no. 7, 1970, pp 3003-3004.

44. F. Povolo. "On the Granato-Lücke expression for the amplitude dependent damping," Scripta Metallurgica, vol 9, 1975, pp 865-872.

45. C.F. Burdett and T.J. Queen. "The role of dislocations in damping," Review 143 (Part II), Metallurgical Reviews, Institute of Metals, Jun 1970, pp 65-67.

46. W.F. Brown and J.E. Srawley. "Plane strain crack testing of high strength metallic materials," American Society for Testing and Materials, S.T.P. 410, 1966.

47. C.E. Feltner and J.D. Morrow. "Microplastic strain hysteresis energy as a criterion for fatigue fracture," Transactions of the American Society of Mechanical Engineers, Journal of Basic Engineering, vol 83, 1961, p 20.

48. H.E. Davis, G.E. Troxell, and C.T. Wiskocil. The testing and inspection of engineering materials. New York, NY, Third edition, McGraw-Hill Book Co., 1964, pp 37-38.

49. G.R. Halford and J.D. Morrow. "Low-cycle fatigue in torsion," in Proceedings of the American Society for Testing and Materials, vol 62, 1962, p 695-702.

50. J.F. Tavernelli and L.F. Coffin. "A compilation and interpretation of cyclic strain fatigue tests on metals," Transactions, American Society of Metals, vol 51, 1959, p 438.

51. L.M. Clarebrough, M.E. Hargreaves, A.K. Head, and G.K. West. "Energy stored during fatigue of copper," Journal of Metals, vol 7, 1955.

52. A.H. Cottrell. Dislocations and plastic flow in crystals. London, England, Oxford University Press, 1953.

53. G.T. Hahn. "A model for yielding with special reference to the yield-point phenomena of iron and related b.c.c. metals," Acta Metallurgica, vol 10, 1962, p 727.

54. Y. Bergström. "A dislocation model for the stress-strain behaviour of polycrystalline α-Fe with special emphasis on the variation of the densities of mobile and immobile dislocations," Materials Science and Engineering, vol 5, 1970, p 193.

55. H.M. Otte and J.J. Hren. "The observation of crystalline imperfections and their role in plastic deformation," Experimental Mechanics, vol 6, 1966, p 177.

56. R. Vetter and A. van den Beukel. "Dislocation production in cold worked copper," Scripta Metallurgica, vol 11, 1977, p 143.

57. K. Ishikawa. "On distribution of the plastic strain around the crack tip at the onset of ductile fracture," Technical Note, International Journal of Fracture, vol 11, 1975, p 974.

58. F.W. Young, Jr. "On the yield stress of copper crystals," Journal of Applied Physics, vol 33, no. 2, 1962, p 964.

59. Del Research Corporation. The stress analysis of cracks handbook, by H. Tada, P.C. Paris, and G.R. Irwin. Hellertown, PA, 1973, pp 2.13-2.14.

60. N.E. Frost, K.J. Marsh, and L.P. Pook. Metal fatigue. Oxford, England, Clarendon Press, 1974, pp 234-235.

61. W.A. Wood. "Some basic studies of fatigue in metals," in Fracture. New York, NY, John Wiley and Sons, 1959.

62. H.L. Ewalds and R.J.H. Wanhill. Fracture mechanics. Baltimore, MD, Edward Arnold Ltd, 1986.

63. C. Atkinson and M.F. Kanninen. "A simple representation of crack plasticity: the inclined strip yield superdislocation model," International Journal of Fracture, vol 13, no. 2, Apr 1977.

64. H. Miyamoto, H. Okamura, K. Kageyama, and H. Marita. "Elastic-plastic analysis of a crack by using continuously distributed dislocations," Numerical Methods in Fracture Mechanics. West Cross, Swansea, Pineridge Press Limited, 1980.

65. B. Budiansky and R.J. O'Connell. "Elastic moduli of a cracked solid," International Journal of Solids and Structures, vol 12, no. 2, Feb 1976, pp 81-97.

66. T. Baumeister, E.A. Avallone, and T. Baumeister, III. Marks' standard handbook for mechanical engineers. New York, NY, 8th ed., McGraw-Hill, 1978, p 5-4; ibid, p 6-11.

67. G.E.P. Box, W.G. Hunter, and J.S. Hunter. Statistics for experimenters. New York, NY, John Wiley and Sons, 1978, pp 453-461.

68. M.S. Caceci and W.P. Cacheris. "Fitting curves to data," BYTE, May 1984, pp 340-361.

69. L.H. Van Vlack. Elements of material science & engineering. Reading, MA, Fourth edition, Addision-Wesley Publishing Company, 1980, p 193.

70. American Society for Testing and Materials. "Standard test method for plane-strain fracture toughness of metallic materials," Designation: E399-83, Annual Book of ASTM Standards, vol 3.01, 1985, pp 547-582.

71. A.M. Freudenthal. The inelastic behavior of engineering materials and structures. New York, NY, John Wiley and Sons, 1950, pp 336-339.

72. W.T. Thomson. Theory of vibration with applications. Englewood Cliffs, NJ, Prentice-Hall, Inc., 1972, p 310.

73. Naval Civil Engineering Laboratory. Memorandum to files on internal damping and crack propagation in steel: Constitutive relation equations, by R.L. Jones. Port Hueneme, CA, Nov 1984.

74. National Aeronautics and Space Administration. NASA Technical Note D-1467: On scaling laws for material damping, by S.H. Crandall. Washington, DC, Dec 1962.

75. W.N. Sharpe, Jr. "Interferometric systems for measuring crack-opening displacements of small cracks," Joint BSSM/SEM Conference, London, England, Aug 1987.

76. W.C. Hurty and M.F. Rubenstein. Dynamics of structures. Englewood Cliffs, NJ, Prentice-Hall, Inc., 1964, pp 278-289.

77. M.F. Spotts. Design of machine elements. Englewood Cliffs, NJ, 4th ed., Prentice-Hall, Inc., 1971, pp 10 and 16.

78. C.M. Harris and C.E. Crede. Shock and vibration handbook. New York, NY, 2nd edition, McGraw-Hill Book Company, 1976.

79. T.G. Chondros and A.D. Dimarogonas. "Identification of cracks in welded joints of complex structures," Journal of Sound and Vibration, vol 69, 1980, pp 531-538.

LIST OF SYMBOLS

α	Linear expansion coefficient and constant
α_c	Material-dependent, crack growth rate constant
$\delta(x-\xi)$	Unit impulse or delta function at the location ξ
Δ	Total decrement, $\Delta_H + \Delta_I$
$\bar{\Delta}$	Average specific damping capacity
$\bar{\Delta}^c$	Average corrected total decrement, $\bar{\Delta}_H^c + \bar{\Delta}_I^c$
Δ_{ext}	External damping
Δ_H	Amplitude-dependent decrement
Δ_H^c	Povolo's corrected amplitude-dependent decrement
$\bar{\Delta}_H$	Average amplitude-dependent decrement
$\bar{\Delta}_H^c$	Average Povolo's corrected amplitude-dependent decrement
Δ_I	Frequency-dependent decrement
$\bar{\Delta}_I^c$	Average corrected frequency-dependent decrement
Δ_{Ii}	Frequency-dependent decrement for the i^{th} mode
ΔK	Difference between the maximum and minimum values of the stress intensity factor during fatigue cycle, $K_{max} - K_{min}$
Δ_p	Internal damping due to plastic strain
Δ_0	$4(1-\nu)/\pi^2$
Δw	Energy dissipated per cycle in a volume element
Δ^0	Damping decrement for beam specimen with no sets of wires removed
Δ^1	Damping decrement with one set of strain gage wires removed
Δ^2	Damping decrement with two sets of strain gage wires removed
Δ^3	Damping decrement with three sets of wires removed
Δ^4	Damping decrement with all strain gage wires removed

Δ^4_i	Damping decrement of i^{th} mode with all wires removed
Δa_j	Crack growth during j^{th} fatigue cycle
ε'	Cottrell misfit factor
ε_a	Fatigue cycle elastic strain at maximum load
ε_{min}	Fatigue cycle strain at minimum load
ε_p	Plastic strain
ε_{pi}	Plastic strain per cycle
ε_{pj}	Plastic strain for j^{th} fatigue cycle
ε_{pu}	Static plastic strain fracture value at 1/2 cycle
ε_u	Ultimate strain for static fracture
ε_p	Critical strain above which plastic strain occurs
$\bar{\varepsilon}_p$	Average value of the cyclic plastic-strain range
ε_t	$\ln(A_o/A_i)$, true strain
$\varepsilon(x_o)$	Strain in beam at location x_o
ε_0	Cyclic strain amplitude
ζ_i	Viscous damping ratio for the i^{th} mode, $\zeta_i = C_i/C_{ci}$
θ	Phase angle, $\theta \rightarrow \pi/2$ as $\omega \rightarrow \omega_i$
θ^c_H	Δ^c_H/Λ
κ_i	Eigenvalue of i^{th} mode of vibrating beam
Λ	Total length of movable dislocation line per unit volume (dislocation density)
Λ_e	Dislocation density in elastic region
Λ_i	Immobile dislocation density
Λ_p	Dislocation density in plastic zone
ν	Poisson's ratio
ξ	Location of unit impulse function
ρ	Density

σ	Nominal outer fiber stress
σ_a	Maximum cyclic stress
σ_{io}	Stress constant
σ_t	P/A_i, true strain
σ_u	Ultimate stress for static fracture
$\sigma(0)$	Stress at zero plastic strain
τ	Relaxation time for heat flow across a beam, $\tau = h^2c/\pi^2k$
Φ	Orientation factor (0.5 and 0.32 for b.c.c. and f.c.c., respectively)
$\phi_i(x)$	Characteristic shape function associated with i^{th} mode of vibrating beam
$\phi_i'(x)$	Derivative of i^{th} characteristic shape function with respect to x, describes slope of beam
$\phi_i''(x)$	Second derivative of i^{th} characteristic shape function with respect to x, describes curvature of beam
χ	Strain independent probability for the remobilization of immobile dislocations
ψ	Strength parameter
ω	Frequency of forcing function
ω_i	Resonant frequency of the i^{th} mode, $\omega_i = (K_i/M_i)^{1/2}$
ω_{n1}	Fundamental beam frequency
Ω	Orientation factor
a	Crack length
a_0	Initial crack length
a_{j-1}	Crack length after j^{th}-1 fatigue cycle
a_j	Crack length after j^{th} fatigue cycle
A	Dimensionless constant and for the G-L Theory $A = \pi\rho b^2$
A_i	Instantaneous cross-sectional area under a given load
A_o	Original cross-sectional area before any load is applied

A'	$1/\Phi bKf$
A_2	Material constant
b	Burger's vector and beam thickness
B	Material temperature-dependent term
B_i	Amplitude scaling factor associated with i^{th} mode of vibrating beam
b_c	Material constant relating crack length to beam torsional stiffness at crack
C	Material constant; for the G-L Theory $C = 2Gb^2/\pi(1-\nu)$; and for the Manson-Coffin law, the ductility exponent
C_1	$\Omega\Delta_0 L_N{}^3/\pi L_c$
C_2	$K\varepsilon' a/L_c$
C_3	$\Omega\Delta_0 L_c{}^4 B\omega/\pi^2 C$
C_i	Generalized damping of i^{th} mode
C_{ci}	Generalized critical damping of i^{th} mode
c	Specific heat per unit volume
c_{ck}	Crack damping coefficient
c_{eq}	Equivalent viscous damping
c(x)	Beam damping coefficient
d	Dislocation cell size, $d = K/\Lambda^{1/2}$
dw	Plastic energy absorbed per cycle
D%	Fatigue life damage assessment in percent, 100% (N_c/N_{fp})
E	Young's modulus of beam material
E_1	Exponential integral function of first order
E_n	Exponential integral function
f	Constant of order 1
F(a/b)	$1.122 - 1.4(a/b) + 7.33(a/b)^2 - 13.08(a/b)^3 + 14.0(a/b)^4$
f_{ex}	Amplitude scaling factor of exciter forcing function

$F_{ex}(x,t)$	Exciter forcing function
G	Shear modulus
h	Height of beam
i	Mode number
I	Moment of inertia of beam, $I = th^3/12$
j	Fatigue cycle number
k	Thermal conductivity; for Manson-Coffin law, 1/C
K	Orientation and anisotropy parameter and material constant, K = 20 for Fe
K_{ave}	Average stress intensity factor over fatigue test
$k_c(a)$	Torsional spring stiffness of crack
K_i	Generalized stiffness of i^{th} mode
K_I	Stress intensity factor
K_{Ic}	Critical stress intensity factor
k_{ke}	Torsional spring stiffness of knife-edge support
K_{max}	Maximum value of stress intensity factor during fatigue cycle
K_{min}	Minimum value of stress intensity factor during fatigue cycle
k_p	Strength coefficient
l	Length of beam
L	Mobile dislocation density
l_a	Fatigue specimen distance from knife edge to loading point
L_c	Impurities loop length
L_e	Effective length of dislocation loop
l_{ex}	Distance from knife-edge support to exciter
LF	Fraction of fatigue life expended
L_N	Network loop length
m	Hysteresis energy exponent

M	Moment on beam section
M_c	Moment due to crack
M_i	Generalized mass of i^{th} mode
M_{ke}	Moment due to knife-edge support
$m(x)$	Mass per unit length of beam
$M(x)$	Moment along beam, $M(x) = EI\ B_i\ \phi_i''(x)$
n	Strain hardening exponent
N	Fatigue cycle number
N_c	Number of fatigue cycles completed
N_f	Number of cycles to complete fracture
N_{fp}	Predicted number of cycles to complete fracture
N^*	Number of cycles in a stage of fatigue life
P	Fatigue or static load
q_i	Generalized coordinate of i^{th} mode
$\dot{q}_i$	First derivative of generalized coordinate with respect to time
$\ddot{q}_i$	Second derivative of generalized coordinate with respect to time
R_i	Characteristic shape function ratio of nonzero constants
r_p	Plastic zone radius
s	Dislocation mean free path
SD	Standard deviation
t	Time variable or thickness of beam
T	Absolute temperature
TF	Transfer function amplitude ratio at ω_{n1}
U	Integrated plastic work expended in the plastic zone or peak potential energy per cycle
U_i	Rate of immobilization of mobile dislocations or peak potential energy per cycle of i^{th} mode
V	Specimen volume

V_e	Elastic region volume
V_p	Plastic zone volume
W	Amplitude scaling factor for beam support displacement
$w_b(t)$	Time-dependent displacement of beam support
$\ddot{w}_b(t)$	Time-dependent acceleration of beam support
W_d	Energy dissipated per cycle
W_{di}	Energy dissipated per cycle of i^{th} mode
W_f	Total hysteresis energy to cyclic failure
W_u	Total hysteresis energy to static failure
$w(x,t)$	Time- and location-dependent displacement of beam
$\dot{w}(x,t)$	Time- and location-dependent velocity of beam
$\ddot{w}(x,t)$	Time- and location-dependent acceleration of beam
$w'(x,t)$	Derivative of $w(x,t)$ with respect to x
$w''(x,t)$	Second derivative of $w(x,t)$ with respect to x
$w'''(x,t)$	Third derivative of $w(x,t)$ with respect to x
w	Peak potential energy per cycle in a volume element
x	Coordinate of longitudinal axis of beam
x_o	Known location on beam
$\ddot{z}_i(t)$	Forcing function for generalized coordinate equation of motion
$z_i(t)$	Displacement function for i^{th} generalized coordinate equation of motion
Z_i	Amplitude scaling factor for displacement function of i^{th} mode

Table 1. Characteristics of SAE 4340 Steel

Item	Description
Material	SAE 4340 Steel
Composition	C - 0.40, Mn - 0.81, P - 0.018, S - 0.019, Si - 0.25, Ni - 1.73, Cr - 0.87, Mo - 0.24
Heat Treatment	The fatigue, tension, compact tension and damping specimens were austenitized at 1525°F in a neutral salt bath, quenched in still oil and room temperature and tempered at 1100°F for 2 hours.
Engineering Tensile Properties	Average tensile properties for three specimens are given below: Engineering 0.2% offset, yield strength (psi) - 141,300 Engineering ultimate strength (psi) - 150,200 Hardness Rockwell C - 37

Table 2. Summary of Static Test Results

Parameters	Units	Values
s_u	psi	225,000
ε_{pu}	in./in.	0.748
W_u	lb-in./in.^{3} (Equation 37)	153,800
W_u	lb-in./in.^{3} (Equation 38)	154,000

Table 3. Fatigue Specimens at Failure

Specimen	Load at Failure, P (lb)	Crack Length, a (in.)	Estimated Outer Fiber Stress, σ (ksi)	Estimated Stress Intensity Factor, K_I (ksi-in.$^{1/2}$)
A	1240	0.277	50.1	80.3
B	690	0.393	14.4	71.2
C	260	0.413	11.1	78.6
D	345	0.402	11.5	90.1

Table 4. Values Used in Equation 40 to Obtain the Curve Shown in Figure 26 (Ref 74) for Steel

Parameters	Units	Values
α	strain/°F	6.7×10^{-6}
E	psi	29×10^{6}
c	psi/°F	245
k	lb/sec °F	6.5
h	in.	0.125
T	°R	530

Table 5. Computation of Internal Damping in Fatigue Model

Step	Drescription
1	Define material and crack growth constants
2	Repeat step 2 for fatigue cycle j = 1 to N
2.1	Using the crack growth constant, α_c, and crack length from the previous fatigue cycle, a_{j-1}, compute the crack length for the current fatigue cycle a_j (Equations 31 and G-10)
2.2	From known values of the static plastic strain fracture value, ε_{pu}, the final crack length, a_f, and the ductility exponent, C, compute the estimeted plastic strain, ε_{pj} in the current fatigue cycle (Equation 30)
2.3	Compute the fraction of fatigue life expended, LF (Equation 29)
2.4	Determine the plastic zone radius, r_{pj}, for the current fatigue cycle (Equation 11 or 12)
2.5	Calculate the crack torsional stiffness, k_{cj}, for the current fatigue cycle (Equation G-12)
2.6	With the knife-edge stiffness, k_{ke}, determine the eigenvalue, κ_1, eigenvector, $\phi_1(x)$, and resonant frequency, ω_1, of the fundamental mode of vibration (Equation G-4)
2.7	Determine amplitude scaling factor, B_{1j} (Equation F-8)
2.8	Calculate plastic zone dislocation density (Equation 21)
2.9	Compute the average amplitude-dependent damping, $\bar{\Delta}^c_{Hj}$, from the vibration strain level, ε_0 (Equation 13)
2.10	Determine the frequency-dependent damping, Δj (Equation F-16)
3	stop.

Table 6. Material-Dependent Constants for 1018 and 4340 Steel

Constant	Description	Units	1018	4340
A_i	Dislocation density to plastic strain coefficient	$disl/in.^2$	2.41×10^6	6.13×10^6
b_c	Crack length to beam torsional stiffness coefficient	lb/in.	124×10^3	124×10^3
C	Manson-Coffin ductility exponent		646×10^{-3}	690×10^{-3}
C_1	Internal damping coefficient		50×10^{-3}	50×10^{-3}
C_2	Internal damping coefficient	in./in.	150×10^{-6}	100×10^{-6}
c	Specific heat per unit volume	psi/°F	245	245
EI	Young's modulus x beam moment of inertia	$lb/in.^2$	300×10^3	300×10^3
k	Thermal conductivity		6.5	6.5
α	Expansion coefficient	in./in.°F	6.7×10^{-6}	6.7×10^{-6}
α_c	Crack growth rate coefficient	$in.^7/lb^4$ - cycle	16×10^{-24}	9.66×10^{-24}
ε_{pu}	Static plastic fracture value at 1/2 cycle	in./in.	550×10^{-3}	748×10^{-3}
A_0	Dislocation density for plastic strain equal to zero	$disl/in.^2$	1×10^8	1×10^8
σ_y	Yield stress	psi	62×10^3	144×10^3
χ	Strain independent probability for the remobilization of immobile dislocations		10.7	8.61

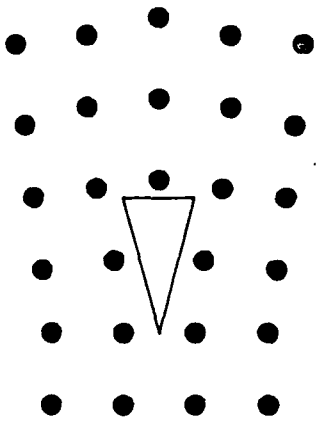

Figure 1. Edge dislocation.

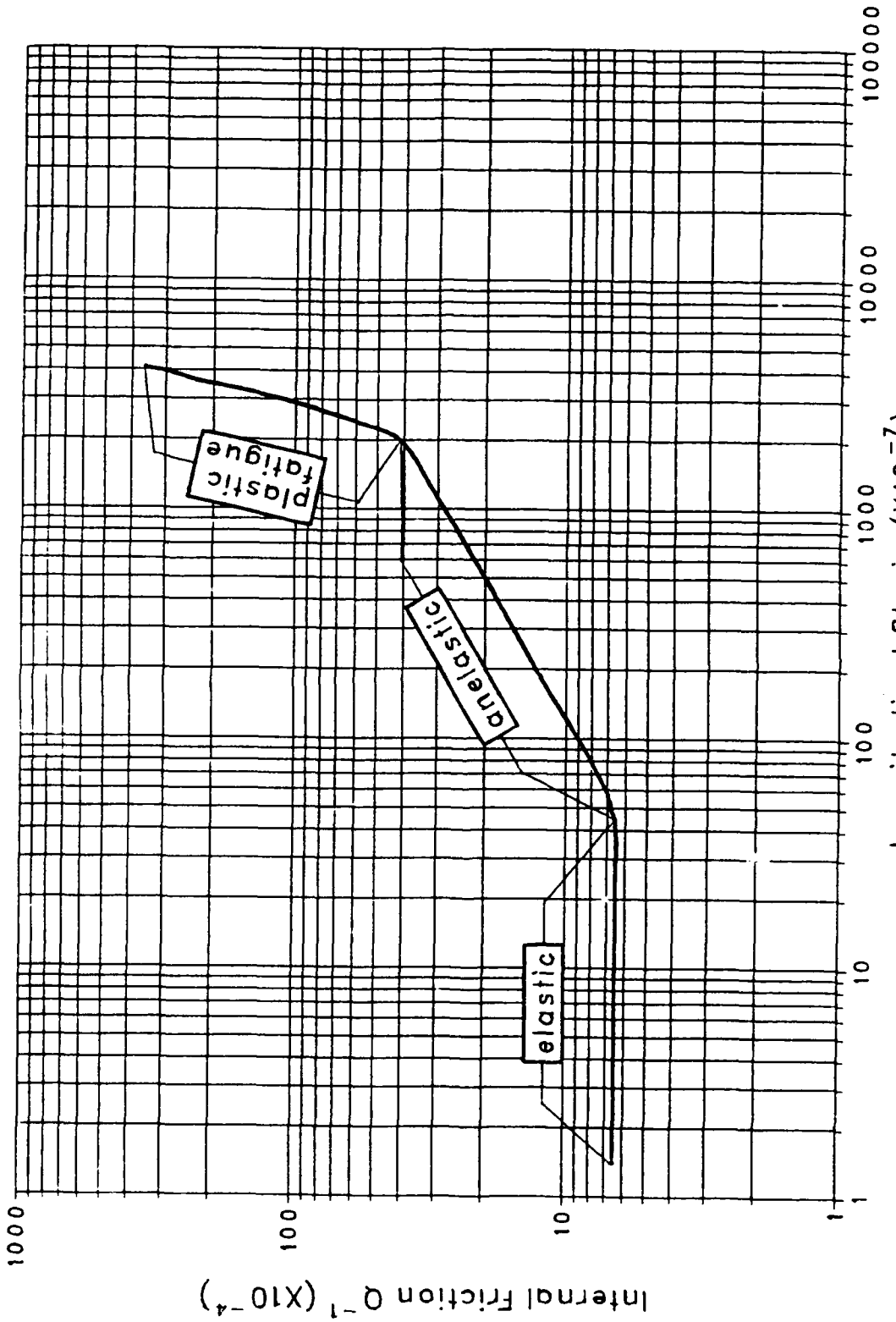

Figure 2. Internal friction of 99.999% pure aluminum (from Mason, Ref 3).

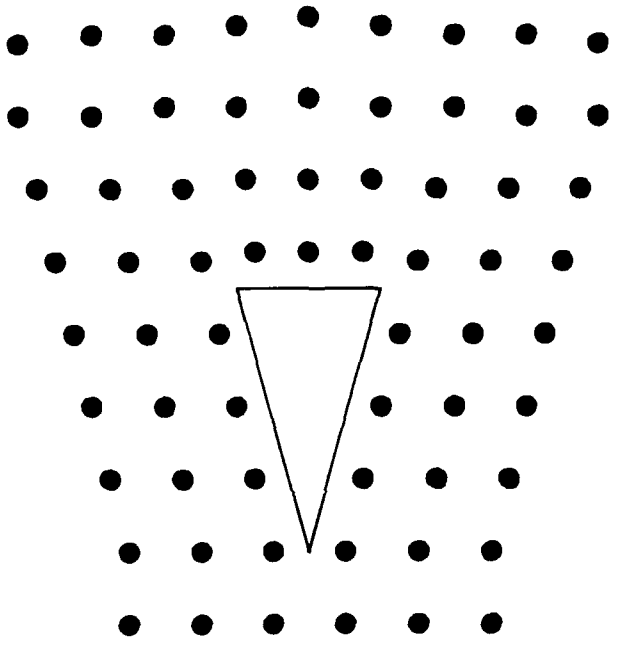

Figure 3. Formation of a microcrack by a combination of (three) dislocations (from Yokobori, Ref 11).

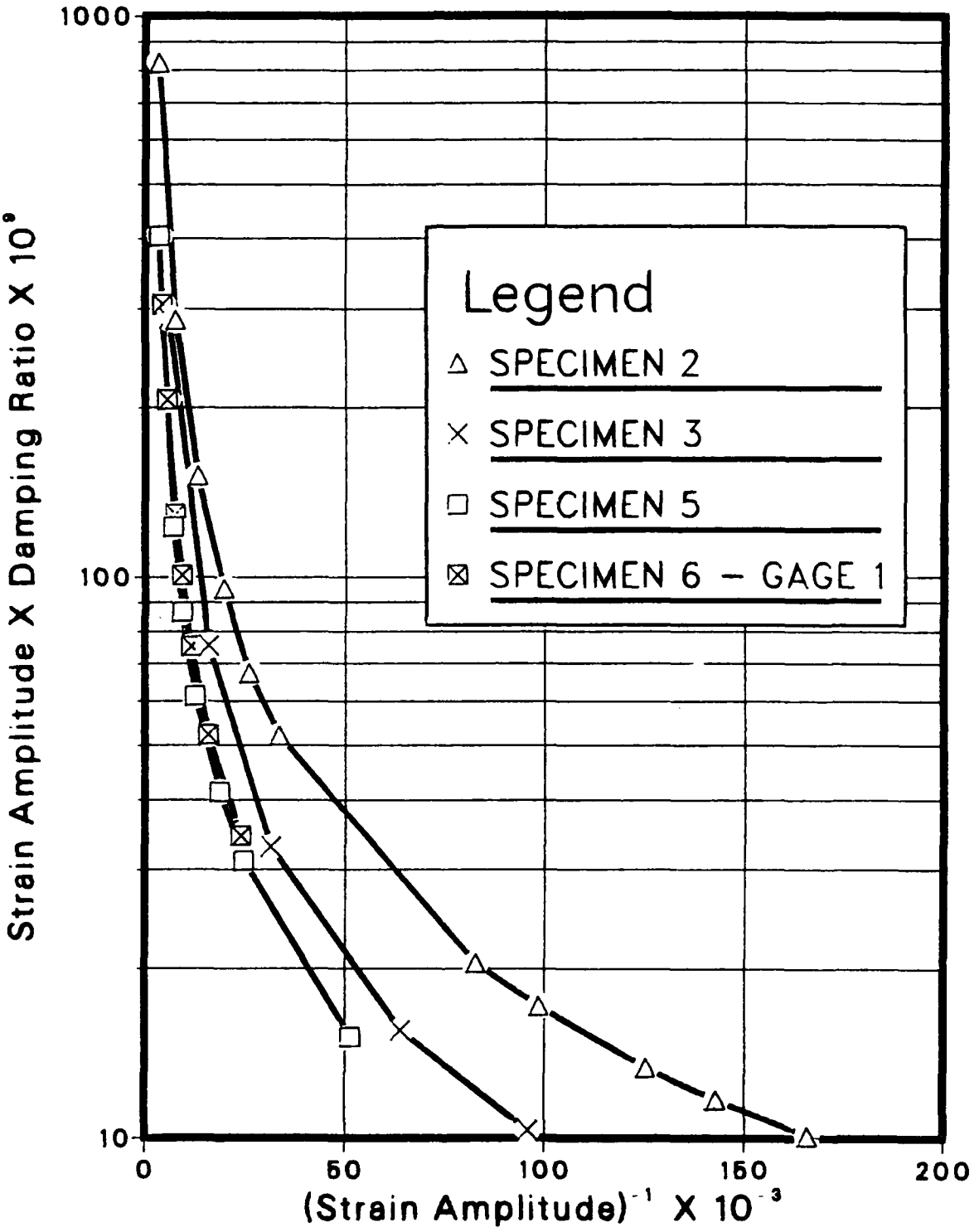

Figure 4. Granato-Lucke plot of a 1018 steel cantilever beam.

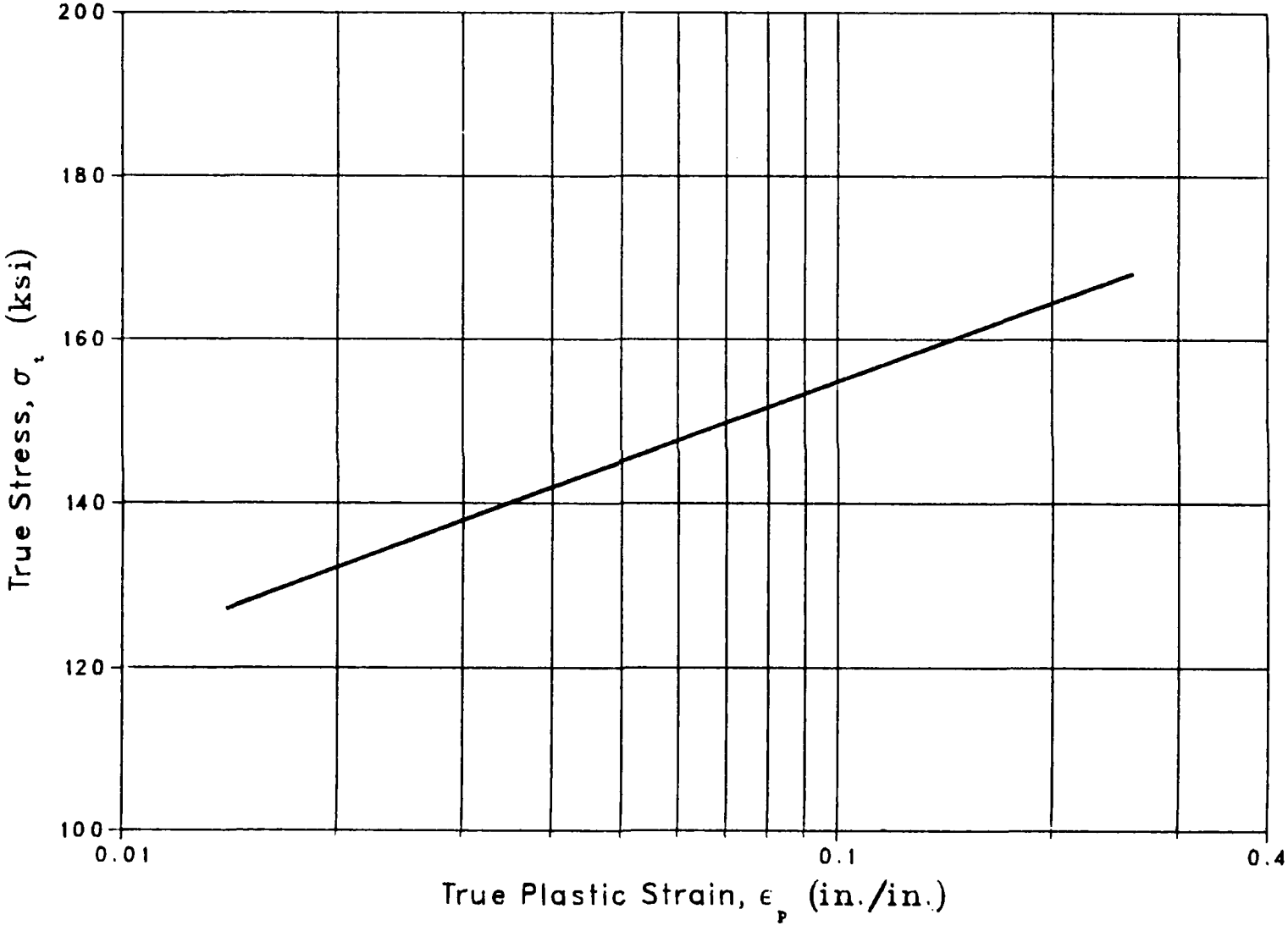

Figure 5. Logarithmic stress-plastic strain curve (from Feltner and Morrow, Ref 47).

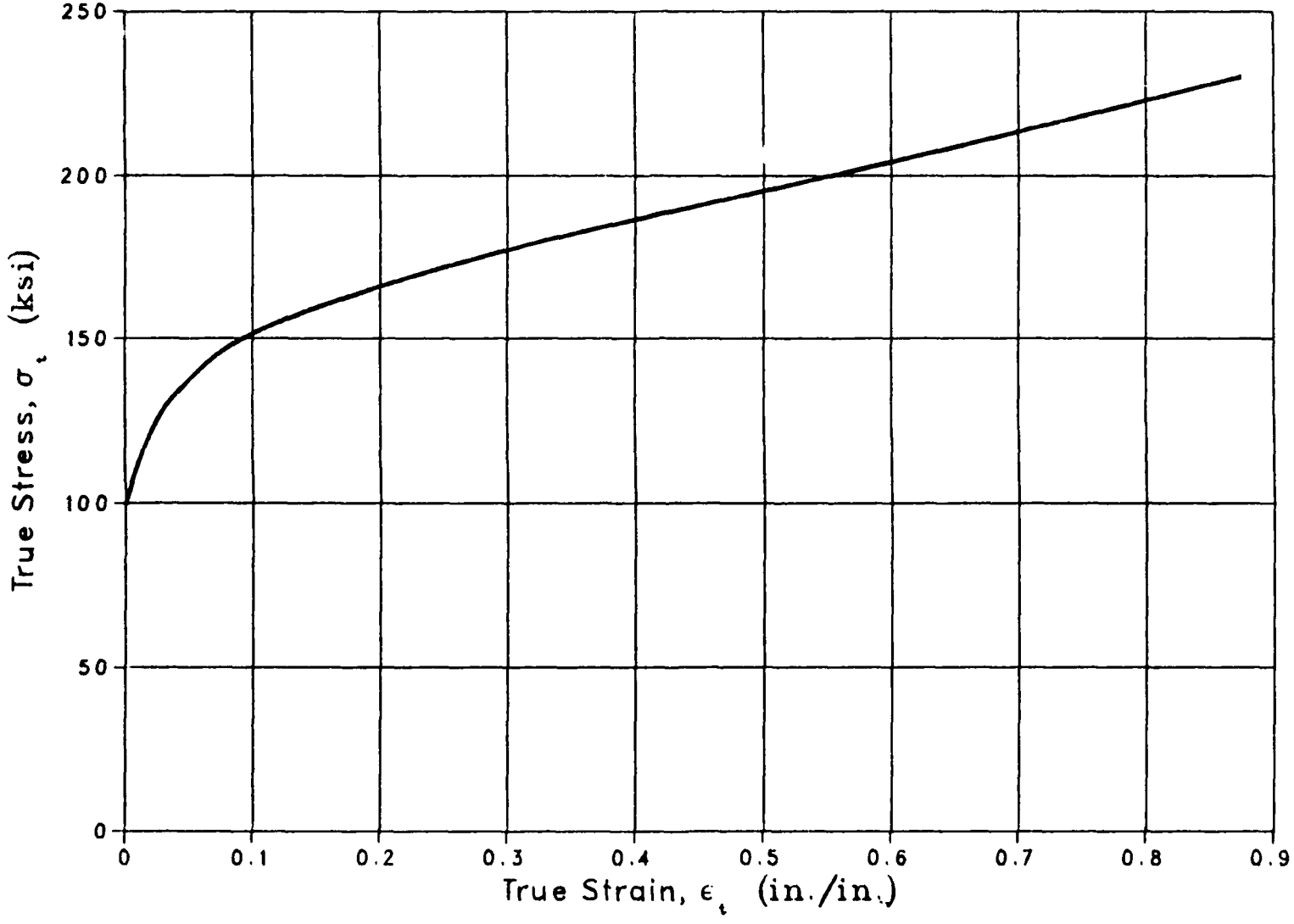

Figure 6. True stress-strain curve: 4340 steel (from Feltner and Morrow, Ref 47).

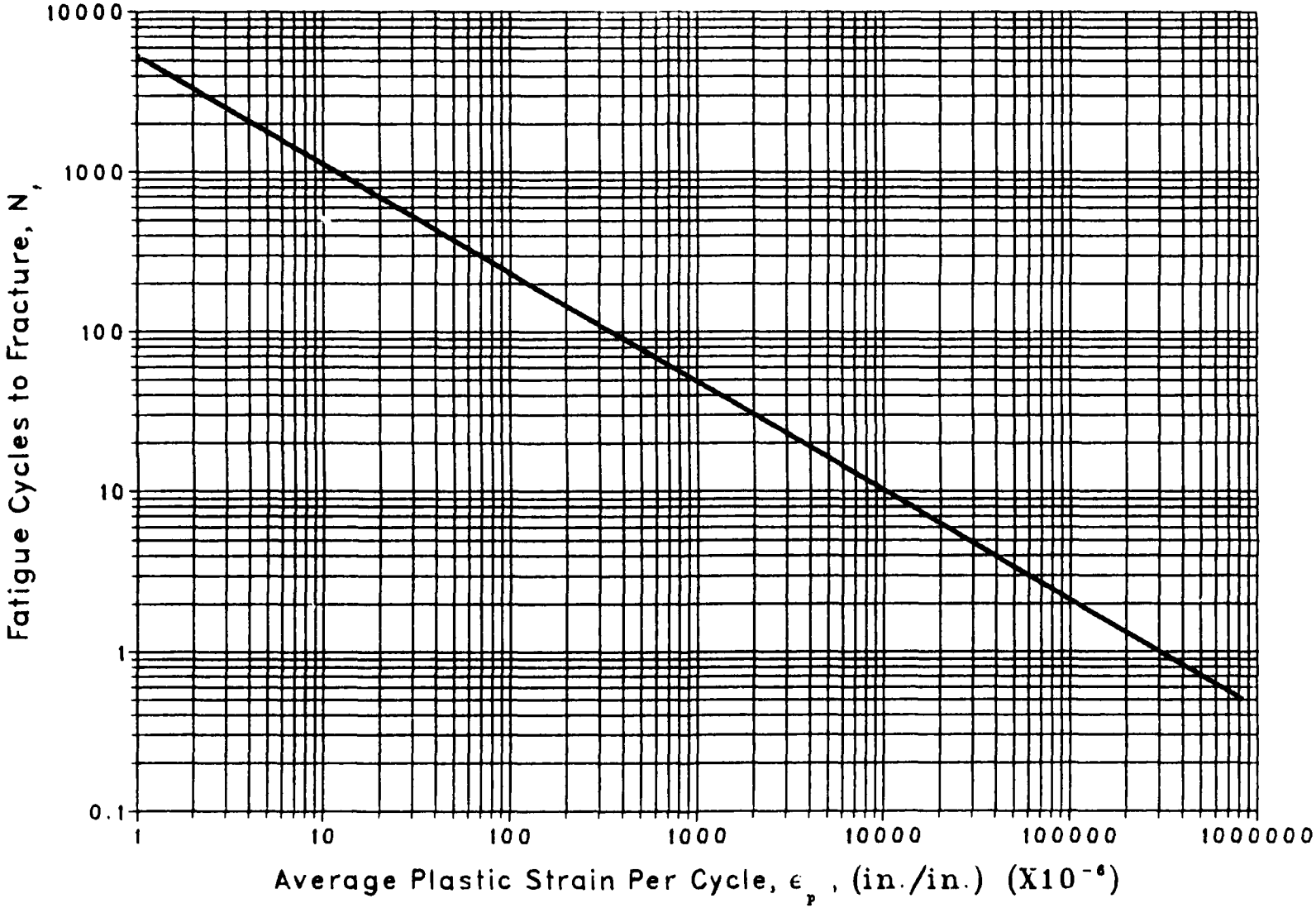

Figure 7. Fatigue life-average plastic strain curve.

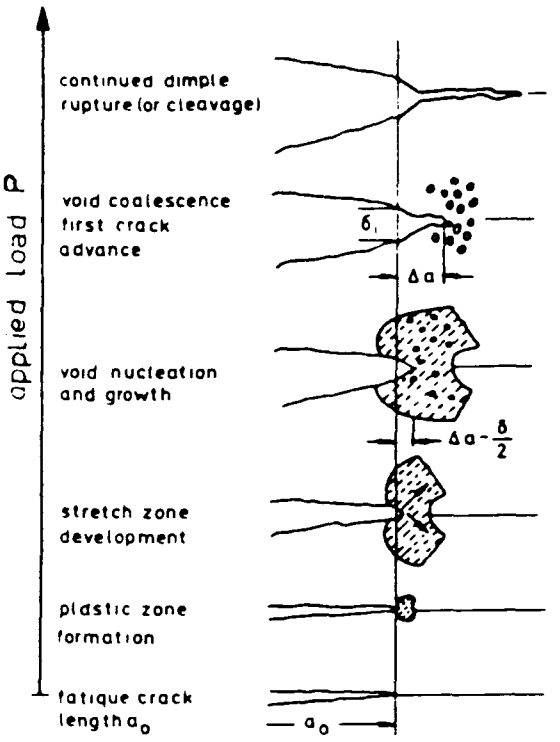

Figure 8. Successive stages of ductile failure (from Blauel, Ref 12).

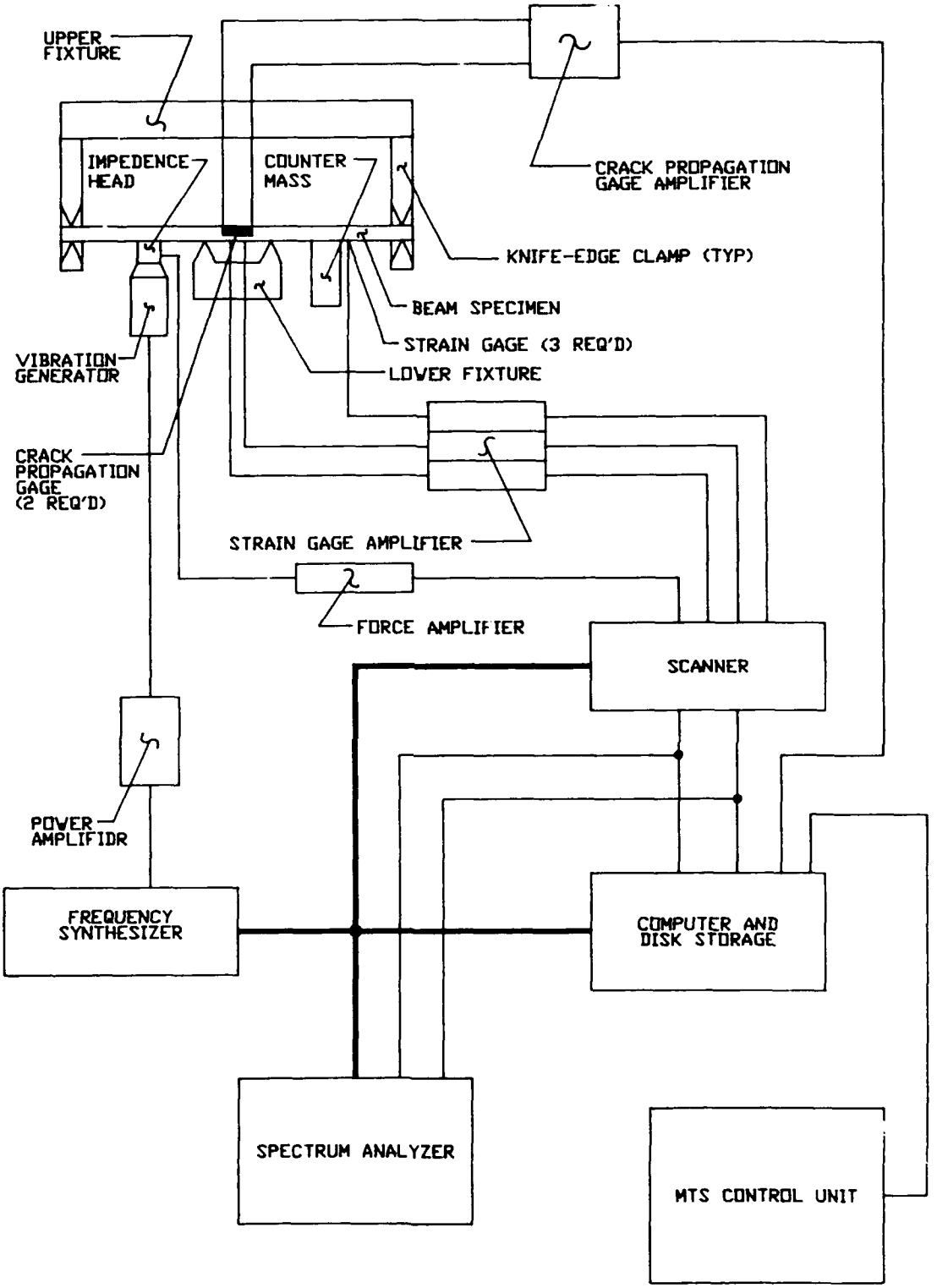

Figure 9. Fatigue test equipment schematic.

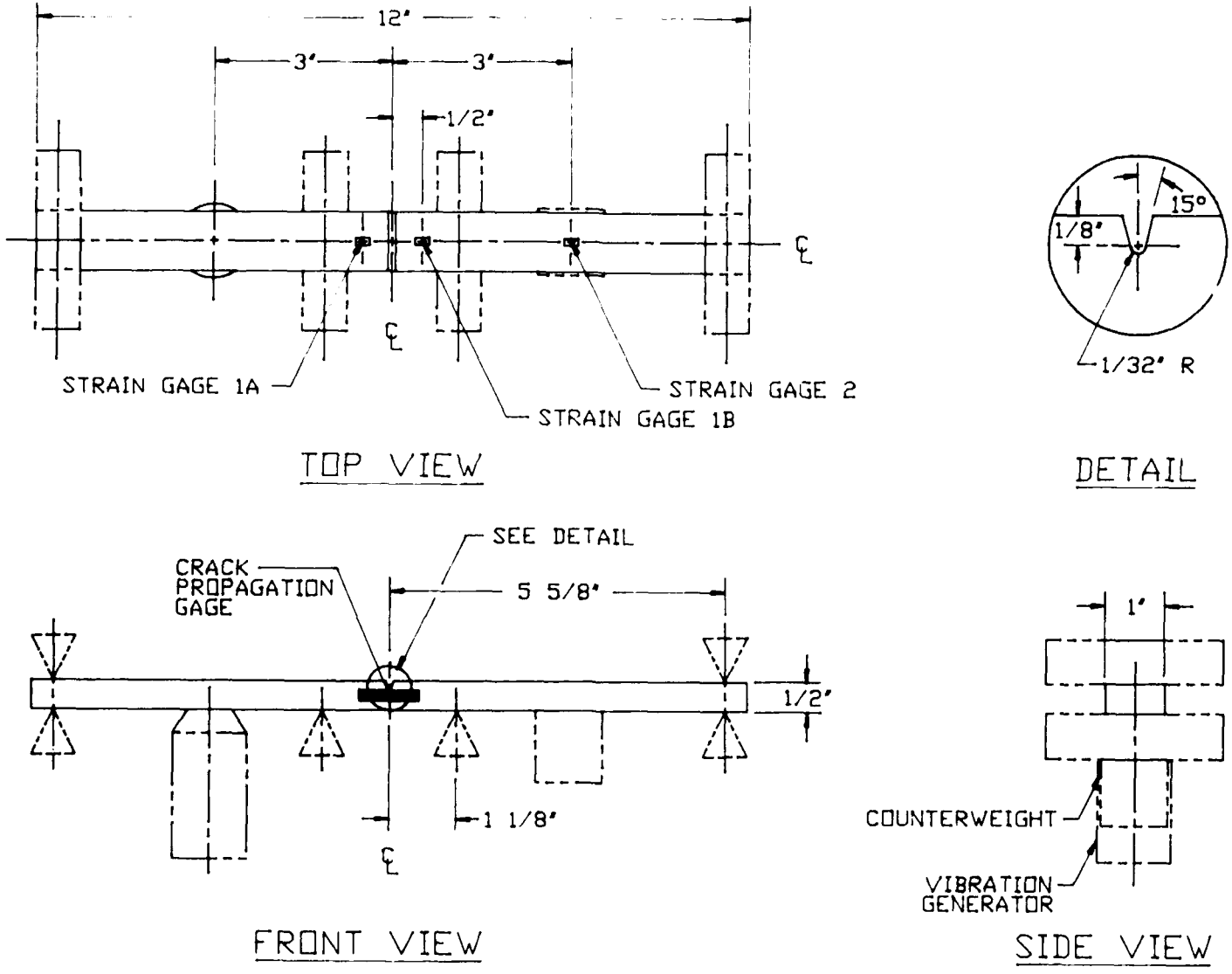

Figure 10. Fatigue test beam specimen.

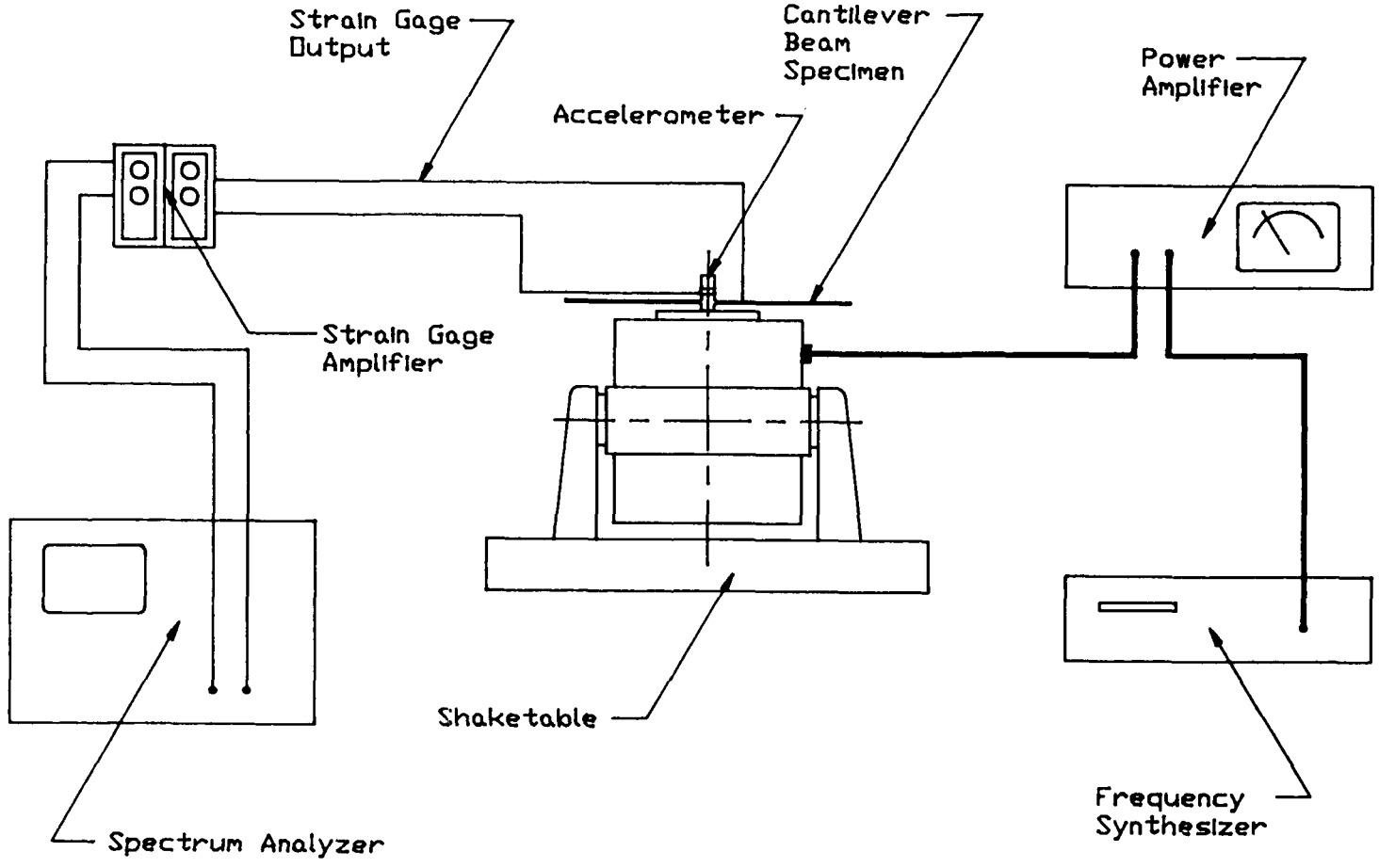

Figure 11. Damping test equipment schematic.

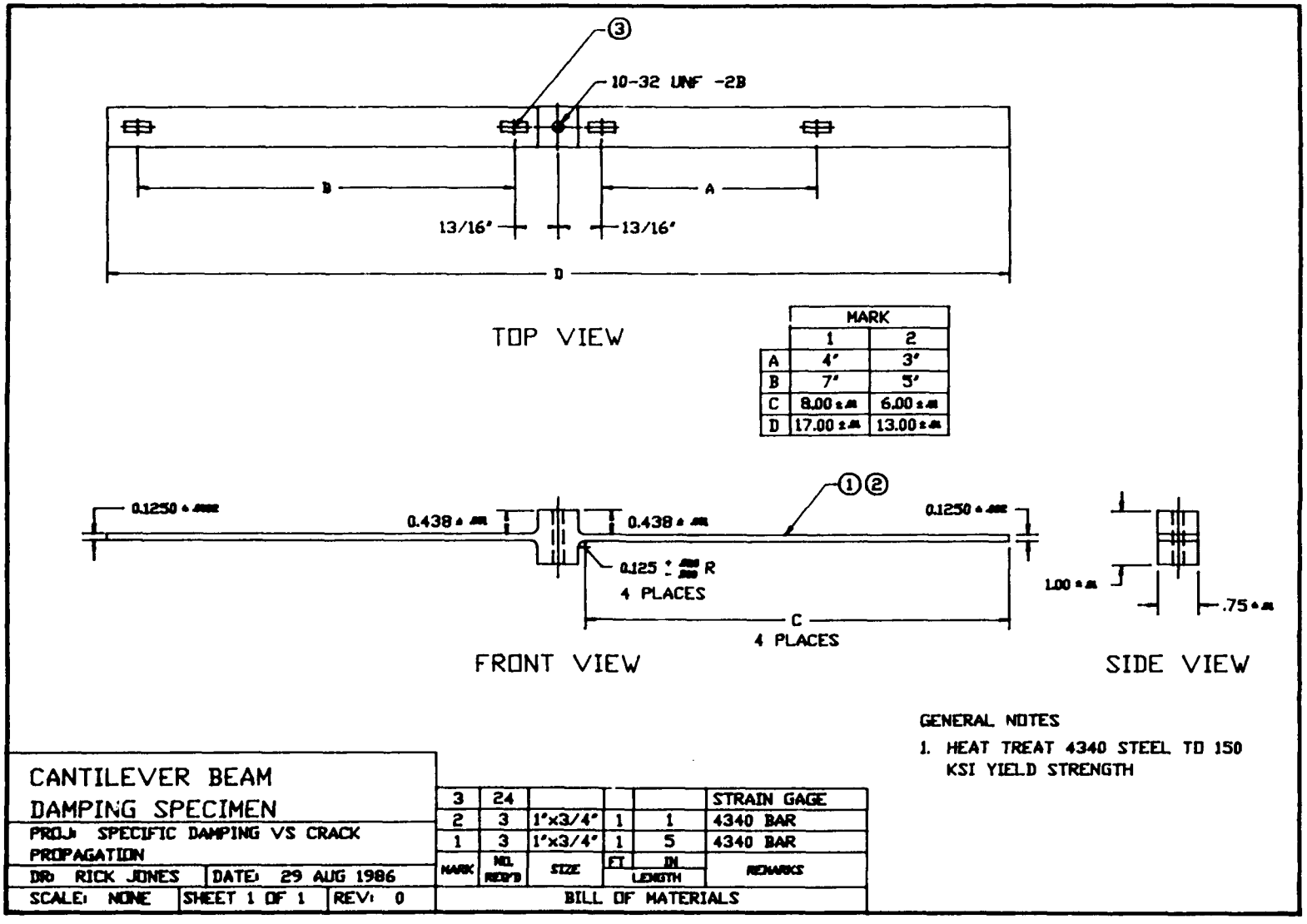

Figure 12. Damping test beam specimen.

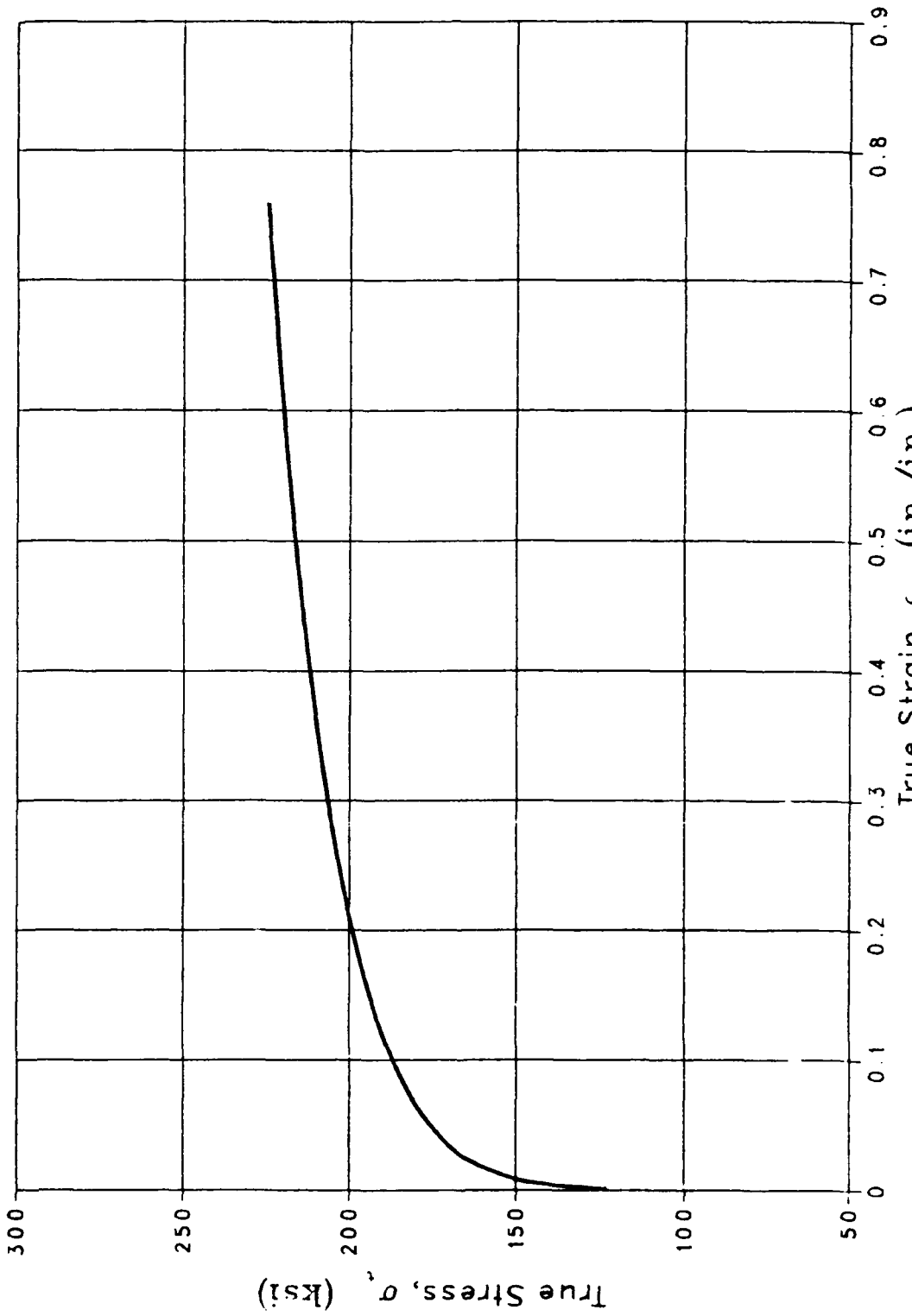

Figure 13. True stress-strain curve: 4340 steel.

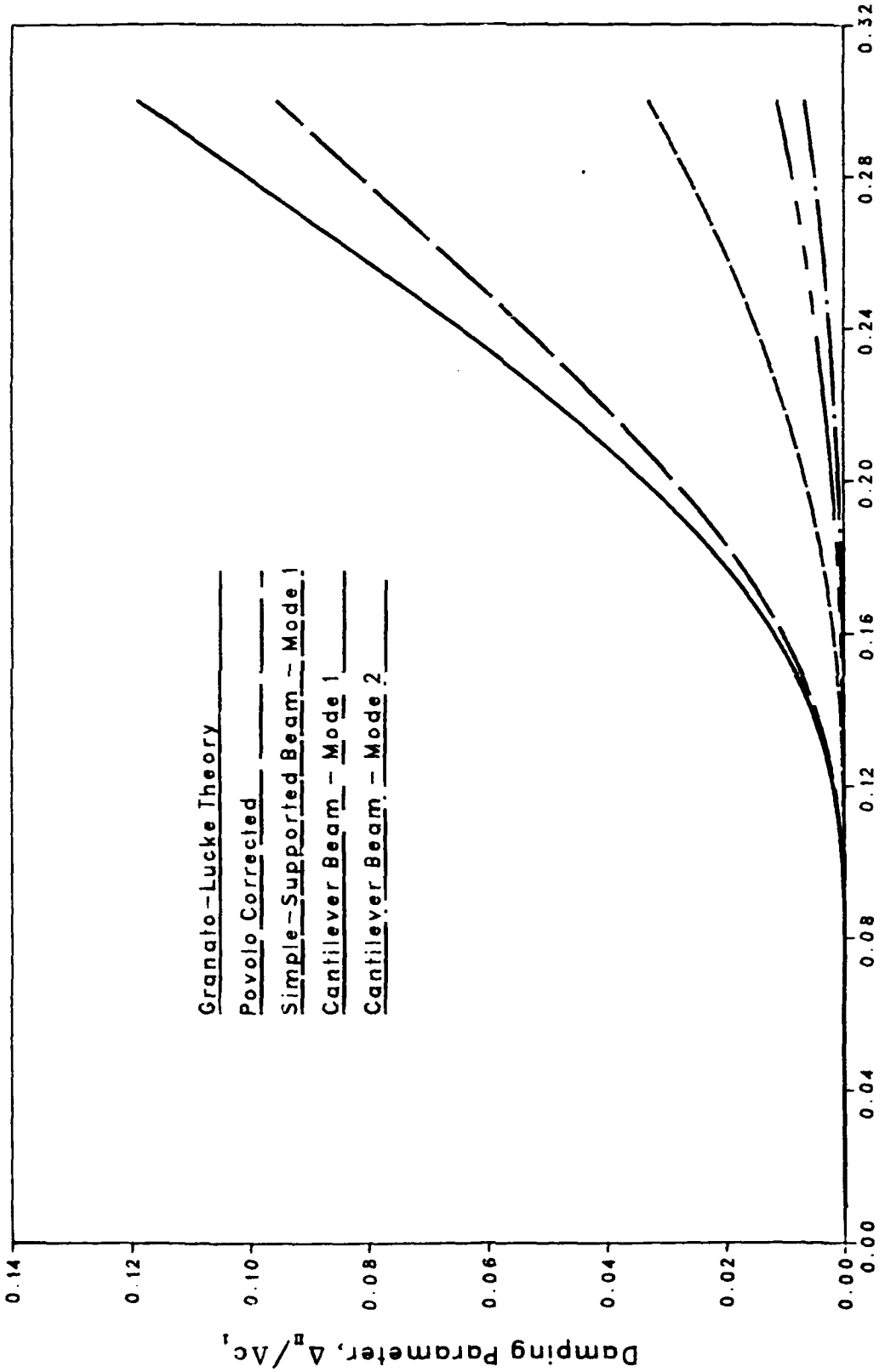

Figure 14. Strain amplitude dependent dislocation damping.

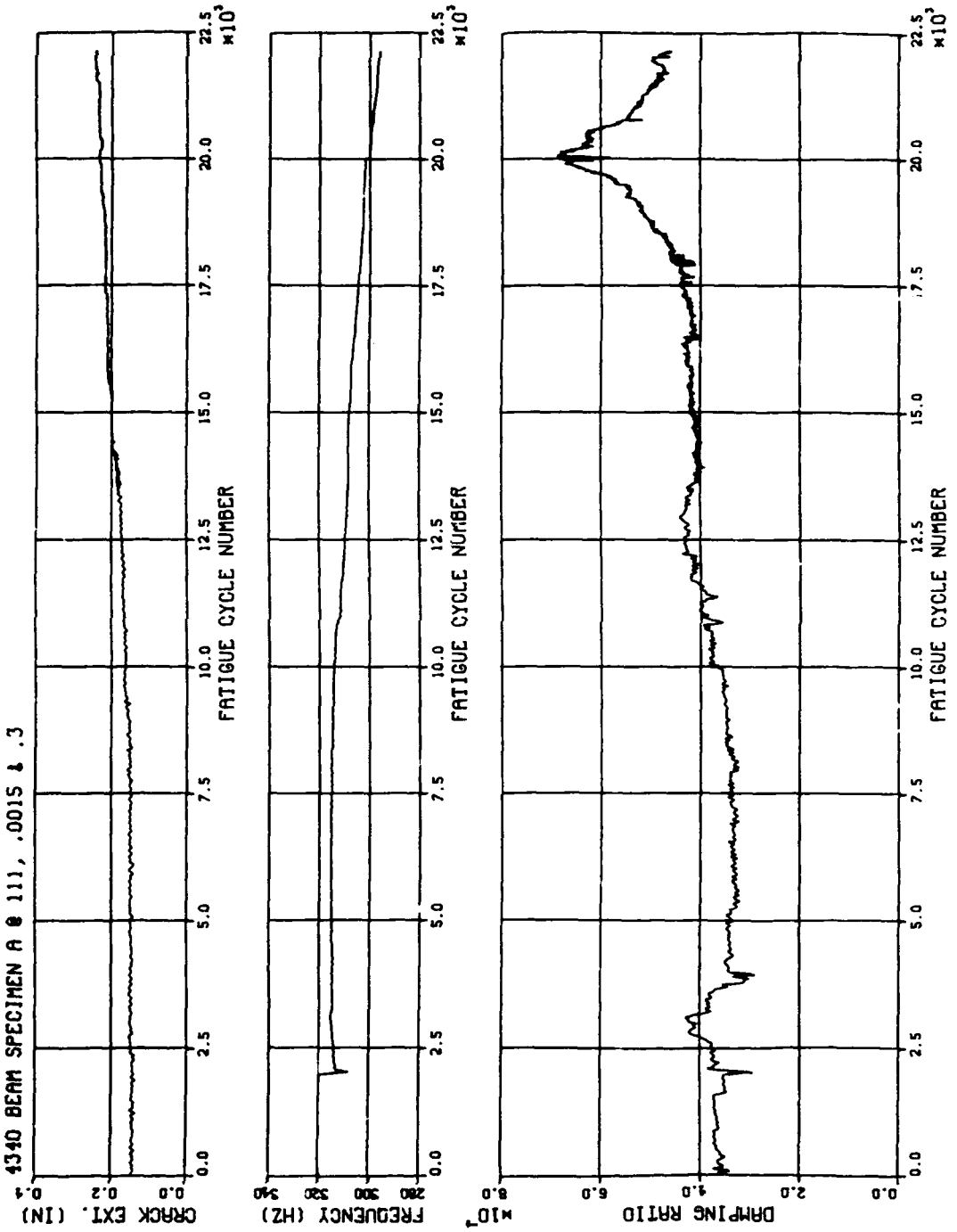

Figure 15. Beam Specimen A: Crack extension, resonant frequency and damping ratio.

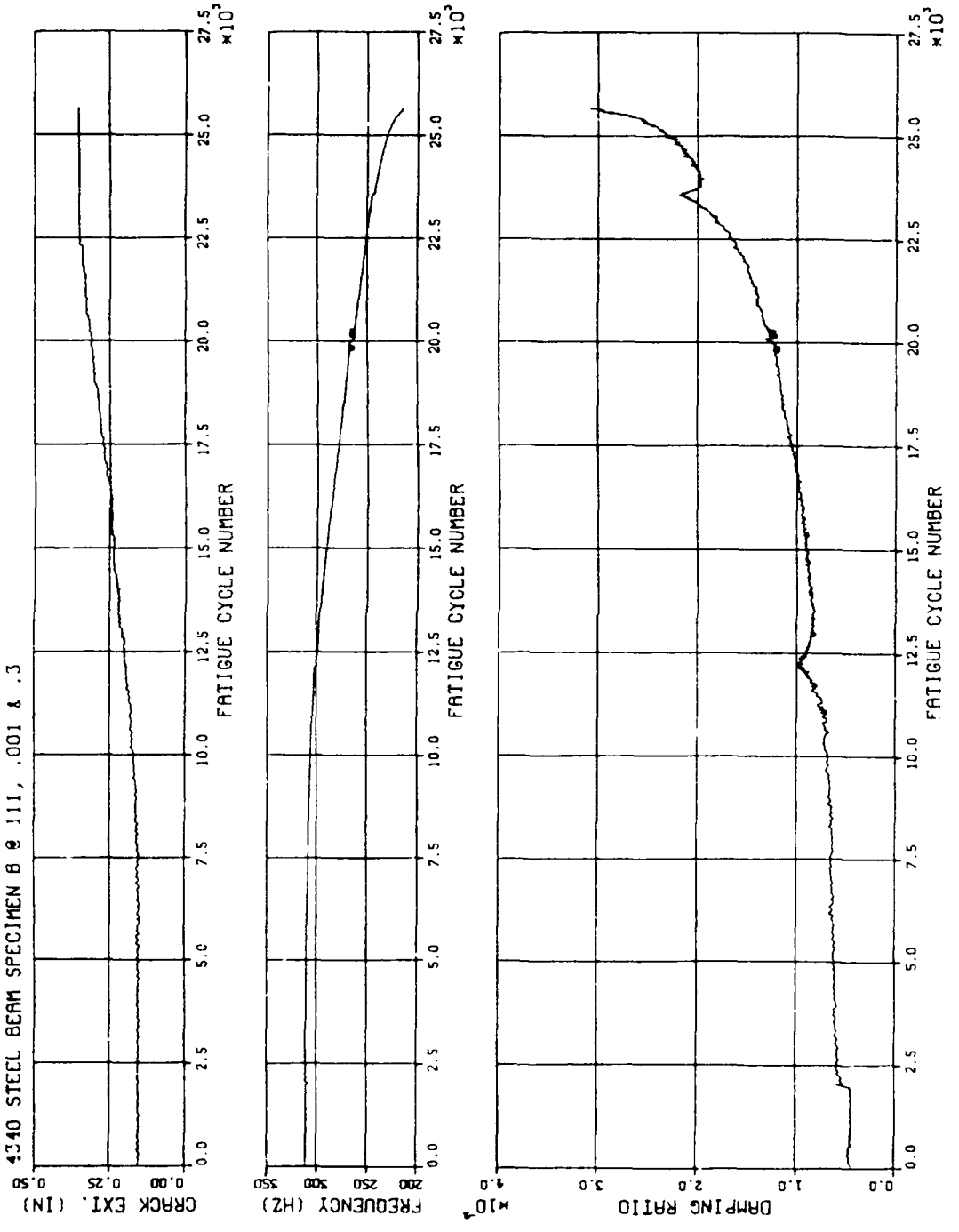

Figure 16. Beam Specimen B: Crack extension, resonant frequency and damping ratio.

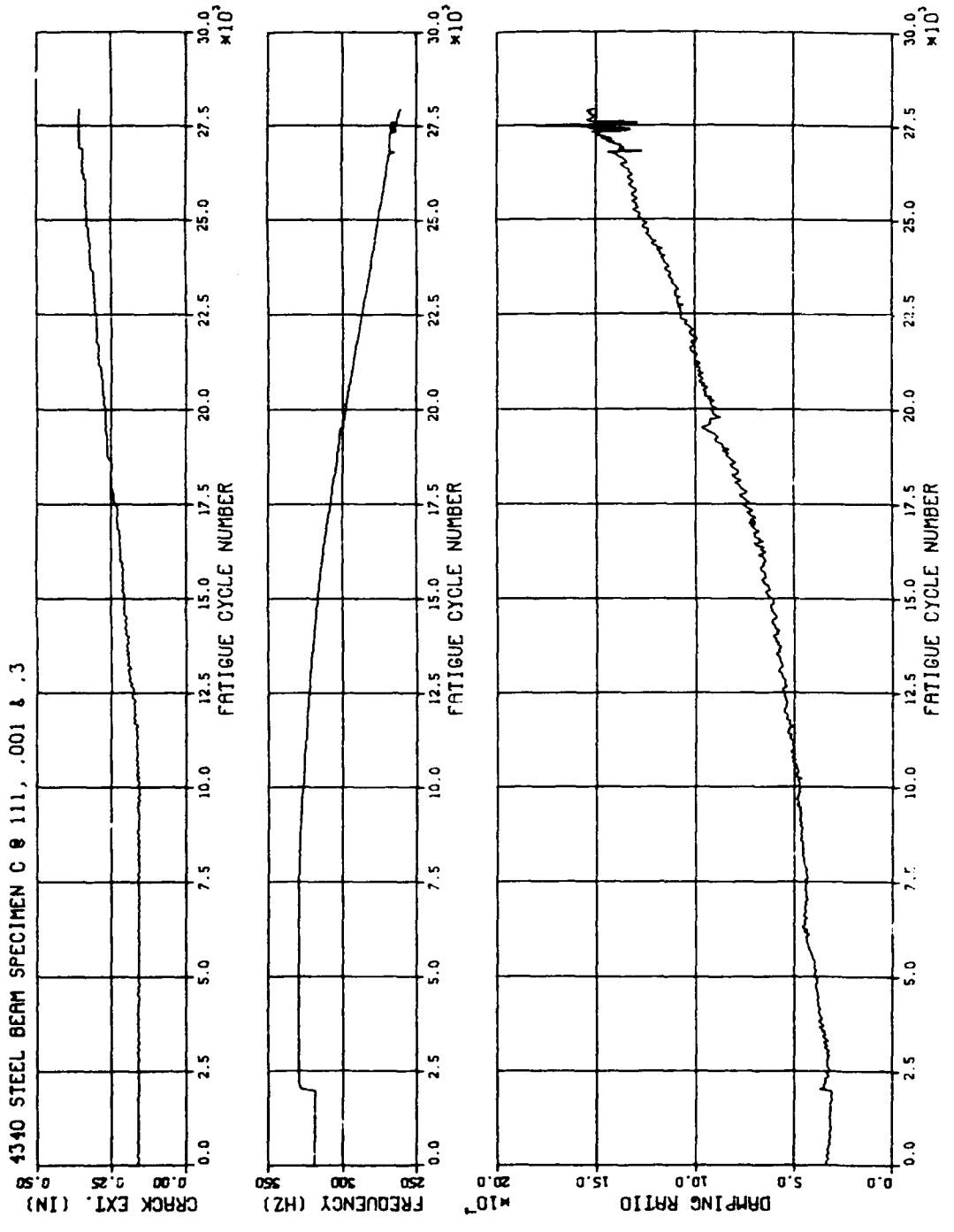

Figure 17. Beam Specimen C: Crack extension, resonant frequency and damping ratio.

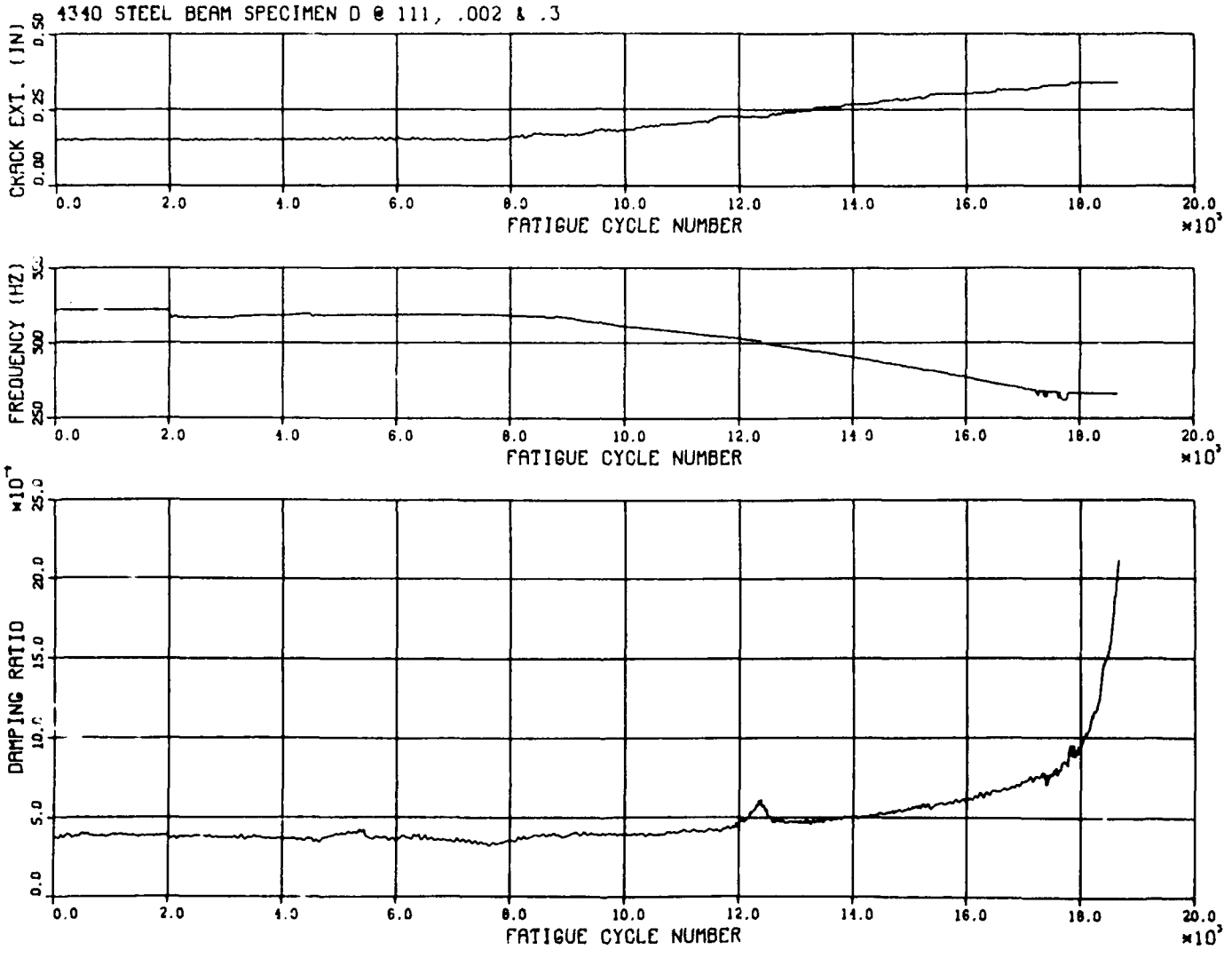

Figure 18. Beam Specimen D: Crack extension, resonant frequency and damping ratio.

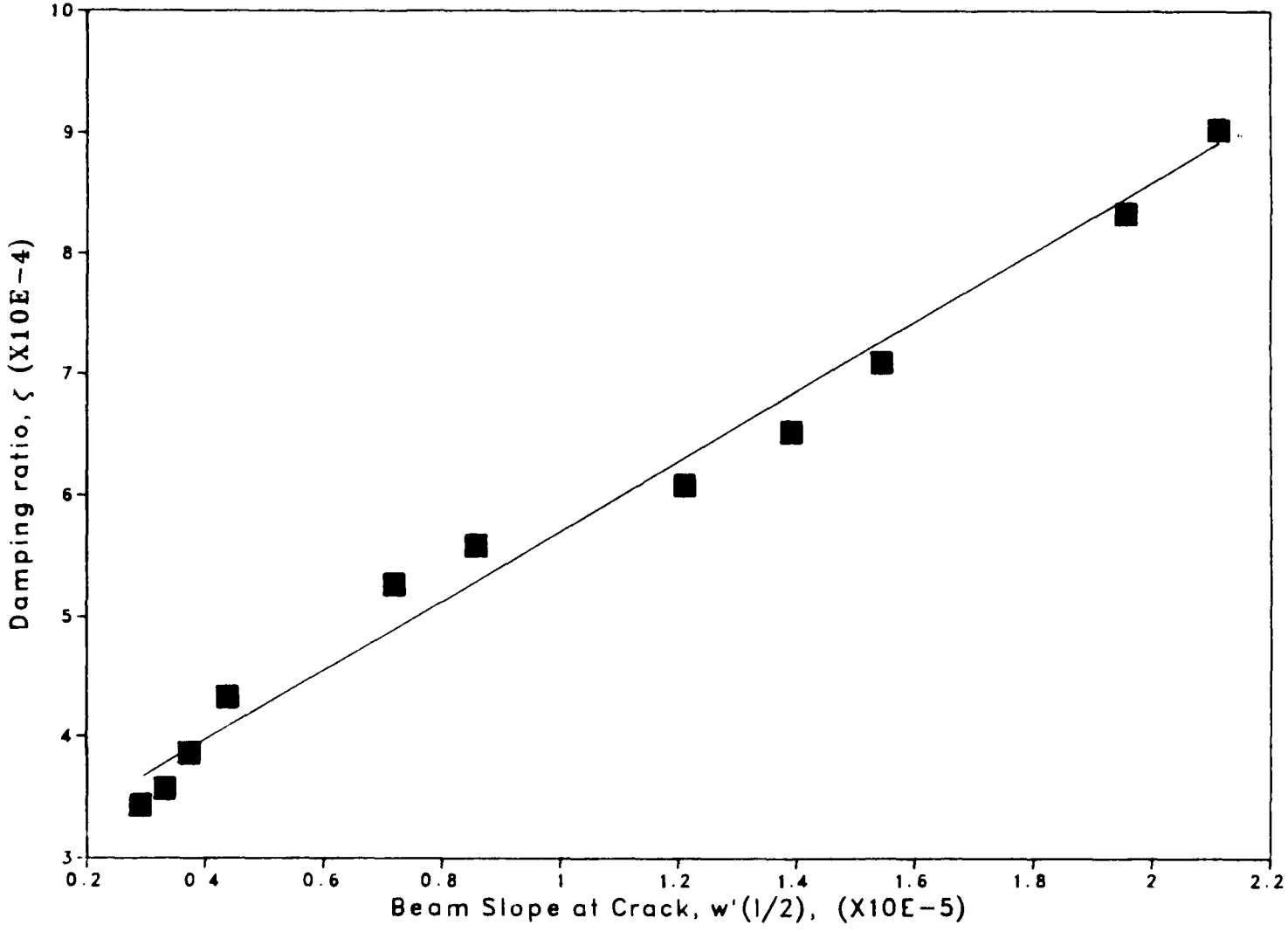

Figure 19. Beam Specimen B: Damping versus beam slope.

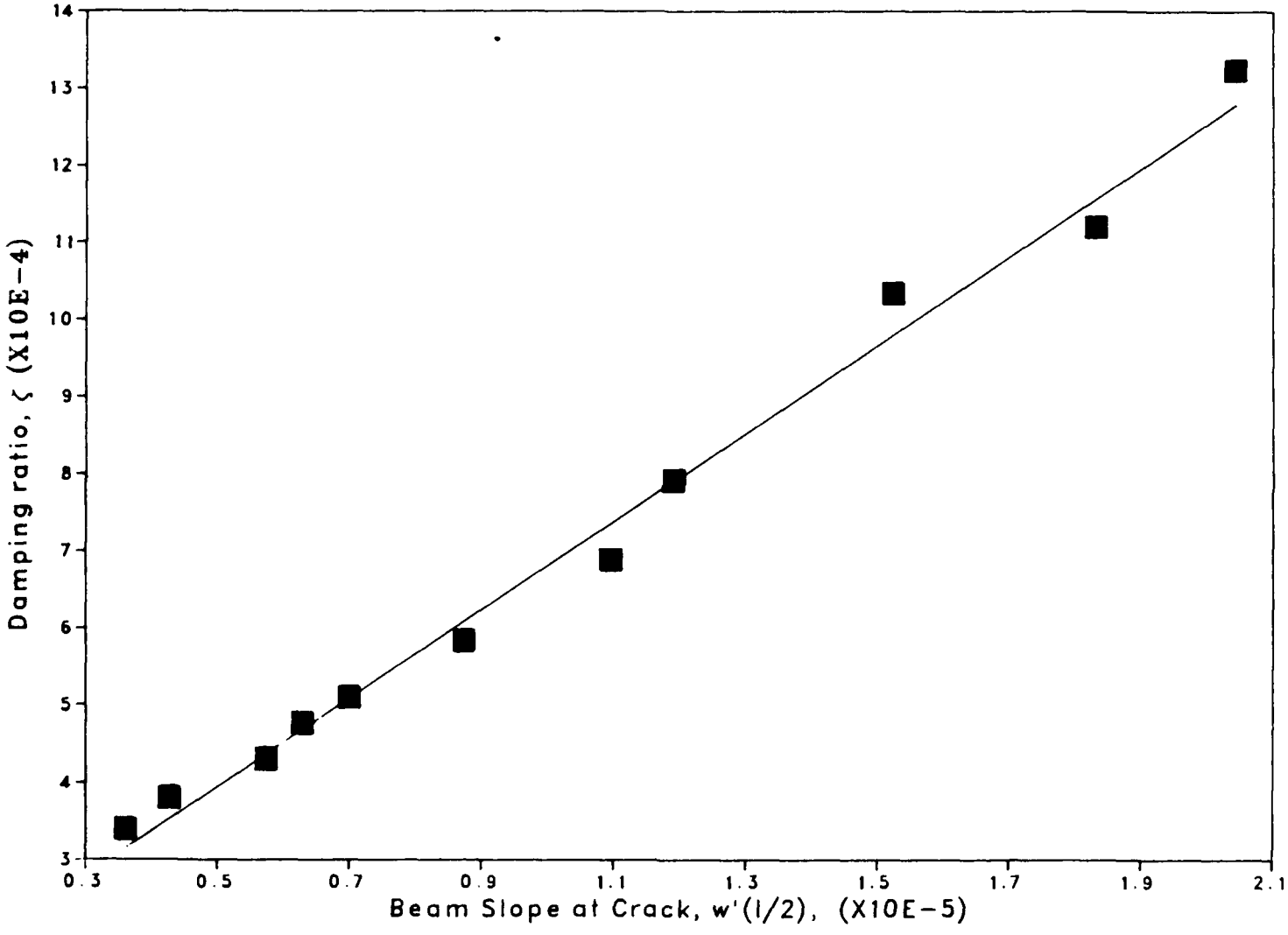

Figure 20. Beam Specimen C: Damping versus beam slope.

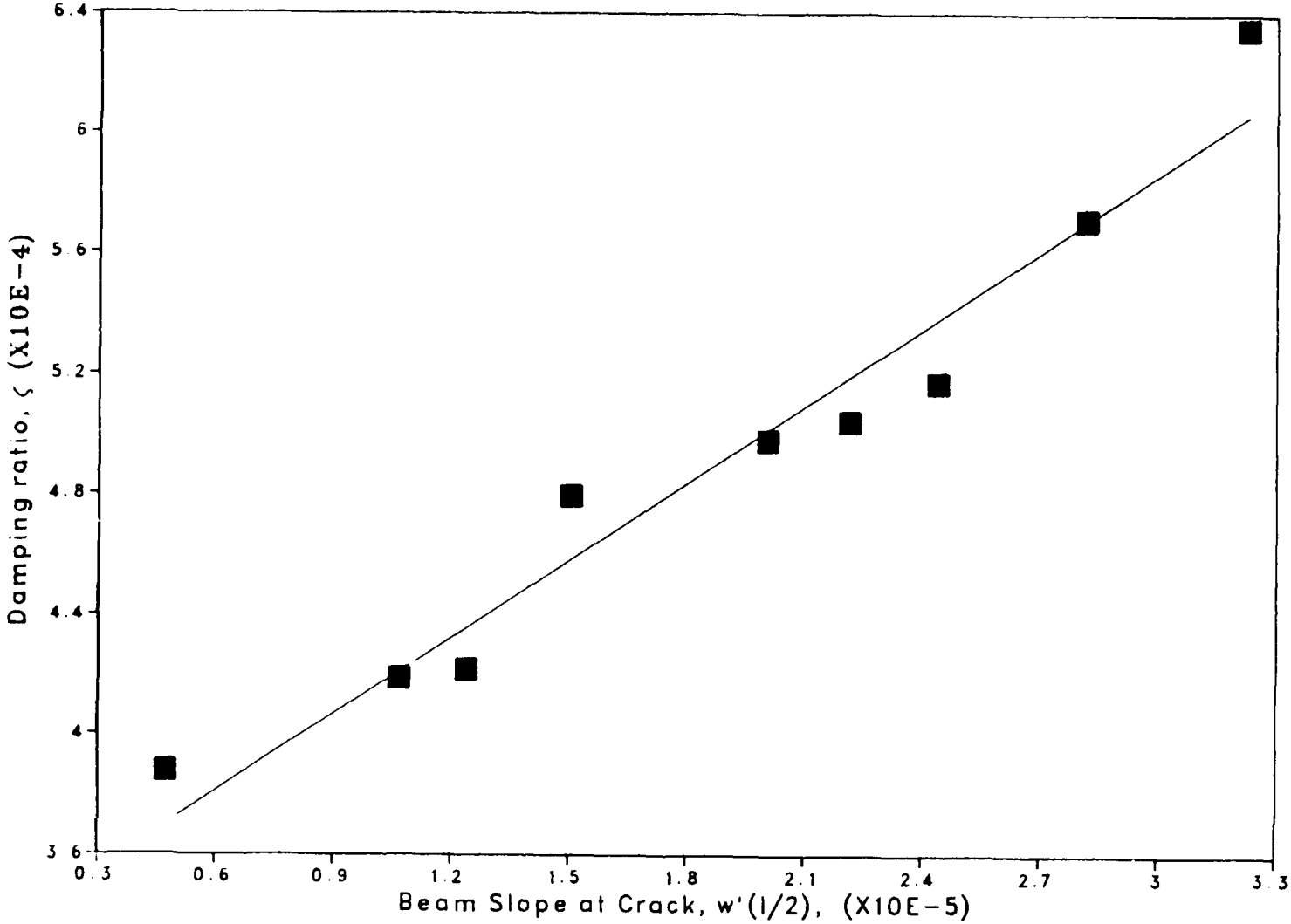

Figure 21. Beam Specimen D: Damping versus beam slope.

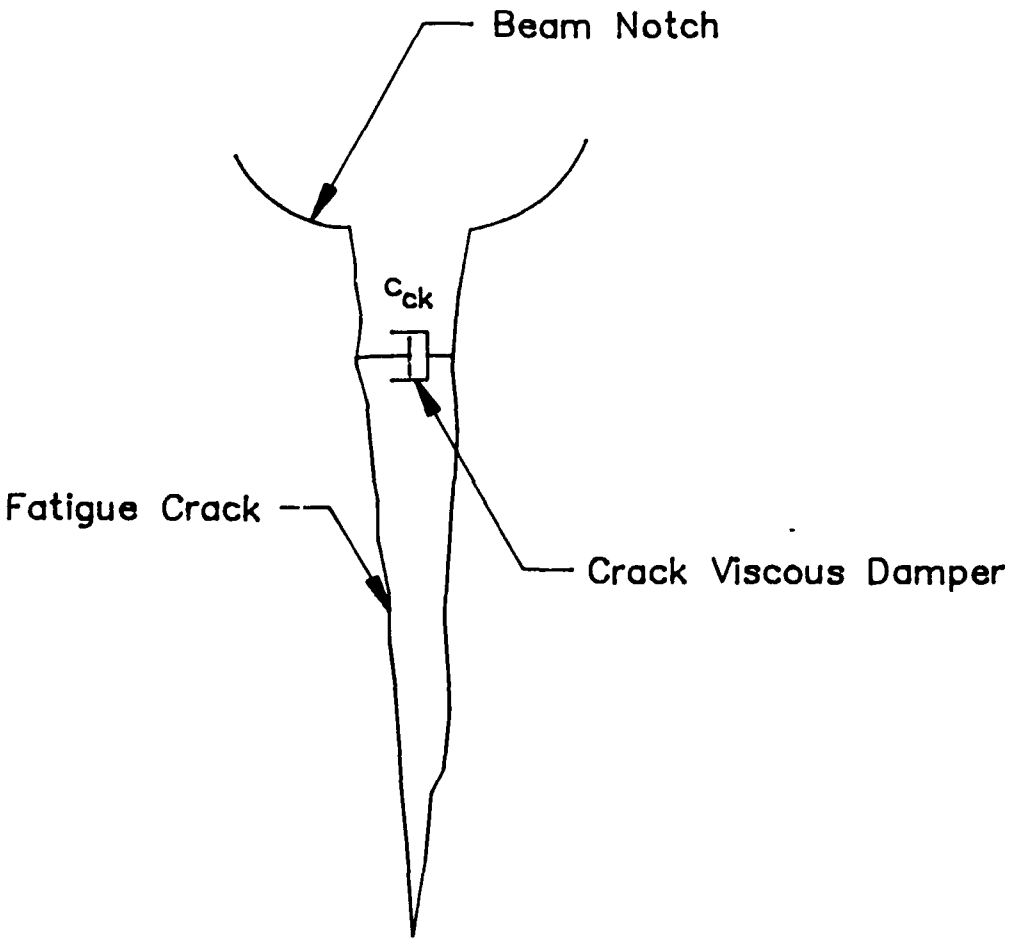

Figure 22. Crack damping model.

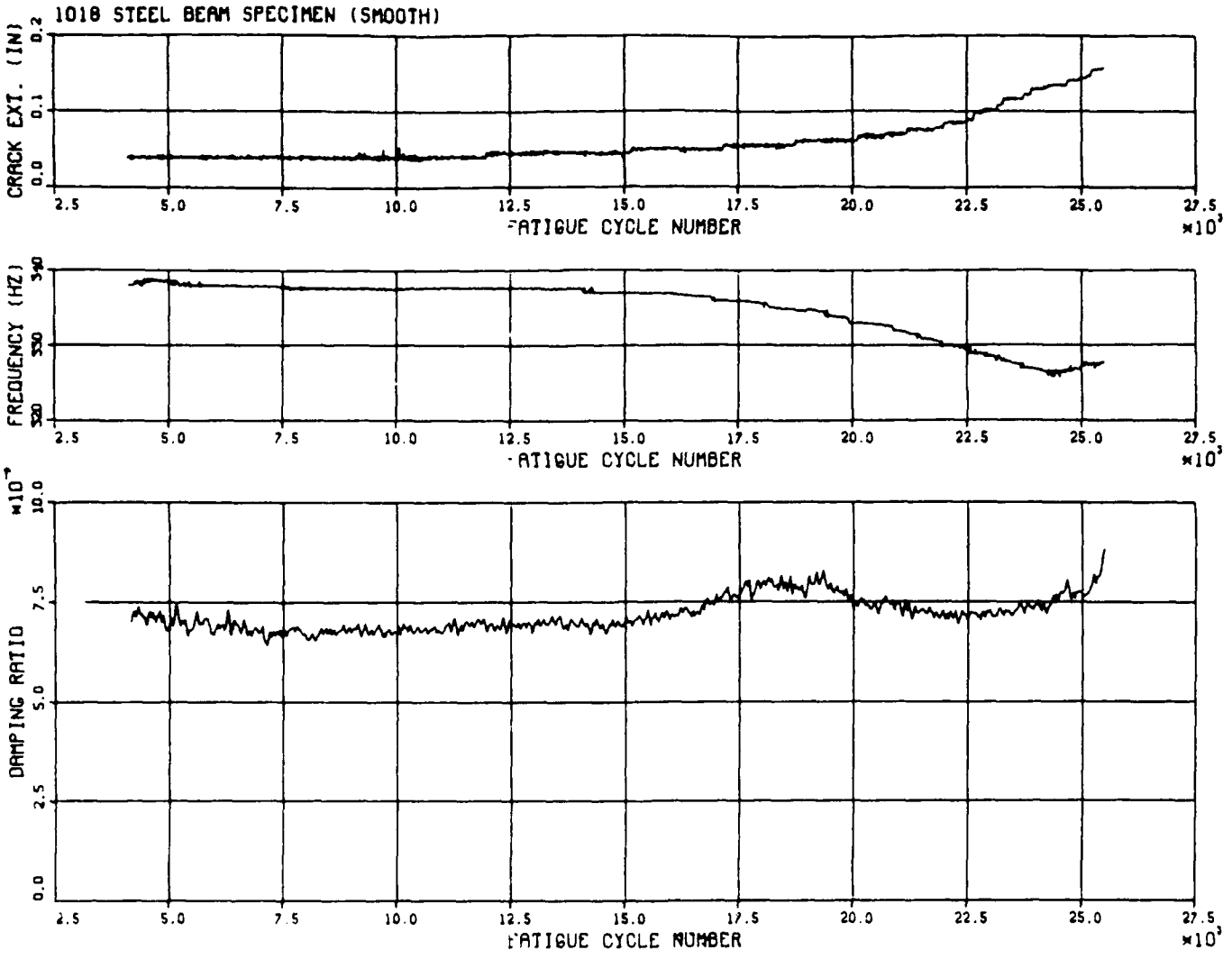

Figure 23. 1018 steel beam specimen: Crack extension, resonant frequency and damping ratio.

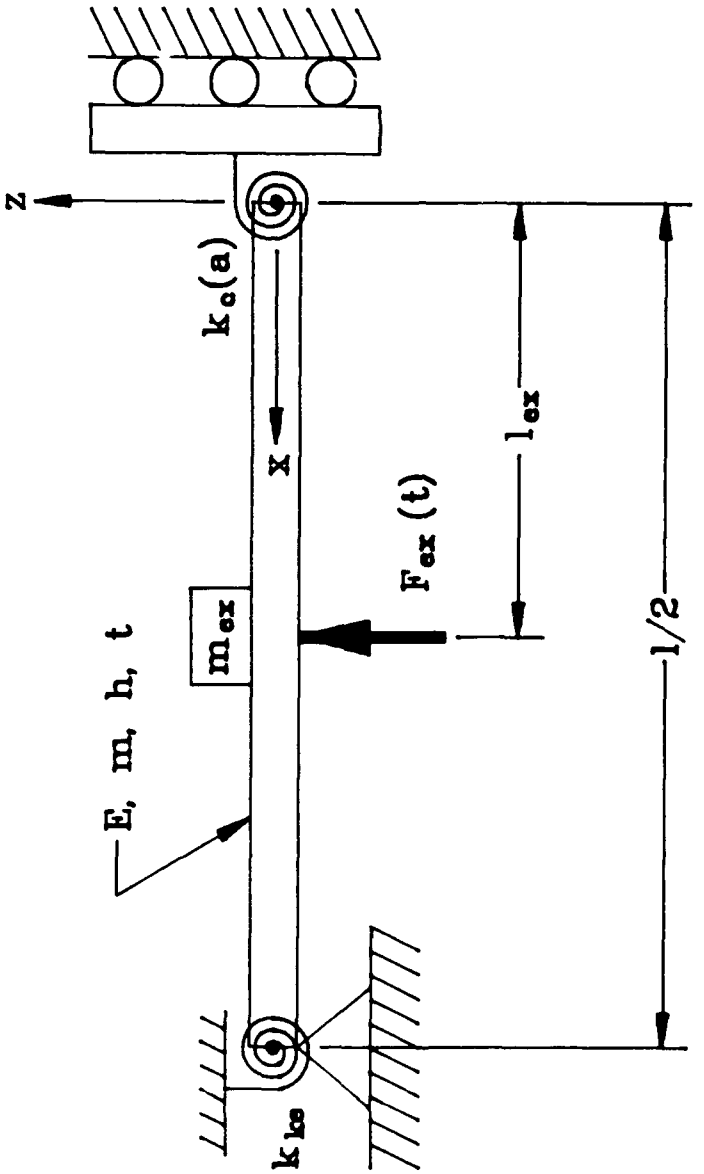

Figure 24. Four-point beam model.

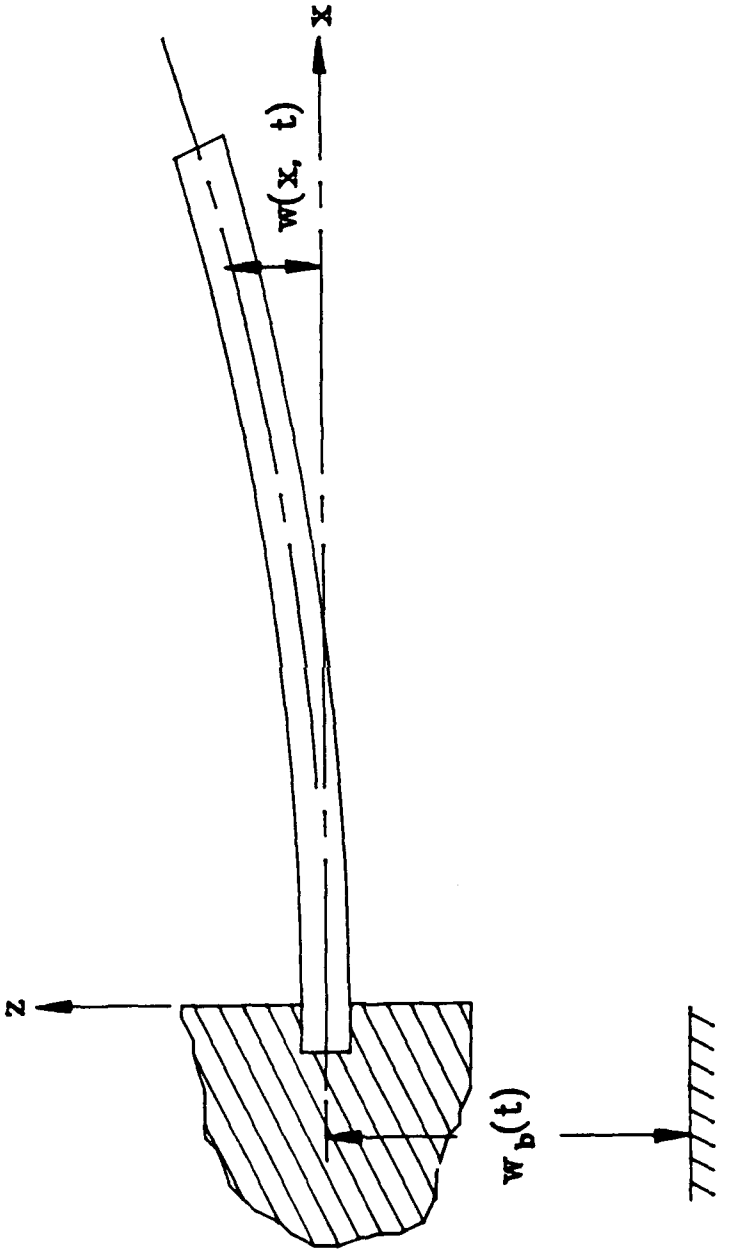

Figure 25. Cantilever beam model.

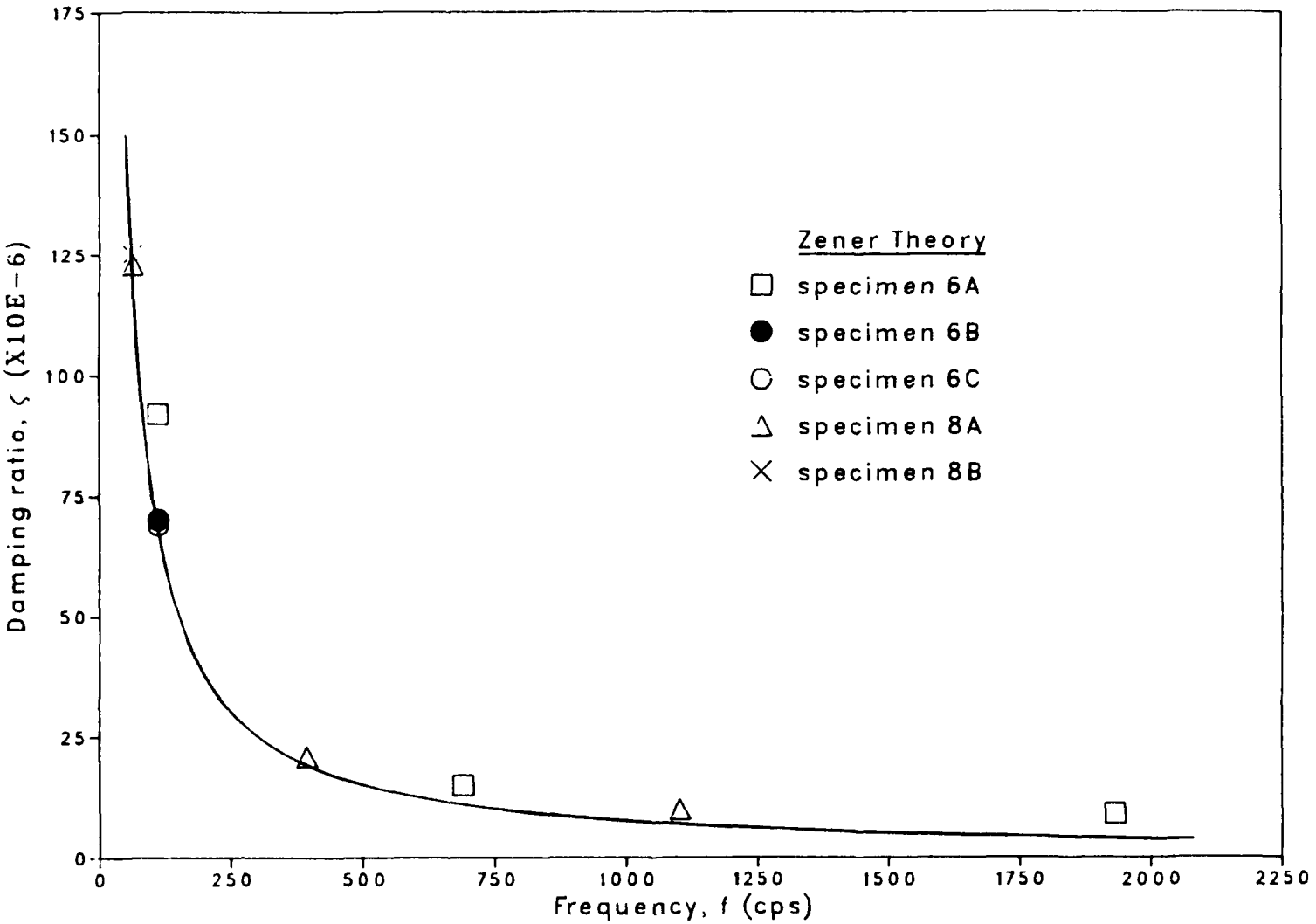

Figure 26. Frequency dependent damping, experimental results.

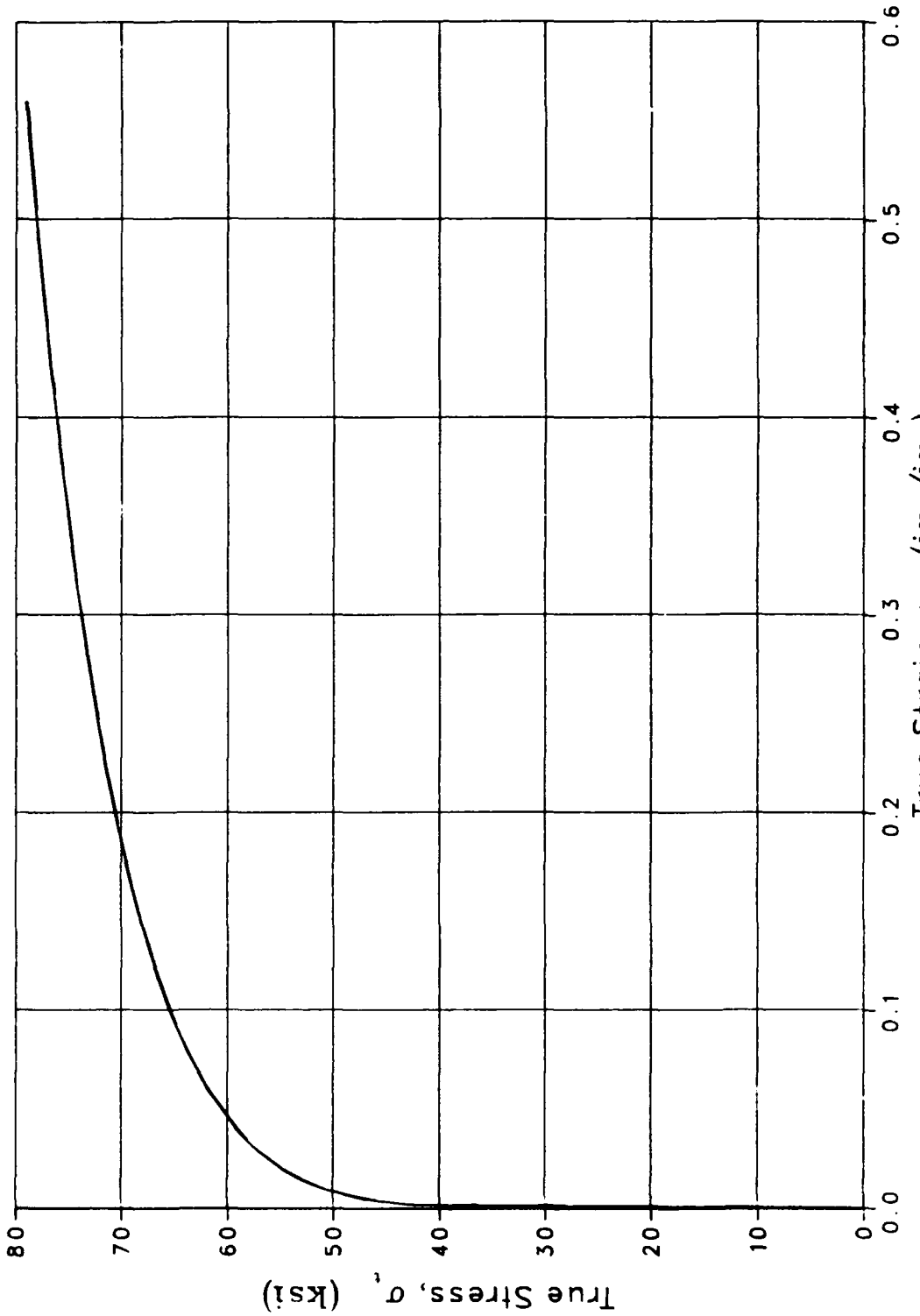

Figure 27. True stress-strain curve: 1018 steel.

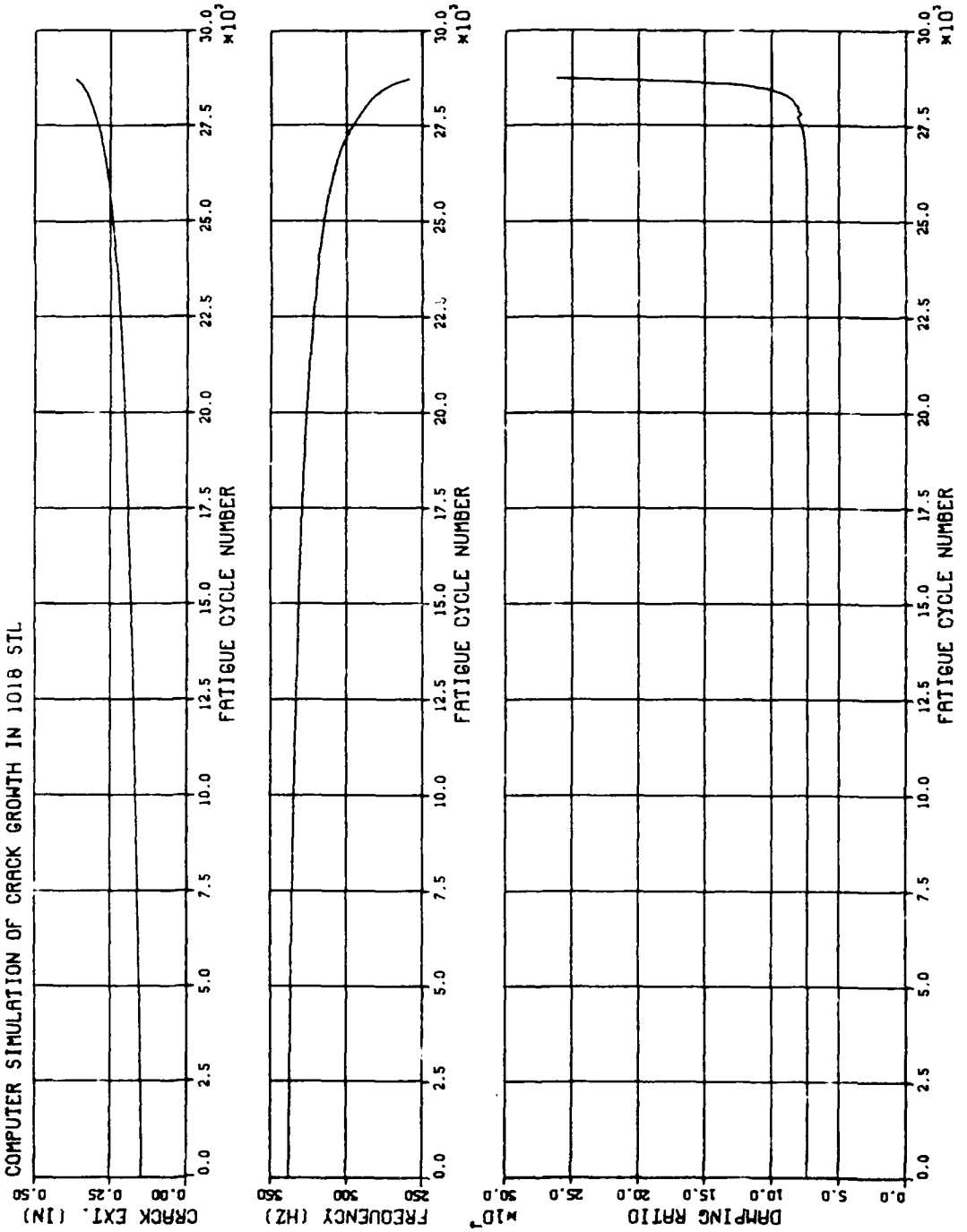

Figure 28. 1018 steel beam simulation: Crack extension, resonant frequency and damping ratio.

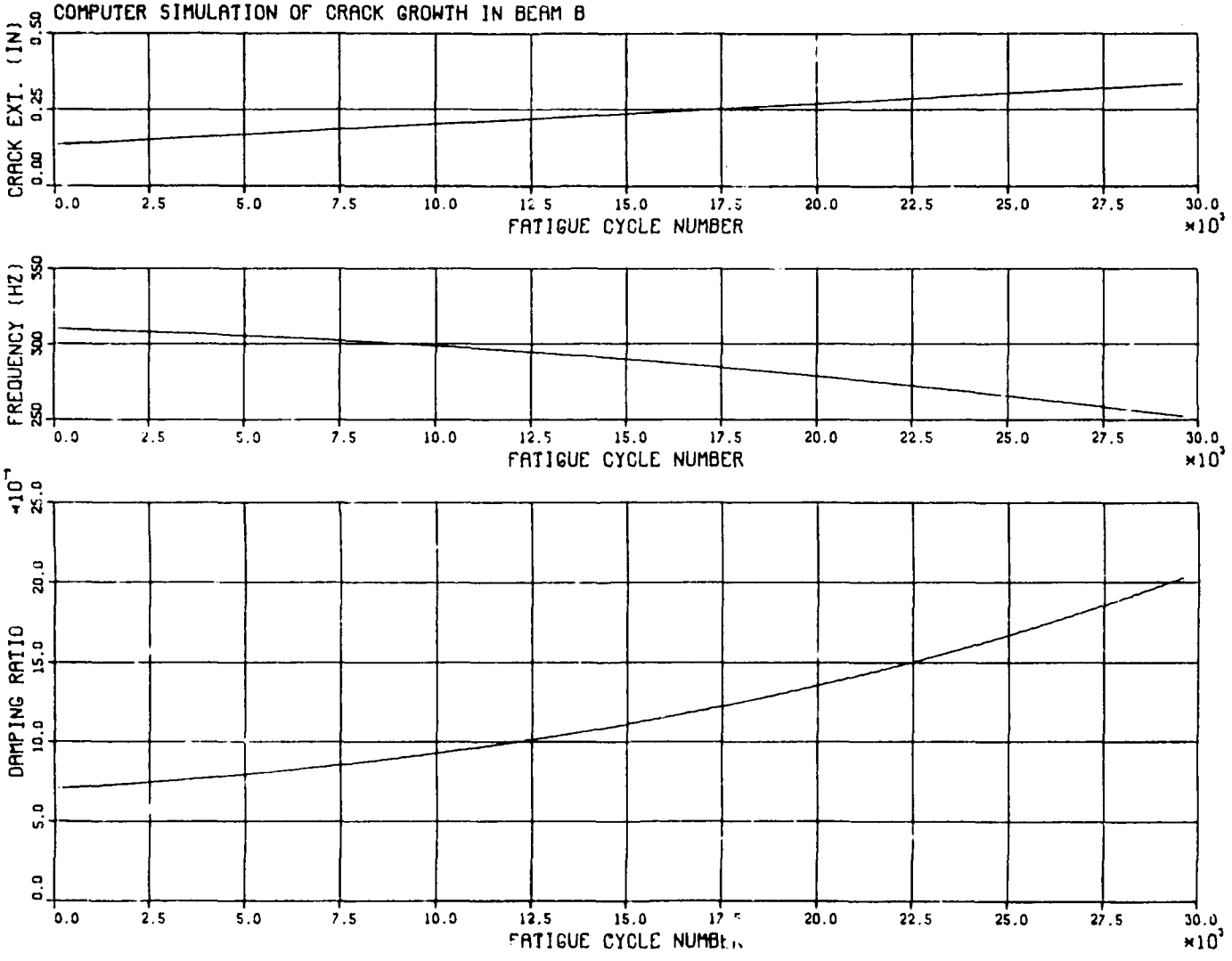

Figure 29. Beam Specimen B simulation: Crack extension, resonant frequency and damping ratio.

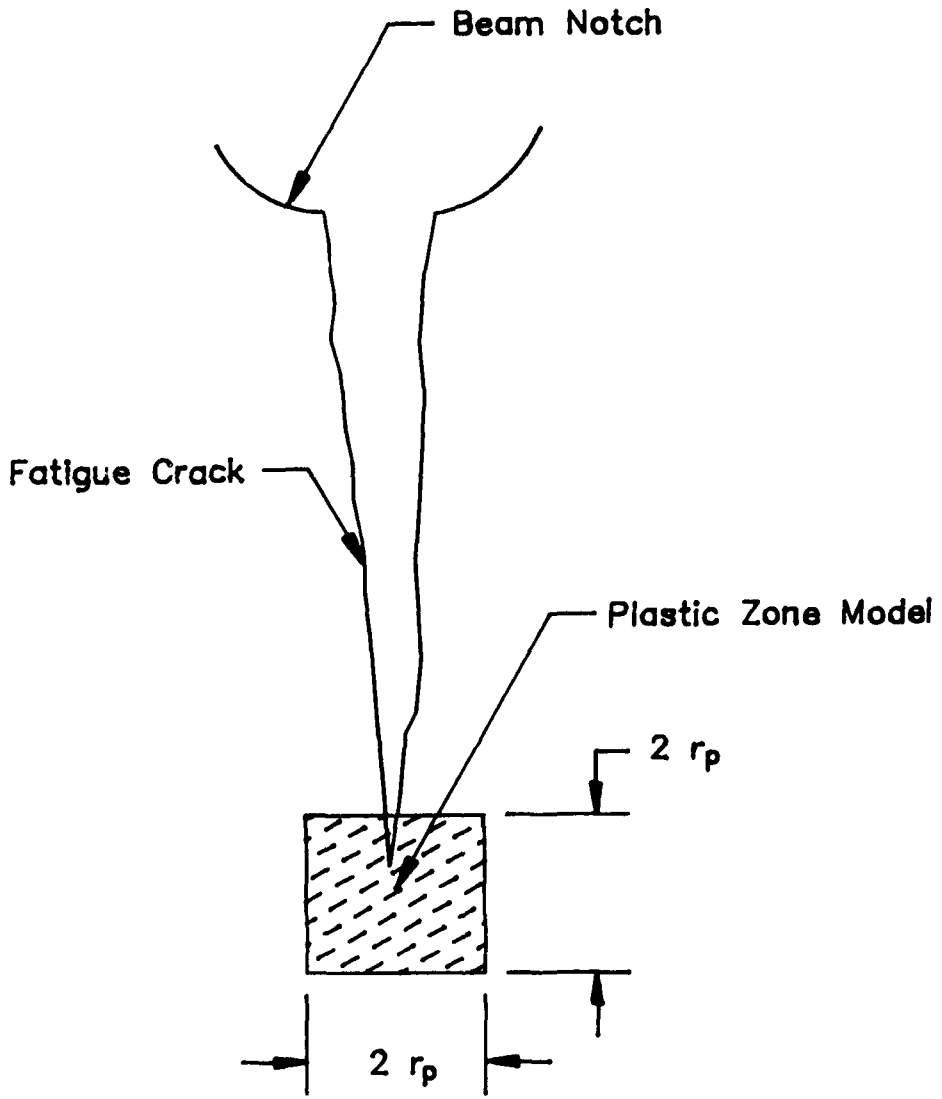

Figure 30. Plastic zone model.

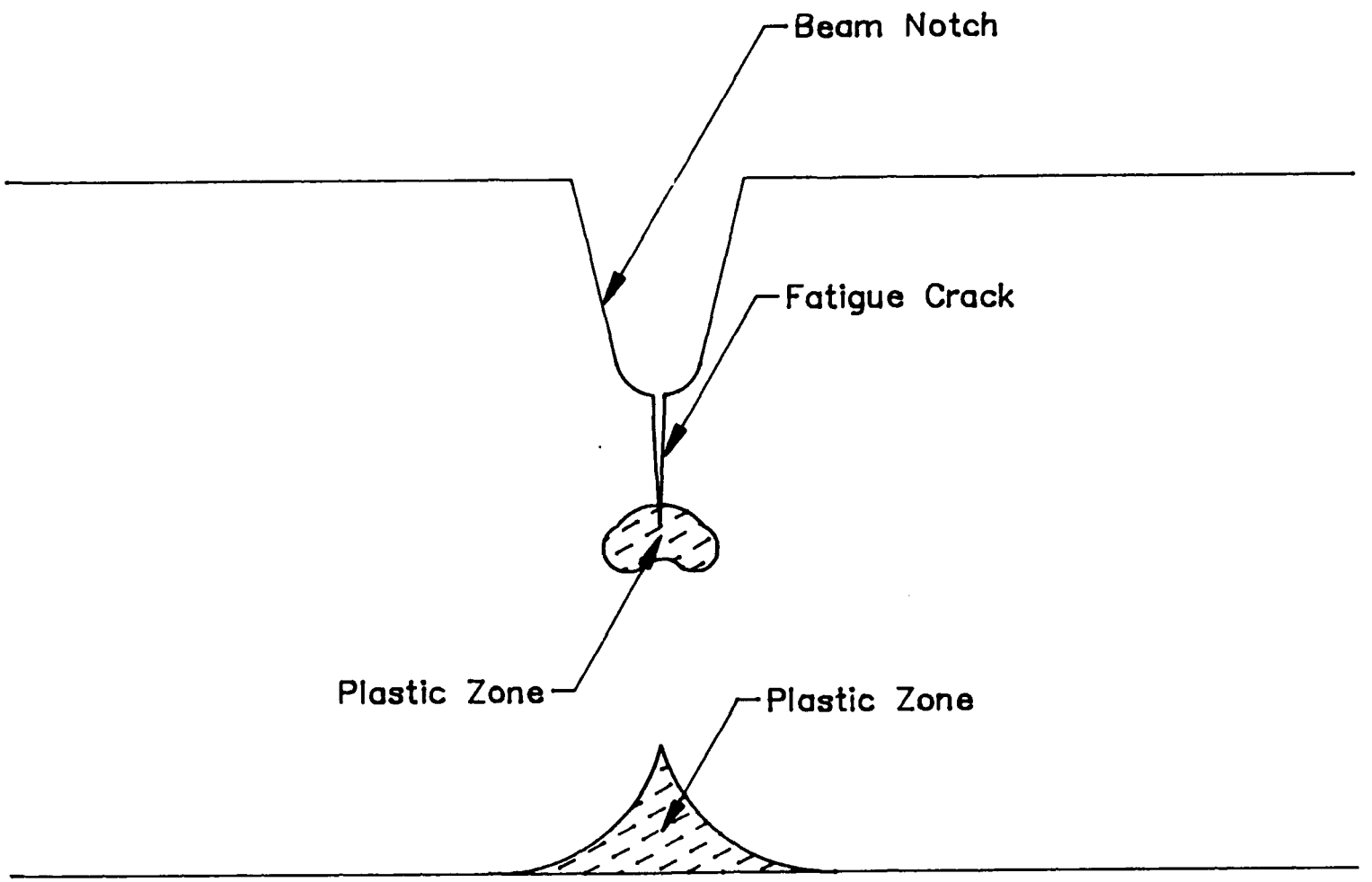

Figure 31. Plastic hinge.

Appendix A

FATIGUE TEST PROCEDURE

This appendix presents a detailed description of the procedure used to fatigue test 1018 and 4340 steel beam specimens.

TEST EQUIPMENT

Table A-1 contains a list of equipment used in the fatigue test. Refer to Figure 9 in the main text of this report for a general arrangement of the equipment listed in Table A-1.

A vibration generator excites a fatigue specimen to collect strain and force data used in the calculation of internal damping for the beam. An impedance head located between the vibration generator and specimen provides the force data for the damping calculation. Three strain gages are attached to the specimen (see Figure 10). These gages provide strain measurements during fatigue loading and vibration generator excitation. The specimen is vibrated at a frequency selected via computer control on the frequency synthesizer. The frequency synthesizer output signal is boosted by a power amplifier to provide strains of measurable amplitude.

The Lab-Datax Computer controls the fatigue load of the MTS test machine and performs the calculations to determine internal damping. Crack propagation gages connected to an analog to digital port on the computer monitor the fatigue crack length that the computer uses to maintain a constant stress intensity factor. The computer also controls the number of fatigue cycles between damping data cycles and the frequency range selected on the frequency synthesizer.

Table A-1. Fatigue Test Equipment

1 - Data Translation Lab-Datax Computer w/Hard Disk Drive, D/A Converter, and A/D Converter
1 - Scientific Atlanta Model SD375 Spectrum Analyzer
1 - Wilcoxon Research Model F5B Vibration Generator
1 - Wilcoxon Research Model Z12 Impedance Head
1 - Accelerometer - Force Amplifier Unit
1 - Validyne Model MC1-3 Amplifier Enclosure
2 - Validyne Model SG71 Strain Gage Amplifier
1 - Hewlett Packard Model 3325A Frequency Synthesizer
1 - Hewlett Packard Model 3495A Scanner w/Optional 001 Relay Assembly
1 - Hewlett Packard Model 467A Power Amplifier
1 - MTS Test Machine
2 - Micro-Measurements Model TK-09-CPA01-005 Crack Propagation Gage
3 - Micro-Measurements Model EA-06-125BZ-350 Strain Gage

The spectrum analyzer collects strain and force data and converts them to a transfer function ratio. The transfer function is transferred to the computer where the damping calculation is made and the frequency range selection is updated. Strain input to the spectrum analyzer is under computer control with the switching function handled by the scanner.

SPECIMENS

The 1018 or 4340 steel beam specimen, shown in Figure 10, is mounted in the MTS test machine using a knife-edge support fixture. The specimen is initially uncracked, with a small notch at its midpoint. A four-point load is applied to the beam by the hydraulic ram of the MTS test machine.

The initial fatigue load, ranging from 1,250 to 1,400 pounds for the four specimens tested, produce a maximum stress in the notch of 160 ksi and a maximum stress intensity factor of 36 ksi-in.$^{1/2}$.

For the heat treatment used, the 4340 steel has a yield strength of 141 ksi and a critical stress intensity factor of 77 ksi-in.$^{1/2}$. With the specimen fatigued at a constant stress intensity factor, the maximum plastic radius is estimated at 3.5×10^{-3} inches, as calculated from Equation 12 in the main text of this report.

The 1018 steel was untreated, having a yield strength of 62 ksi. The 1018 steel is too soft to obtain a valid critical stress intensity factor and no attempt was made to determine one. At 800 pounds, the uncracked specimen has a maximum plastic radius estimated at 7.2×10^{-3} inches, as calculated from Equation 12.

TEST PROCEDURE

After mounting the specimen in the fixture on the MTS test machine, the Lab-Datax computer program is initialized. The initialization process sets the number of fatigue cycles, crack gage parameters,and exciter frequency range. After initializing the system, 2,000 load cycles, 100 pounds each, are applied to the beam specimen. This series of load cycles is used to establish a damping datum for the uncracked specimen.

For each load cycle, maximum strain and load are saved on disk by the computer. After each set of forty load cycles, the computer program executes a damping data cycle. A damping data cycle begins when the frequency synthesizer is set to sweep a range of frequencies starting 10 Hz below and ending 10 Hz above the fundamental resonant frequency of the specimen. As the vibration generator sweeps the frequency range, exciting the specimen, strain gage and force transducer data are transferred to the spectrum analyzer. These data are transformed into a transfer function consisting of two components: real and imaginary. Data from the real component of the strain-force transfer function are interpreted in terms of the phase shift between the input forcing function and output strain. The damping ratio, ζ, may be calculated from

the real component after determining the frequencies of minimum and maximum magnitudes, f_1 and f_2, respectively, using the following formula,

$$\zeta = \frac{f_2^2 - f_1^2}{2(f_2^2 + f_1^2)} \qquad \text{(A-1)}$$

Equation A-1 was not used for calculating the damping ratio within the computer program because the term $f_2^2 - f_1^2$ is a small difference between large numbers and has poor accuracy.

A better technique for measuring damping, during steady-state vibration, is to measure the maximum amplitude of the imaginary component of the transfer function, $TF_{I,max}$. Inverting $TF_{I,max}$ and dividing by two is the equivalent of Equation F-13 in Appendix F, which is equal to the damping ratio. $TF_{I,max}$ occurs at the resonant frequency of the beam, f_r. Steady-state vibration was selected instead of using a ring-down technique because the damping ratio changes with vibration amplitude as the specimen rings down.

A correction factor must be included in the $TF_{I,max}$ calculation. The spectrum analyzer collects data while the synthesizer sweeps discrete frequencies, resulting in an averaged transfer function, rather than the true value at each discrete frequency. The correction factor is the inverse of the number of data sets collected per frequency sweep.

After establishing the damping datum, the computer applies the full fatigue load to the specimen. As before, the fatigue load is cycled forty times between damping data collection cycles. During the load cycle, crack length measurements are made, and the fatigue load is adjusted to maintain a constant stress intensity factor. This procedure continues until the crack passes beyond the crack propagation gages. At this point, feedback from the crack propagation gages indicates a constant crack length and the system produces a constant fatigue load through the remainder of the test.

NOISE

The principal sources of noise in the fatigue and damping tests are fluorescent lights and electomagnetic fields from vibration generators. In the case of fluorescent lights, the spectrum analyzer filters out the noise occurring at 60 and 120 Hz. For the vibration generators, tests showed there were electomagnetic effects only when the strain gage wires were in direct contact with the generator. During the fatigue and damping tests, care was taken to assure that the strain gage wires never came into direct contact with a vibration generator.

Appendix B

DAMPING TEST PROCEDURE

This appendix describes the procedure used to collect damping data from 4340 steel symmetrical cantilever beam specimens.

TEST EQUIPMENT

Table B-1 contains a list of the equipment used to conduct the damping tests. Refer to Figure 11 in the main text of this report for a schematic of the test equipment.

Table B-1. Damping Test Equipment

1 - Scientific Atlanta Model SD375 Spectrum Analyzer
1 - Validyne Model MC1-3 Amplifier Enclosure
2 - Validyne Model SG71 Strain Gage Amplifier
1 - Hewlett Packard Model 3325A Frequency Synthesizer
1 - Hewlett Packard Model 467A Power Amplifier
1 - MB Electronics Model PM-50 Shaketable
4 - Micro-Measurements Model EA-06-125BZ-350 Strain Gage

The frequency synthesizer is set to operate the shaketable at the resonant frequency of the symmetric cantilever beam damping specimen. Output from a strain gage and accelerometer are transmitted to the spectrum analyzer where the data are transformed into a transfer

function. The amplitude of the transfer function is read from the analyzer and converted to a damping ratio using Equation F-13 in Appendix F.

Amplitude of vibration is adjusted through the power amplifier. At each setting, the maximum cyclic strain is read from the spectrum analyzer.

SPECIMEN

Figure 12 in the main text illustrates the symmetric cantilever beam specimen used in the damping tests. The beam material is 4340 steel that has been heat treated to 150 ksi yield strength.

TEST PROCEDURE

A damping specimen is mounted on the shaketable. The amplitude of vibration is initialized to a low level and the frequency synthesizer is adjusted to the fundamental resonant frequency of the specimen, f_r. From the spectrum analyzer, the amplitudes of maximum cyclic strain, ε_0, and acceleration, a_0, are read. The ratio of a_0 to ε_0 is a transfer function. To pinpoint the exact resonant frequency and its associated damping ratio, strain and acceleration data are collected from frequencies 0.05 Hz above and below f_r. Interpolation is used on these three data points to compute the beam's damping ratio. The damping interpolation process is based on fitting the three data points to a curve generated by Equation F-11.

The above procedure is repeated for the second and third modes of the specimen. Having completed the damping data collection for the first three modes of the specimen, at the selected strain levels, the amplitude of vibration is increased and the procedure repeated.

Appendix C

ALGORITHM FOR MODELING INTERNAL DAMPING FROM CRACK GROWTH

The internal damping of a beam undergoing fatigue crack growth is calculated based on an estimation of the plastic zone size and material dependent constants related to crack growth rate and internal damping. The following algorithm is used to calculate the internal damping of a four-point beam with a propagating crack.

STEP 1. Input material and crack growth constants

a_0	Initial crack length (in.)
A_i	Dislocation density coefficient (disl/in.^{2})
a_f	Final crack length (in.)
α	Linear expansion coefficient (in./in./°F)
b_c	Material constant relating crack length to torsional stiffness (lb-in.)
C	Manson-Coffin ductility exponent
C_1	Internal damping coefficient
C_2	Internal damping coefficient (in./in.)
c	Specific heat per unit volume (psi/°F)
χ	Strain independent probability for the remobilization of immobile dislocations
E	Young's modulus (psi)
EI	Young's modulus x moment of inertia (lb-in.^{2})
ε_{pu}	Static plastic fracture value at 1/2 cycle (in./in.)
ε_0	Maximum strain in beam during damping data collection (in./in.)
α_c	Crack growth rate constant based on dislocation theory of crack growth (in.^{7}/lb^4-cycle)

h	Beam height (in.)
k	Thermal conductivity (lb/sec-°F)
k_{ke}	Torsional stiffness at knife-edge support (lb-in.)
l_{ex}	Location of exciter relative to knife-edge support (in.)
l_a	Location of load relative to knife-edge support (in.)
Λ_0	Dislocation density for $\varepsilon_p = 0$ (disl/in.^{2})
m	Mass of beam per unit length (slug/in.)
m_{ex}	Mass of exciter and counterweight (slug)
P	Fatigue load applied to beam (lb)
σ_y	Yield stress (psi)

STEP 2. Initialize variables

$LF = 0.,$	life expended variable
$a_{old} = a_0,$	crack length
$j = 1,$	fatigue cycle counter
$\tau = \frac{h^2 c}{\pi^2 k},$	relaxation time for heat flow

STEP 3. while ($a_{old} <= a_f$)

STEP 3.1 Calculate crack length for current cycle based on

$$\int_{a_{old}}^{a_{new}} \frac{da}{K_I^4(a)} = \alpha_c$$

Begin by calculating the stress intensity factor using an empirical formula

$$f(a/h) = 1.122 - 1.4(a/h) + 7.33(a/h)^2 - 13.08(a/h)^3 + 14.0(a/h)^4,$$

or

$$f(a/h) = \left(\frac{\tan(\psi)}{\psi}\right)^{1/2} \frac{0.923 + 0.199(1 - \sin\psi)^4}{\cos\psi},$$

where $\psi = \frac{\pi a}{2h}$.

$k_c = b_c\ (h/a)^3$ torsional stiffness at crack

Rotation of beam at knife-edge support

$$\theta = -\frac{(2EI + l_a k_c)\ l_a\ P}{+EI\ (k_{ke} + k_c)},$$

Nominal bending moment between load points

$$M_{nom} = 1/2\ l_a\ P - k_{ke}\ \theta,$$

$$\sigma_{nom} = \frac{6\ M_{nom}}{h^2}, \quad \text{nominal bending stress}$$

$$K_I = \sigma_{nom}\ \sqrt{\pi a}\ f(a/h), \quad \text{stress intensity factor.}$$

STEP 3.1.1 Assume a value for a_{new}^{0}

STEP 3.1.2 Use Newton-Raphson Iteration for the i^{th} iteration of a_{new}

$$R = \int_{a_{old}}^{a_{new}} \frac{da}{K_I^4(a)} = \alpha_c, \quad \text{residual amount}$$

$$R' = \frac{1}{K_I^4(a_{new}^{i})}, \quad \text{slope of function}$$

$$a_{new}i+1 = a_{new}i - R/R', \quad i+1^{st} \text{ iteration of } a_{new}.$$

Step 3.1 requires numerical integration and Newton-Raphson iteration. This case has one equation and one unknown and should not require extensive computing.

STEP 3.2 Sum the new value of life expended

$$\Delta a = a_{new} - a_{old}, \quad \text{incremental crack growth}$$

$$\varepsilon_p = \varepsilon_{pu} \left(\frac{\Delta a}{a_f}\right)^C, \qquad \text{plastic strain}$$

$$LF \mathrel{+}= \frac{\varepsilon_p}{\varepsilon_{pu}}, \qquad \text{specimen is loaded on upstroke only}$$

STEP 3.3 Compute new plastic zone size

$$\sigma_\pi = \frac{1}{6\pi} \left(\frac{K_I(a_{new})}{\sigma_y}\right)^2 .$$

STEP 3.4 Calculate new torsional stiffness at crack

$$k_c = b_c \, (h/a)^3 .$$

STEP 3.5 Compute beam fundamental mode characteristics including eigenvalue, κ; eigenvector, $\phi(x)$; and resonant frequency, ω. The six unknowns, κ; four from $\phi(x)$: A, B, C, and D; and ω, are computed from the four boundary conditions:

$w(0) = 0,$	deflection at knife edge is zero
$EIw''(0) = k_{ke}w'(0),$	moment at knife edge is equal to the torsional stiffness x slope
$EIw''(1/2) = k_c w'(1/2),$	moment at crack is equal to the torsional stiffness x slope
$w'''(1/2) = 0,$	shear at crack is zero.

Frequency equation (ignoring the small amount of damping):

$$\omega^2 M_i - K_i = 0,$$

where

$$K_i = \int_0^1 EI[\phi_i''(x)]^2 \, dx,$$

and

$$M_i = \int_0^1 \phi_i^2(x) m(x) \, dx + \phi_i^2(l_{ex}) m_{ex}.$$

Step 3.5 requires Newton-Raphson iteration to solve the six nonlinear equations for the six unknowns. In addition, numerical integration is needed to calculate the generalized mass and stiffness. For the initial cycle, this is a time consuming process and will require 50 to 100 iterations. Subsequent cycles should have sufficiently small changes in the variables to require less than ten iterations.

STEP 3.6 Determine amplitude scaling factor

$$B = \frac{2\,\varepsilon_0}{h\kappa^2\,\phi''(1/2)},$$

$\phi(x) = B\,\phi(x)$, scale eigenvector accordingly.

STEP 3.7 Calculate plastic zone dislocation density

$$\Lambda_p = \frac{U_i}{\chi}\,[1 - \exp(-1/2\chi\varepsilon_p)] + \Lambda_0\exp(-1/2\chi\varepsilon_p).$$

STEP 3.8 Compute average amplitude-dependent damping ratio

$$\bar{\Delta}_H^c = [\Lambda_e \int_e \varepsilon^2\theta_H^c(\varepsilon)dV + \Lambda_p \int_p \varepsilon^2\theta_H^c(\varepsilon)dV]/\int \varepsilon^2 dV$$

Step 3.8 has several numerical integration computations and computes the exponential integral function inside an integral. This is a time consuming process and, along with step 3.5, will determine the overall program runtime.

STEP 3.9 Compute frequency-dependent damping ratio

$$\Delta_I = \frac{2\pi\alpha^2 ET}{c}\,\frac{\omega\tau}{1 + \omega^2\tau^2}.$$

STEP 3.10 Sum average amplitude- and frequency-dependent damping

$$\bar{\Delta} = \bar{\Delta}_H + \Delta_I.$$

STEP 3.11 Output results for (j % 100) == 0

Fatigue cycle number, j

Fatigue crack length, a_{new}

Stress intensity factor, K_I

Torsional stiffness at crack, k_c

Fraction of life expended, LF

Plastic zone size, r_p

Plastic zone strain, ε_p

Resonant frequency, ω

Average amplitude-dependent damping ratio, $\bar{\Delta}_H$

Frequency-dependent damping ratio, Δ_I

Total damping ratio, $\bar{\Delta}$

STEP 3.12 Increment fatigue cycle counter

j++

$a_{old} = a_{new}$, reset crack length variable.

STEP 4. stop

Appendix D

MATHEMATICAL COMPUTER MODEL LISTING

Table of Contents

```
/* <p> d:\lc\header\ */
/* ************************************************************************
   NAME

      dmp_crck.exe..............calculate internal damping for a beam
                                undergoing fatigue crack growth

   SYNOPSIS

      dmp_crck <data filename> [data plot filename]   execute program
                                dmp_crck with input data provided via a
                                data file

      data filename             file containing input data of beam and
                                material characteristics

      data plot filename        file containing output data for DISSPLA
                                plots on PRIME
   DESCRIPTION

      The internal damping of a beam undergoing fatigue crack growth is
      calculated based on an estimation of the plastic zone size and
      material dependent constants related to crack growth rate and
      internal damping.  The following algorithm is used to calculate
      the internal damping of a four-point beam with a propagating
      crack.

      STEP 1.  Input material and crack growth constants

         a_0            = initial crack length (in).
         a_disl         = dislocation density coefficient (disl/in^2).
         a_final        = final crack length (in).
         alpha          = linear expansion coefficient (in/in/xF).
         b_crack        = material constant relating crack length to
                          torsional stiffness (lb-in).
         c              = Manson-Coffin ductility exponent.
         c_1            = internal damping coefficient.
         c_2            = internal damping coefficient (in/in).
         c_heat         = specific heat per unit volume (psi/xF)
         chi            = strain independent probability for the
                          remobilization of immobile dislocations.
         delta_ext      = damping ratio due to external source
         e              = Young's modulus (psi).
         ei             = Young's modulus x moment of inertia (lb-in^2).
         n_max          = maximum strain in beam during damping data
                          collection (in/in).
         n_ult          = static plastic fracture value at 1/2 cycle
                          (in/in).
         g_check        = minimum crack growth before updating
                          eigenvector results (in).
         growth_rate    = crack growth rate constant based on
                          dislocation theory of crack growth
                          (in^7/lb^4-cycle).
         h              = beam height (in).
         k              = thermal conductivity (lb/sec-xF)
         k_knife_edge   = torsional stiffness at knife-edge support
                          (lb-in).
         l              = beam length
         lambda_0       = dislocatin density for n_p = 0 (disl/in^2).
         l_exciter      = location of exciter relative to knife-edge
                          support (in).
         l_load         = location of load relative to knife-edge
                          support (in).
         m_beam         = mass of beam per unit length (slug/inch).
         m_exciter      = mass of exciter and counterweight (slug).
         p              = fatigue load applied to beam (lb).
         e_yield        = yield stress (psi).
         slope_factor   = constant relating beam slope and damping.
         temperature    = ambient temperature of specimen (xF)
```

STEP 2. Initialize variables

```
a_old = a_0  crack length
j     = 1    fatigue cycle counter
life  = 0.   life expended variable
tau   = h^2*c_heat/c^2*k  relaxation parameter
```

STEP 3. while a_last <= a_final

STEP 3.1 Calculate crack length for current cycle based on

$$\int_{a\_old}^{a\_new} (da/ki^4) = growth\_rate.$$

Begin by calculating the stress intensity factor using an empirical formula

```
f(a/h) = 1.122 - 1.4*(a/h) + 7.33*(a/h)^2 -
         13.08*(a/h)^3 + 14*(a/h)^4,
```

or

```
f(a/h) = dsqrt(tan(psi)/psi)*
         (.923 + .199*(1 - sin(psi))^4/cos(psi),
```

where psi = c*a/(2*h)

```
k_crack = b_crack*(h/a)^3  torsional stiffness
                           at crack
```

Rotation of beam at knife-edge support

```
theta = (2*ei + l_load*k_crack)*l_load*p/
        (4*ei*(k_knife_edge + k_crack)
```

Nominal bending moment between load points

```
moment = .5*l_load*p - k_knife_edge*theta
e_nominal = 6*moment/h^2  nominal bending stress
ki = e_nominal*dsqrt(c*a)*f(a/h)   stress intensity
                                   factor
```

STEP 3.1.1 Assume a value for a[j][0]

STEP 3.1.2 Use Newton-Raphson Interation with

$$residual = \int_{a\_old}^{a\_new[i-1]} (da/(ki(a))^4) - growth\_rate,$$

```
slope = 1/(ki(a_new[i-1]))^4,

a_new[i] = a_old[i-1] - residual/slope.
```

This step requires numerical integration and Newton-Raphson iteration. This case has one equation and one unknown and should not require extensive computing.

STEP 3.2 Sum the new value of life expended

```
delta_a = a_new - a_old    incremental crack growth
n_p = n_ult*(a_new/a_final)^c   plastic strain
life += 2*n_p/n_ult  include 2 only if loading occurs on
                     both up and down stroke of piston
```

STEP 3.3 Compute new plastic zone size

```
r_plastic = (ki/e_yield)^2/(c*6),
```

where ki is computed from a_new.

STEP 3.4 Calculate new torsional stiffness at crack

```
k_crack = b_crack*(h/a_new)^3
```

STEP 3.5 Compute beam fundamental mode characteristics including eigenvalue, kappa, eigenvector, phi(x), and resonant frequency, omega. The six unknowns, kappa, four from phi(x) and omega, are computed from the four boundary conditions:

```
w(0) = 0  deflection at knife_edge is zero
ei*w"(0) = k_knife_edge*w'(0)  moment at knife-edge is
                               equal to the torsional
                               stiffness x slope
ei*w"(l/2) = k_crack*w'(l/2)   moment at crack is equal
                               to the torsional stiffness
                               x slope
w'''(l/2) = 0  shear at crack is zero
```

Frequency equation (ignoring the small amount of damping):

$$\text{omega}^2 * m\_general - k\_general = 0$$

where

$$m\_general = \int_0^l m\_beam*phi(x)^2\ dx + phi(l\_exciter)^2*m\_exciter$$

and

$$k\_general = \int_0^l ei[phi"(x)]^2\ dx.$$

This step requires Newton-Raphson iteration to solve the six nonlinear equations for the six unknowns. In addition, numerical integration is needed to calculate the generalized mass and stiffness. For the initial cycle, this is a time consuming process and will require 50 to 100 iterations. Subsequent cycles should have sufficiently small changes in the variables to require less than ten iterations.

STEP 3.6 Determine amplitude scaling factor

```
scale_factor = 2*n_max/(h*kappa^2*phi"(l/2))
phi(x) = scale_factor*phi(x)   scale eigenvector accordingly
```

STEP 3.7 Calculate plastic zone dislocation density

```
lambda_p = ( (a_disl/chi)*(1-exp(.5*chi*n_p) +
           dsqrt(lambda_0)*exp(.5*chi*n_p) )^2
```

STEP 3.8 Compute average amplitude-dependent damping ratio

$$delta\_h = \left(lambda\_p * \int_p n(x,z)^2 * theta\_h(n(x,z))\ dV + lambda\_0 * \int_e n(x,z)^2 * theta\_h(n(x,z))\ dV \right) \Big/ \int n(x,z)^2\ dV$$

where the functions n(x,z) and theta_h(n(x,z)) are defined by

```
            n(x,z) = z*scale_factor*kappa^2*phi"(x)
            theta_h(n(x,z)) = c_1*(c_2/n(x,z))^2*ei1(c_2/n(x,z))

         and ei1() is the exponential integral function.

      This step has several numerical integration computations and
      computes the exponential integral function inside an integral.
      This is a time consuming process and along with step 3.6 will
      determine the overall program runtime.

      STEP 3.9  Compute frequency dependent damping ratio

         delta_i = (2*c*alpha^2*e*temperature)/c_heat*
                   omega*tau/(1 + (omega*tau)^2)

      STEP 3.10  Sum average amplitude- and frequency dependent
         damping

         delta = delta_i + delta_h

      STEP 3.11  Output results for j%100 == 0:

         fatigue cycle number, j
         fatigue crack length, a_new
         stress intensity factor, ki
         torsional stiffness at crack, k_crack
         fraction of life expended, life
         plastic zone size, r_plastic
         plastic zone strain, n_p
         resonant frequency, omega
         average amplitude-dependent damping ratio, delta_h
         frequency dependent damping ratio, delta_i
         total damping ratio, delta

   STEP 4.  stop

FUNCTIONS USED

   beam_mode.................compute beam eigenvector, eigenvalue
                               and frequency
   crack_integral............compute crack length residual
   d_modal...................derivative of beam characteristic
                               equation coefficients
   da_dn.....................change in crack length as a function of
                               fatigue cycle number
   data_plot.................output to file data for DISSPLA plot
   data_print................output to screen data printout
   ddphi.....................second derivative of beam
                               characteristic equation with respect
                               to the beam coordinate
   dexp......................Lattice SSP exponential function
   dsqrt.....................Lattice SSP square root function
   ezb_limit.................starting limit for second integration
                               of multiple integration
   eze_limit.................ending limit for second integration of
                               multiple integration
   strain2...................strain squared function
   n2_theta_h................strain squared, amplitude dependent
                               damping function
   f.........................stress intensity factor empirical
                               formula for pure bending
   get_data..................input material data from file
   input_print...............print input data to screen
   ki........................stress intensity factor
   mat_assign................MATRIX structure assignment function
   modal.....................beam characteristic equation
                               coefficients
   multi_al..................multiple integral algorithm
   newton_raphson............solves nonlinear equation using Newton-
```

```
                                    Raphson algorithm
      phi.......................beam characteristic equation
      phi2......................square of beam characteristic equation
      power.....................Lattice SSP power function
      pzb_limit.................starting limit for second integration
                                    of multiple integration
      pze_limit.................ending limit for second integration of
                                    multiple integration
      simpson...................numerical integration using Simpson's
                                    rule

   REFERENCES

      Burden, R.L. and Faires, J.D.  "Numerical Analysis," third
      edition, Prindle, Weber and Schmidt, Boston, 1984, pp. 153-
      195.

      Frost, N.E., Marsh, K.J. and Pook, L.P.  "Metal Fatigue,"
      Clarendon Press, Oxford, 1974, pp 234-235.

      Harris, C.M. and Crede, C.V. (eds).  Shock and Vibration Handbook,
      2nd edition, McGraw-Hill, New York, pp. 7-13 through 7-15, 1976.

      Hoag, A.L. and McNeese, D.C.  Engineering and Technical Handbook,
      Prentice-Hall, Inc., Englewood Cliffs, NJ, 1957, p. 176.

      Povolo, F.  "On the Granato-Lucke expression for the amplitude-
      dependent damping," Scripta Metallurgica, vol. 9, pp. 865-872.

      Thomson, W.T.  "Theory of Vibration with Applications," Prentice-
      Hall, Inc. Englewood Cliffs, NJ, 1972.

   AUTHOR:   Rick Jones
   VERSION:  1.0
   DATE:     11 AUG 1987

********************************************************************** */

#include <stdio.h>
#include <math.h>
#include <numeric.h>
#include <storage.h>

#define cube(x) ((x)*(x)*(x))     /* cube function */
#define sqr(x) ((x)*(x))          /* square function */
#define quad(x) sqr(x)*sqr(x)     /* fourth power function */
#define PVERSION "1.0"            /* program version number */
#define PDATE "11 AUG 1987"       /* program date */
/* program title */
#define PTITLE "Internal damping vs. crack propagation model"
#define MAX_INT 6                 /* number of integers input from file */
#define MAX_REAL 36               /* number of reals input from file */

unsigned _STACK = 4096;           /* stack size */

main( argc, argv )
int argc;
char *argv[];
{
   double a_0, a_disl, a_final, a_new, a_old, b_crack, c, c_1, c_2, c_heat;
   double chi, delta, delta_crack, delta_ext, delta_h, delta_i, depth, e;
   double ei, g_check, g_last, gen_mass, growth_rate, h, k, kappa, k_crack;
   double k_knife_edge, l, lambda_0, lambda_p, l_exciter, life, l_load;
   double m_beam, m_exciter, moment, omega, p, r_plastic, sif, slope_factor;
   double tau, temperature, theta, toler;
   double alpha, n_max, n_p, n_ult, e_nominal, e_yield;

   /* double arrays */
   double crack[9], ez_limit[2], input_real[MAX_REAL], mode_data[8];
```

```
double phi_data[5], plot_pak[7], print_pak[12], pz_limit[2], theta_h[7];
double theta_p[7];

/* double functions */
double crack_integral(), da_dn(), ddphi(), dexp(), dphi(), dsqrt();
double ezb_limit(), eze_limit(), f(), ki(), multi_al();
double newton_raphson(), power(), pzb_limit(), pze_limit(), simpson();
double strain(), strain2(), n2_theta_h(), phi(), phi2();

D_SUPPLD a_fun, da_fun, e_begin, e_end, e_fun, p_begin, p_end, p_fun;
D_SUPPLD n_begin, n_end, n_fun, h_fun;
FILE *f1, *f2;
FILE *fopen();
int data_rate, i, j, m, maxum, n;
int input_int[MAX_INT];
int data_plot(), fclose(), get_data();
MATRIX mode;
MATRIX beam_mode(), d_modal(), mat_assign(), modal();
M_SUPPLD m_fun, dm_fun;
unsigned int is_type_sif, is_plot_file;
void data_print(), input_print();

printf( "     Title:  %s\n", PTITLE );
printf( "   version:  %s\n", PVERSION );
printf( "      Date:  %s\n\n", PDATE );

/* check for data file in command line */
if( ( argc < 2 ) || ( argc > 3 ) ) {   /* invalid number of data files */
   printf( " \n Usage: programname filename [output filename]" );
   exit( 1 );
}

/* open data file */
if( ( f1 = fopen( argv[1], "r" ) ) == NULL ) {
   printf( " Cannot open %s\n", argv[1] );
   exit( 1 );
}

/* make or overwrite output file */
is_plot_file = FALSE;         /* do not output to file */
if ( argc == 3 ) {
   if ( ( f2 = fopen( argv[2], "w" ) ) == NULL ) {
      printf( " Cannot open %s\n", argv[2] );
      exit( 1 );
      }
   else {
      is_plot_file = TRUE;    /* output to file */
      printf( " Creating data output file %s\n\n", argv[2] );
  }

}

/* STEP 1.  Input material and crack growth constants

   in addition to material and crack growth constants, the following
   program control data must also be input:

   data_ ate   = number of fatigue cycles between data output
   is_type_sif = 0 for constant load
                 1 for constant stress intensity factor
   j           = initial cycle number
   m           = number of subintervals for integration
   maxum       = number of iteration cycles
   n           = number of subintervals for second integration
   toler       = accuracy tolerance for Newton-Raphson iteration  */

if (  get_data( f1, input_int, input_real ) ) {
   printf( " Error in data input from %s\n", argv[1] );
   exit( 1 );
```

```
}

if ( fclose( f1 ) )              /* finished with input file */
   {
   printf( " Error in closing input data file %s\n", argv[1] );
   exit( 1 );                    /* could not close data file */
   }

/* print input data to screen */
input_print( input_int, input_real );

/* set constants from input file */
a_0             = input_real[0];
a_disl          = input_real[1];
a_final         = input_real[2];
alpha           = input_real[3];
b_crack         = input_real[4];
c               = input_real[5];
c_1             = input_real[6];
c_2             = input_real[7];
c_heat          = input_real[8];
chi             = input_real[9];
data_rate       = input_int[0];
delta_ext       = input_real[10];
e               = input_real[11];
ei              = input_real[12];
n_max           = input_real[13];
n_ult           = input_real[14];
g_check         = input_real[15];
growth_rate     = input_real[16];
h               = input_real[17];
is_type_sif     = input_int[1];
j               = input_int[2];
k               = input_real[18];
k_knife_edge    = input_real[19];
l               = input_real[20];
l_exciter       = input_real[21];
l_load          = input_real[22];
lambda_0        = input_real[23];
m               = input_int[3];
maxum           = input_int[4];
m_beam          = input_real[24];
m_exciter       = input_real[25];
n               = input_int[5];
p               = input_real[26];
e_yield         = input_real[27];
slope_factor    = input_real[28];
temperature     = input_real[29];
toler           = input_real[30];

/* STEP 2.  Initialize variables */

a_old         = a_0;             /* crack length */
depth         = 0.5;             /* plastic zone depth factor */
g_last        = 0.;              /* eigenvector update parameter */
life          = 0.;              /* life expended variable */
phi_data[4]   = 1.;              /* assume an initial scale factor of 1 */
tau           = sqr( h/PI )*c_heat/k;  /* relaxation constant */
mode          = mat_assign( 5, 1, NULL );  /* set aside memory for the
                                              beam mode characteristics */

/* initial guess of mode variables */
for ( i = 0; i < 5; i++ )
   mode.element[i] = input_real[31 + i];

a_fun.funct  = crack_integral; /* crack length integral function pointer */
da_fun.funct = da_dn;          /* da/dN function pointer */
a_fun.coeff  = crack;          /* the same coefficients are required to   */
da_fun.coeff = crack;          /* calculate the crack length and the      */
```

```
crack[0]     = b_crack;       /* da/dN function.                          */
crack[1]     = ei;            /* pass seven coefficients to a_fun &       */
crack[2]     = growth_rate;   /* df_fun.                                  */
crack[3]     = h;             /* these coefficents calculate e_nominal    */
crack[4]     = k_knife_edge;  /* which is used to determine the stress    */
crack[5]     = l_load;        /* intensity factor on which the functions  */
crack[6]     = p;             /* are based.                               */
crack[7]     = (double) m;    /* number of subdivisions for integration   */

m_fun.funct  = modal;         /* beam mode characteristics equations      */
dm_fun.funct = d_modal;       /* derivative of characteristics equations  */
m_fun.coeff  = mode_data;     /* the same coefficients are required to    */
dm_fun.coeff = mode_data;     /* calculate the characteritics equations   */
mode_data[0] = k_knife_edge;  /* and their derivatives.  knife-edge       */
mode_data[2] = l;             /* stiffness.  beam length                  */
mode_data[3] = m_beam;        /* beam mass per unit length                */
mode_data[4] = m_exciter;     /* mass of exciter                          */
mode_data[5] = ei;            /* modulus and moment of inertia            */
mode_data[6] = l_exciter;     /* position of exciter relative to knife-   */
                              /* edge                                     */
mode_data[7] = (double) m;    /* number of subdivisions for integration   */

e_begin.funct = ezb_limit;    /* lower elastic limit function             */
e_end.funct   = eze_limit;    /* upper elastic limit function             */
e_fun.funct   = n2_theta_h;   /* strain squared x amplitude-dependent     */
e_begin.coeff = ez_limit;     /* damping function                         */
e_end.coeff   = ez_limit;
e_fun.coeff   = theta_h;
ez_limit[0]   = 0.;           /* lower elastic limit is 0.                */
ez_limit[1]   = h/2.;         /* upper elastic limit is one half h        */
theta_h[0]    = c_1;          /* internal damping coefficient             */
theta_h[1]    = c_2;          /* internal damping coefficient             */

p_begin.funct = pzb_limit;    /* lower plastic limit function             */
p_end.funct   = pze_limit;    /* upper plastic limit function             */
p_fun.funct   = n2_theta_h;   /* strain squared x amplitude-dependent     */
p_begin.coeff = pz_limit;     /* damping function                         */
p_end.coeff   = pz_limit;
p_fun.coeff   = theta_p;
theta_p[0]    = c_1;          /* internal damping coefficient             */
theta_p[1]    = c_2;          /* internal damping coefficient             */

n_begin.funct = ezb_limit;    /* use elastic functions for integrating    */
n_end.funct   = eze_limit;    /* strain over the volume of the beam       */
n_fun.funct   = strain2;      /* strain                                   */
n_begin.coeff = ez_limit;
n_end.coeff   = ez_limit;
n_fun.coeff   = phi_data;     /* use coefficients of ddphi                */

h_fun.funct   = phi2;         /* beam characteristic equation             */
h_fun.coeff   = phi_data;     /* eigenvector data                         */

/* calculate constant stress intensity factor */
k_crack = b_crack*cube( h/a_old );  /* torsional stiffness at crack */

/* Rotation of beam at knife-edge support */
theta = ( 2.*ei + l_load*k_crack )*l_load*p/
        ( 4.*ei*( k_knife_edge + k_crack ) );

/* Nominal bending moment between load points */
moment    = .5*l_load*p - k_knife_edge*theta;
e_nominal = 6.*moment/sqr(h);  /* nominal bending stress */

sif = ki( a_old, h, e_nominal );    /* constant stress intensity
                                       factor */
r_plastic = sqr( sif/e_yield )/(PI*6.);   /* constant plastic zone
                                             radius */

/* STEP 3.  while a_old <= a_final */
```

```
while ( a_old <= a_final ) {

   /* STEP 3.1  Calculate crack length for current cycle */

      /* STEP 3.1.1  Assume a value for a_new */
   a_new = a_old + growth_rate*quad( sif );

   if ( !( is_type_sif ) )

      {
      /* constant fatigue load */
      /* STEP 3.1.2  Use Newton-Raphson Interation */
      crack[8] = a_old;          /* lower limit of integral */
      a_new    = newton_raphson( a_new, maxum, toler, a_fun, da_fun );

      }

   /* STEP 3.2  Sum the new value of life expended */
   n_p     = n_ult*power( ( a_new - a_old )/a_final, c );  /* plastic
                                                              strain */
   life   += power( n_p/n_ult, 1./c );  /* include 2 only if loading
                                           occurs on both up and down
                                           stroke of piston */

   /* STEP 3.3  Calculate new torsional stiffness at crack */
   k_crack = b_crack*cube( h/a_new );
   mode_data[1] = k_crack;        /* pass on crack stiffness */

   if ( is_type_sif )
      {
      /* calculate new load */
      e_nominal = sif/( dsqrt( PI*a_new )*f( a_new/h ) );   /* nominal
                                                               bending
                                                               stress */
      moment    = sqr( h )*e_nominal/6.;  /* nominal bending moment */
      p         = 4.*ei*( k_crack + k_knife_edge )*moment/
                  ( ( 2.*ei - l_load*k_knife_edge )*l_load*k_crack );
      }
   else
      {
      /* for constant load, calculate new plastic zone radius
         Rotation of beam at knife-edge support */
      theta = ( 2.*ei + l_load*k_crack )*l_load*p/
              ( 4.*ei*( k_knife_edge + k_crack ) );

      /* Nominal bending moment between load points */
      moment    = .5*l_load*p - k_knife_edge*theta;
      e_nominal = 6.*moment/sqr( h );  /* nominal bending stress */

      /* STEP 3.4  Compute new plastic zone size */

      r_plastic = sqr( ( sif = ki( a_new, h, e_nominal ) ) /e_yield )/
                  (PI*6.);
      }

   /* STEP 3.5  Compute beam fundamental mode characteristics
   including eigenvalue, kappa, eigenvector, phi(x), and resonant
   frequency, omega.  Use the nonlinear system of equations function
   to solve this 5 equation system.  Assign the vector x as follows

      element[0] - eigenvalue, kappa
      element[1] - resonant frequency, omega
      element[2] - B coefficient
      element[3] - C coefficient
      element[4] - D coefficient

   where phi(x) = cos( kappa*x ) + B*sin( kappa*x ) +
                  C*cosh( kappa*x ) + D*sinh( kappa*x ),
```

```
and ddphi(x) = sqr( kappa )*( -cos( kappa*x ) - B*sin( kappa*x ) +
               C*cosh( kappa*x ) + D*sinh( kappa*x ) ) */

if ( abs( a_new - g_last ) > g_check )  /* only update for large
                                           crack growth */
   {
   mode   = beam_mode( mode, maxum, toler, m_fun, dm_fun );
   g_last = a_new;         /* reset crack length of last update */

   kappa = mode.element[0];      /* eigenvalue */
   omega = mode.element[1];      /* resonant frequency */

   /* STEP 3.6  Determine amplitude scaling factor */
   phi_data[0]  = kappa;
   phi_data[1]  = mode.element[2];
   phi_data[2]  = mode.element[3];
   phi_data[3]  = mode.element[4];
   phi_data[4]  = 1.;
   phi_data[4]  = n_max/strain( l, .5*h, phi_data );

   /* STEP 3.7  Calculate plastic zone dislocation density */
   lambda_p = ( a_disl/chi )*( 1 - dexp( -.5*chi*n_p ) ) +
              dsqrt( lambda_0 )*dexp( -.5*chi*n_p );
   lambda_p = sqr( lambda_p );

   /* STEP 3.8  Compute average amplitude-dependent damping ratio

         delta_h = ( lambda_0*t n(x,z)^2*theta_h(n(x,z)) dV +
                              up

                   lambda_0*t n(x,z)^2*theta_h(n(x,z)) dV )/
                            ue

                   t n(x,z)^2 dV
                   u

         where the functions n(x,z) and t eta_h(n(x,z)) are defined by

            n(x,z) = z*scale_factor*kappa^2*h"(x)
            theta_h(n(x,z)) = c_1*(c_2/n(x,z))^2*ei1(c_2/n(x,z))

        and ei1() is the exponential integral function. */

   /* check size of plastic zone relative to remaining section depth */
   if ( ( pz_limit[0] = 0.5*(h - a_new) - r_plastic ) < 0.0 )
      /* r_plastic is too large for remaining section depth */
      {
      r_plastic = 0.5*(h - a_new);  /* r_plastic is half of
                                       remaining section depth    */
      pz_limit[0] = 0.0;            /* treat plastic zone as full
                                       depth of section           */
      depth       = 1.0;
      }
   pz_limit[1]   = 0.5*(h - a_new); /* upper plastic limit is one
                                       half h less crack length   */

   theta_h[2]  = kappa;             /* eigenvalue                 */
   theta_h[3]  = mode.element[2];   /* phi(x) coefficient B       */
   theta_h[4]  = mode.element[3];   /* phi(x) coefficient C       */
   theta_h[5]  = mode.element[4];   /* phi(x) coefficient D       */
   theta_h[6]  = phi_data[4];       /* amplitude scale factor     */

   theta_p[2]  = kappa;             /* eigenvalue                 */
   theta_p[3]  = mode.element[2];   /* phi(x) coefficient B       */
   theta_p[4]  = mode.element[3];   /* phi(x) coefficient C       */
   theta_p[5]  = mode.element[4];   /* phi(x) coefficient D       */
   theta_p[6]  = .25*sqr( h/pz_limit[1] )*phi_data[4];
                                    /* amplitude scale factor
```

```
                                        adjusted for reduced cross-
                                        section in plastic zone     */

   delta_h = ( multi_al( 0., l, m, n, e_begin, e_end, e_fun ) +
             depth*( ( lambda_p - lambda_0 )/lambda_0 )*
             multi_al( l - r_plastic, l, m, n, p_begin, p_end, p_fun ) )/
             multi_al( 0., l, m, n, n_begin, n_end, n_fun );

   /* STEP 3.9  Compute frequency dependent damping ratio */

   delta_i = (2.*PI*sqr( alpha )*e*temperature)/c_heat*
                  omega*tau/( 1 + sqr( omega*tau ) );

   /* calculate damping due to crack surfaces based on slope of beam at
      crack */
   delta_crack = slope_factor*abs( dphi( l, phi_data ) );

   /* STEP 3.10  Sum average amplitude- and frequency dependent
      damping.  Also, sum external and crack related damping */

   delta   = delta_crack + delta_ext + delta_i + delta_h;
   }                       /* end of update block */

/* STEP 3.11  Output results for j % data_rate == 0:

      fatigue cycle number, j
      fatigue crack length, a_new
      stress intensity factor, ki
      torsional stiffness at crack, k_crack
      fraction of life expended, life
      plastic zone size, r_plastic
      plastic zone strain, n_p
      resonant frequency, omega
      average amplitude-dependent damping ratio, delta_h
      frequency dependent damping ratio, delta_i
      total damping ratio, delta */

if ( ( j % data_rate ) == 0 ) {
   if ( is_plot_file ) {

      plot_pak[0]  = p;            /* fatigue load              */
      plot_pak[1]  = e_nominal/e;  /* fatigue nominal strain    */
      plot_pak[2]  = a_new;        /* fatigue crack length      */
      plot_pak[3]  = sif;          /* stress intensity factor   */
      plot_pak[4]  = delta;        /* total internal damping    */
      plot_pak[5]  = omega/(2.*PI);  /* resonant frequency (hz) */
      /* compute ratio of max beam strain to input forcing function.
         generalized mass */
      gen_mass     = m_beam*simpson( 0., l, m, h_fun ) +
                     m_exciter*phi2( l_exciter, phi_data );
      plot_pak[6]  = n_max*abs( phi( l_exciter, phi_data ) )/
                   ( 2.*delta*sqr( omega*gen_mass ) );
      if ( data_plot( f2, j, plot_pak ) != 0 )  /* output results in
                                                   plot format */
         {
         printf( "File write error in main\n" );
         exit( 1 );
         }

   } else {

      print_pak[0]  = a_new;       /* fatigue crack length          */
      print_pak[1]  = sif;         /* stress intensity factor       */
      print_pak[2]  = k_crack;     /* torsional stiffness at crack  */
      print_pak[3]  = life;        /* fraction of life expended     */
      print_pak[4]  = r_plastic;   /* plastic zone size             */
      print_pak[5]  = n_p;         /* plastic zone strain           */
      print_pak[6]  = omega;       /* resonant frequency            */
      print_pak[7]  = delta_h;     /* amplitude-dependent damping   */
```

```
            print_pak[8]  = delta_i;     /* frequency dependent damping   */
            print_pak[9]  = delta_crack; /* crack dependent damping       */
            print_pak[10] = delta;       /* total damping ratio           */
            print_pak[11] = p;           /* fatigue load                  */
            data_print( j, print_pak );  /* put results on screen         */

         }
      }

      a_old = a_new;              /* increment crack length */
      ++j;                        /* increment cycle counter */
   }                              /* end of while loop */

   if ( is_plot_file )
      if ( fclose( f2 ) )            /* finished with output file */
         {
         printf( " Error in closing output data file %s\n", argv[2] );
         exit( 1 );                  /* could not close output file */
         }

   /* STEP 4.  stop */

   printf( " Normal exit\n" );
   exit( 0 );

}
```

```
/* <p> d:\lc\header\ */

/* ************************************************************************

   This set of routines provides specific support for the program
   dmp_crck.  These functions are for use with dmp_crck only and may
   require modification to work with other programs.

      beam_mode.................compute beam eigenvector, eigenvalue
                                  and frequency
      crack_integral............compute crack length residual
      d_modal...................derivative of beam characteristic
                                  equation coefficients
      da_dn.. ..................change in crack length as a function of
                                  fatigue cycle number
      data_plot.................output to file data for DISSPLA plot
      data_print................output to screen data printout
      dddphi....................third derivative of beam characteristic
                                  equation with respect to the beam
                                  coordinate
      ddphi.....................second derivative of beam
                                  characteristic equation with respect
                                  to the beam coordinate
      ddphi2....................square of second derivative of beam
                                  characteristic equation with respect
                                  to the beam coordinate
      dphi......................first derivative of beam characteristic
                                  equation with respect to the beam
                                  coordinate
      ezb_limit.................starting limit for second integration
                                  of multiple integration
      eze_limit.................ending limit for second integration of
                                  multiple integration
      f.........................empirical formula for stress intensity
                                  factor in pure bending
      get_data..................input material data from file
      input_print...............print input data on screen
      ki........................stress intensity factor for pure
                                  bending
      modal.....................beam characteristic equation
                                  coefficients
      strain2...................strain squared function
      n2_theta_h................strain squared, amplitude dependent
                                  damping function
      phi.......................beam characteristic equation
      phi2......................square of beam characteristic equation
      pzb_limit.................starting limit for second integration
                                  of multiple integration
      pze_limit.................ending limit for second integration of
                                  multiple integration
      strain....................beam strain function

************************************************************************ */

#include <stdio.h>
#include <math.h>
#include <numeric.h>
#include <storage.h>

#define cube(x) ((x)*(x)*(x))     /* cube function */
#define sqr(x) ((x)*(x))          /* square function */
#define quad(x) sqr(x)*sqr(x)     /* fourth power function */
#define MAX_INT 6                 /* number of integers input from file */
#define MAX_REAL 36               /* number of reals input from file */
```

```
MATRIX beam_mode( mode, maxum, toler, mode_fun, dmode_fun)
/* ************************************************************************
   NAME

      beam_mode.................Compute beam fundametal characteristics
                                including eigenvalue, eigenvector, and
                                resonant frequency

   SYNOPSIS

      include <numeric.h>

      mode = beam_mode( mode, maxum, toler, mode_fun, dmode_fun);  beam
                                   characteristics computed by Newton-
                                   Raphson iteration

      MATRIX mode;                 vector containing initial guess of
                                      characteristics as input, and final
                                      solution values as output
      int maxum;                   maximum number of Newton-Raphson
                                      iterations
      double toler;                accuracy tolerance on final solution
      M_SUPPLD mode_fun,           user supplied beam characteristic
                                      equations and coefficients
               dmode_fun;          user supplied derivative of beam
                                      characteristic equations and
                                      coefficients

   DESCRIPTION

      A vibrating beam has four boundary conditions and an equation of
      motion.  Applying the Newton-Raphson iteration algorithm to these
      five equations results in a solution for the eigenvalue,
      eigenvector and resonant frequency.

   FUNCTIONS USED


   REFERENCES

      Burden, R.L. and Faires, J.D.  "Numerical Analysis," third
      edition, Prindle, Weber and Schmidt, Boston, 1984, pp. 153-
      195.

      Harris, C.M. and Crede, C.V. (eds).  Shock and Vibration Handbook,
      2nd edition, McGraw-Hill, New York, pp. 7-13 through 7-15, 1976.

      Thomson, W.T.  "Theory of Vibration with Applications," Prentice-
      Hall, Inc. Englewood Cliffs, NJ, 1972.

   AUTHOR:   Rick Jones
   VERSION:  1.0
   DATE:     18 AUG 1987

************************************************************************ */

double toler;
int maxum;
MATRIX mode;
M_SUPPLD dmode_fun, mode_fun;
   {
   MATRIX newton();

   /* begin newton-raphson iterative solution */
   mode = newton( mode, maxum, toler, mode_fun, dmode_fun );

   /* check for convergence */
   if ( mat_err == TRUE )
      printf( "newton solution failed to converge \n" );
```

```
   /* return vector solution */
   return ( mode );

   }


double crack_integral( a, co )
/* ************************************************************************
   NAME

      crack_integral.............computes crack length residual integral
                                 using Simpson's Rule

   SYNOPSIS

      include <numeric.h>

      delta_a = crack_integral( a, co );  Compute crack length residual
                                            from integral of da/dN relation

      double a,                  crack length guess
             *co,                array of coefficients for use in function
             delta_a;            residual due to error in estimate of a

   DESCRIPTION

      This function uses Simpson's rule to calculate an increase in the
      crack length integral.  The function then computes the error in the
      crack length integral increase by subtracting the known solution
      from the numerical integration value.  The resulting error is
      returned to the calling function.

                   ta_new
         residual = 3      (da/(ki(a))^4) - growth_rate,
                   ua_old

         co[0]     = b_crack
         co[1]     = ei
         co[2]     = growth_rate
         co[3]     = h
         co[4]     = k_knife_edge
         co[5]     = l_load
         co[6]     = p
         co[7]     = (double) m
         co[8]     = a_old

   FUNCTIONS USED

      da_dn......................change in crack length at a function of
                                    fatigue cycle number
      simpson....................numerical integration using Simpson's
                                 rule

   REFERENCES

      Frost, N.E., Marsh, K.J. and Pook, L.P.  "Metal Fatigue,"
      Clarendon Press, Oxford, 1974, pp 234-235.

   AUTHOR:   Rick Jones
   VERSION:  1.0
   DATE:     18 AUG 1987

************************************************************************** */
double a, *co;
{
   double da_dn(), simpson();
   D_SUPPLD da_fun;
```

```
   da_fun.funct = da_dn;          /* da/dN function pointer */
   da_fun.coeff = co;             /* da/dN array pointer    */


   /* return integral - crack growth constant */
   return ( simpson( co[8], a, ( int ) co[7], da_fun ) - 1. );
}



MATRIX d_modal( x, co, df )
/* ************************************************************************
   NAME

      d_modal.....................computes the matrix of coefficient
                                  derivatives for Newton_Raphson
                                  iteration

   SYNOPSIS

      include <numeric.h>

      df = d_modal( x, co, df ); compute derivative matrix of nonlinear
                                  equation coefficients

      double *co;                pointer to array of coefficient
                                    parameters
      MATRIX x,                  vector of solution values
             dx;                 matrix containing derivative terms of
                                    nonlinear equation coefficients

   DESCRIPTION

      User supplied routine to calculate the partial derivatives of the
      nonlinear system of equations as a function of x with modifiable
      coefficients

         co[0] = k_knife_edge;  knife-edge stiffness
         co[1] = k_crack;       crack stiffness
         co[2] = l;             beam length
         co[3] = m_beam;        beam mass per unit length
         co[4] = m_exciter;     mass of exciter
         co[5] = ei;            modulus and moment of inertia
         co[6] = l_exciter;     position of exciter relative to knife-
                                edge
         co[7] = (double) m;    number of subdivisions for integration

   FUNCTIONS USED

      coeff_red..................reduction of coefficients
      d_coeff....................partial derivative of coefficient reduction
      d_determ...................partial derivative of determinate
      dcos.....................  .....Lattice SSP cosine function
      dcosh......................Lattice SSP hyperbolic cosine function
      dsin.......................Lattice SSP sine function
      dsinh......................Lattice SSP hyperbolic sine function
      mat_assign.................assign matrix structure
      mat_delete.................delete matrix storage space

   REFERENCES

      Burden, R.L. and Faires, J.D.  "Numerical Analysis," third
      edition, Prindle, Weber and Schmidt, Boston, 1984, pp. 153-
      195.

   AUTHOR:   Rick Jones
   VERSION:  1.0
   DATE:     18 AUG 87
```

```
********************************************************************** */

MATRIX df, x;
double *co;
{
   double ch_ei, c_ei, eigen, gen_mass, gen_stiff;
   double sh_ei, s_ei, stiff_c, stiff_ke;
   double phi_data[5];
   double d_determ(), ddphi2(), p2k(), p2kb(), p2kc(), p2kd(), p2m();
   double p2mb(), p2mc(), p2md(), phi2();
   double dcos(), dcosh(), dsin(), dsinh();
   int i;
   D_SUPPLD ddh_fun[5], h_fun[5];
   MATRIX a, a_p, coeff, coeff_p;
   MATRIX coeff_red(), d_coeff(), mat_assign(), mat_delete();

   /* user supplied equations for beam analysis */

   eigen         = x.element[0]*co[2];       /* eigenvalue * length        */
   ch_ei         = dcosh( eigen );
   c_ei          = dcos( eigen );
   sh_ei         = dsinh( eigen );
   s_ei          = dsin( eigen );
   stiff_c       = co[1]/( x.element[0]*co[5] ); /* characteristic stiffness
                                                    at crack               */
   stiff_ke      = co[0]/( x.element[0]*co[5] ); /* characteristic stiffness
                                                    at boundary            */

   /* characteristic equation coefficients */
   phi_data[0]   = x.element[0];
   phi_data[1]   = x.element[2];
   phi_data[2]   = x.element[3];
   phi_data[3]   = x.element[4];
   phi_data[4]   = 1.;            /* use scale factor of 1                  */

   /* create a matrix and partial derivative matrices */
   a             = mat_assign( 4, 4, NULL );
   a_p           = mat_assign( 4, 4, NULL );

   /* fill a matrix */
   a.element[ 0] = 1 ;
   a.element[ 1] = 1.;
   a.element[ 2] = -( c_ei + stiff_c*s_ei );
   a.element[ 3] = s_ei;
   a.element[ 4] = 0.;
   a.element[ 5] = stiff_ke;
   a.element[ 6] = -s_ei + stiff_c*c_ei;
   a.element[ 7] = -c_ei;
   a.element[ 8] = 1.;
   a.element[ 9] = -1.;
   a.element[10] = ch_ei + stiff_c*sh_ei;
   a.element[11] = sh_ei;
   a.element[12] = 0.;
   a.element[13] = stiff_ke;
   a.element[14] = sh_ei + stiff_c*ch_ei;
   a.element[15] = ch_ei;

   /* partials with respect to eigenvalue */
   a_p.element[ 0] = 0.;
   a_p.element[ 1] = 0.;
   a_p.element[ 2] = co[2]*( ( 1. + stiff_c/eigen )*s_ei - stiff_c*c_ei );
   a_p.element[ 3] = co[2]*c_ei;
   a_p.element[ 4] = 0.;
   a_p.element[ 5] = -co[2]*stiff_ke/eigen;
   a_p.element[ 6] = -co[2]*( ( 1. + stiff_c/eigen )*c_ei + stiff_c*s_ei );
   a_p.element[ 7] = co[2]*s_ei;
   a_p.element[ 8] = 0.;
   a_p.element[ 9] = 0.;
```

```
a_p.element[10] = co[2]*( ( 1. - stiff_c/eigen )*sh_ei + stiff_c*ch_ei );
a_p.element[11] = co[2]*ch_ei;
a_p.element[12] = 0.;
a_p.element[13] = -co[2]*stiff_ke/eigen;
a_p.element[14] = co[2]*( ( 1. - stiff_c/eigen )*ch_ei + stiff_c*sh_ei );
a_p.element[15] = co[2]*sh_ei;

/* 0 partial differential matrix */
for ( i = 0; i <= 24; ++i )
   df.element[i] = 0.;

/* partial derivatives of first equation with respect to eigenvalue.
   all other partials of first equation are 0 */
df.element[0] = d_determ( a, a_p );

/* get coefficients and partials */
coeff      = mat_assign( 4, 1, NULL );
coeff_p    = mat_assign( 4, 1, NULL );

/* fill coefficients in terms of coeff[0] */
coeff      = coeff_red( a, coeff );
coeff_p    = d_coeff( a, a_p, coeff_p );

/* setup array of functions for partial derivatives of generalized mass
   and stiffness */

h_fun[0].funct   = p2m;       /* mass with respect to eigenvalue */
ddh_fun[0].funct = p2k;       /* stiffness with respect to eigenvalue */
h_fun[1].funct   = phi2;      /* mass with respect to frequency */
h_fun[2].funct   = p2mb;      /* mass with respect to coefficient B */
ddh_fun[2].funct = p2kb;      /* stiffness with respect to eigenvalue B */
h_fun[3].funct   = p2mc;      /* mass with respect to coefficient C */
ddh_fun[3].funct = p2kc;      /* stiffness with respect to coefficient C */
h_fun[4].funct   = p2md;      /* mass with respect to coefficient D */
ddh_fun[4].funct = p2kd;      /* stiffness with respect to coefficient D */

/* pass coefficients to integration functions */
for ( i = 0; i < 5; i++ )
   {
   h_fun[i].coeff   = phi_data;
   ddh_fun[i].coeff = phi_data;

   /* partial of beam mass */
   gen_mass      = co[3]*simpson( 0., co[2], (int) co[7], h_fun[i] ) +
                        co[4]*(*h_fun[i].funct)( co[6], phi_data );

   if ( i == 1 )
      /* partial derivative of equation 2 with respect to frequency */
      df.element[6] = 2.*x.element[1]*gen_mass;

   else
      {
      /* partial of beam stiffness */
      gen_stiff     = co[5]*simpson( 0., co[2], (int) co[7], ddh_fun[i] );

      /* partial derivatives */
      df.element[1 + 5*i] = sqr( x.element[1] )*gen_mass - gen_stiff;
      }
   }

/* third - fifth equations, derivative with respect to eigenvalue */
for ( i = 1; i <= 3; ++i ) {
   df.element[i+1] = coeff_p.element[i];
}

/* third - fifth equations, mode shape coefficients */
df.element[12] = -1.;
df.element[18] = -1.;
df.element[24] = -1.;
```

```
   /* release storage */
   a             = mat_delete( a );
   a_p           = mat_delete( a_p );
   coeff         = mat_delete( coeff );
   coeff_p       = mat_delete( coeff_p );

   return ( df );
}



double da_dn( a, co )
/* ************************************************************************
   NAME

      da_dn.....................crack growth per fatigue cycle

   SYNOPSIS

      rate = da_dn( a, co );     crack growth rate per fatigue cycle

      double a,                  crack length estimate
             *co,                array of material coefficients
             rate;               crack growth rate

   DESCRIPTION

      Compute crack growth rate based on dislocation theory.  The
      relation is

         da/dN = alpha*KI^4

      where KI is the stress intensity factor and alpha is a material
      dependent constant.  The function ki is used in the computation
      of the stress intensity factor.  ki requires the following
      calculations

         Calculate new torsional stiffness at crack
         k_crack = b_crack*cube( ( h/a_new ) );

         Rotation of beam at knife-edge support
         theta = ( 2.*ei + l_load*k_crack )*l_load*p/
              ( 4.*ei*( k_knife_edge + k_crack ) );

         Nominal bending moment between load points
         moment    = .5*l_load*p - k_knife_edge*theta;
         e_nominal = 6.*moment/sqr(h);   nominal bending stress

         co[0]     = b_crack
         co[1]     = ei
         co[2]     = growth_rate
         co[3]     = h
         co[4]     = k_knife_edge
         co[5]     = l_load
         co[6]     = p
         co[7]     = (double) m
         co[8]     = a_old

      Express the relation in the form

         da/alpha*KI^4 = dN

   FUNCTIONS USED

      ki.........................compute stress intensity factor

   REFERENCES
```

```
      Frost, N.E., Marsh, K.J. and Pook, L.P.  "Metal Fatigue,"
      Clarendon Press, Oxford, 1974, pp 234-235.

   AUTHOR:   Rick Jones
   VERSION:  1.0
   DATE:     18 AUG 1987

************************************************************************ */
double a, *co;
{
   double k_crack, moment, e_nominal, theta;
   double ki();

   /* Calculate new torsional stiffness at crack */
   k_crack = co[0]*cube( co[3]/a );

   /* Rotation of beam at knife-edge support */
   theta = ( 2.*co[1] + co[5]*k_crack )*co[5]*co[6]/
                                   ( 4.*co[1]*( co[4] + k_crack ) );

   /* Nominal bending moment between load points */
   moment    = .5*co[5]*co[6] - co[4]*theta;
   e_nominal = 6.*moment/sqr( co[3] );  /* nominal bending stress */

   /* return growth rate */
   return ( 1./( co[2]*quad( ki( a, co[3], e_nominal ) ) ) );
}



int data_plot( fp, n, data )
/* ************************ ******************************************
   NAME

      data_plot.      ..........Output to a file data for use with
                                DISSPLA programs on the PRIME

   SYNOPSIS

      data_plot( file, n, data ) Output data to file in specific format

         FILE *fp;               output file
         int n;                  fatigue cycle number
         double *data;           pointer to array of output data

   DESCRIPTION

      This function outputs data in the following format

       n    p   strain              a_new                  ki
      %d5  %f6  %e11.4  xxxxxxxxxxx  %e11.4  xxxxxxxxxxx  %e11.4  xxxxxxxxxxx

      delta   frequency  amplification
      %e11.4    %f7.1        %e11.4

      where

         amplification  = ratio of output strain in beam to input force
                          of exciter (in/in/lb)
         a_new          = crack length (in)
         delta          = internal damping ratio
         frequency      = resonant frequency of beam (cps)
         ki             = stress intensity factor (psi-in^1/2)
         n              = fatigue cycle number
         p              = fatigue load
         strain         = nominal strain in beam under fatigue load

      and small x represents a blank space.
```

```
   FUNCTIONS USED

      fprintf.....................write to file

   REFERENCES

   AUTHOR:   Rick Jones
   VERSION:  1.0
   DATE:     18 AUG 1987

************************************************************************** */

double *data;
FILE *fp;
int n;
{
   char *record_1 = "%5d%6.0f%11.4E          %11.4E          %11.4E\n";
   char *record_2 = "%11.4E%7.1f%11.4E\n";
   int err;

   /* initialize error code */
   err = 0;

   /* display fatigue cycle number and crack length on screen */
   printf( "fatigue cycle number:  %5d\n", n );
   printf( "crack length:          %11.4e (in)\n", data[2] );
   printf( "total damping:         %11.4e\n", data[4] );

   /* write first record to file */
   if ( fprintf( fp, record_1, n, data[0], data[1], data[2], data[3] ) != 67 )
      {
      printf( "File write error in data_plot\n" );    /* error in output */
      err = 1;                    /* set error code */
      }
   else                           /* write second record to file */
      if ( fprintf( fp, record_2, data[4], data[5], data[6] ) != 30 )
         {
         printf( "File write error in data_plot\n" ); /* error in output */
         err = 1;                 /* set error code */
         }

   return( err );                 /* return error code */
}


void data_print( n, data )
/* **************************************************************************
   NAME

      data_print.................Output dmp_crack results to screen

   SYNOPSIS

      data_print( n, data );     Output crack growth and internal
                                   damping results to console

      double *data;              array of results
             n;                  fatigue cycle number

   DESCRIPTION

      Output table of crack growth and internal damping results to
      console.  Table of results

         fatigue cycle number, j
         fatigue crack length, a_new
         stress intensity factor, ki
         torsional stiffness at crack, k_crack
```

```
        fraction of life expended, life
        plastic zone size, r_plastic
        plastic zone strain, n_p
        resonant frequency, omega
        average amplitude-dependent damping ratio, delta_h
        frequency dependent damping ratio, delta_i
        crack length dependent damping ratio, delta_crack
        total damping ratio, delta
        fatigue loading, p

   AUTHOR:   Rick Jones
   VERSION:  1.0
   DATE:     18 AUG 1987

************************************************************************ */

double *data;
int n;
{

   /* print to screen */
   printf( "fatigue cycle number                 %5d       (cycle)\n", n );
   printf( "fatigue crack length                 %11.4le (in)\n", data[0] );
   printf( "stress intensity factor              %11.4le (psi-in^1/2)\n", data[1] );
   printf( "torsional stiffness at crack         %11.4le (lb-in)\n", data[2] );
   printf( "fraction of life expended            %11.4le\n", data[3] );
   printf( "plastic zone size                    %11.4le (in)\n", data[4] );
   printf( "plastic zone strain                  %11.4le (in/in)\n", data[5] );
   printf( "resonant frequency                   %11.4le (rad/sec)\n", data[6] );
   printf( "amplitude-dependent damping ratio    %11.4le\n", data[7] );
   printf( "frequency dependent damping ratio    %11.4le\n", data[8] );
   printf( "crack length dependent damping ratio %11.4le\n", data[9] );
   printf( "total damping ratio                  %11.4le\n", data[10] );
   printf( "fatigue load                         %11.4le (lb)\n\n", data[11] );

   return;
}



double dddphi( x, co )
/* ************************************************************************
   NAME

      dddphi.....................third derivative of beam characteristic
                                 equation with respect to x

   SYNOPSIS

      y = dddphi( x, co );       calculate third derivative of beam
                                    characteristic equation with
                                    respect to x

      double *co,                coefficients of characteristic equation
             x,                  beam coordinate
             y;                  third derivative of beam at location x

   DESCRIPTION

      Calculate third derivative of beam at location x.  Third derivative
      has the following equation form

         dddphi(x) = scale_factor*co[0]^3*(      sin( co[0]*x ) -
                                          co[1]*cos( co[0]*x ) +
                                          co[2]*sinh( co[0]*x ) +
                                          co[3]*cosh( co[0]*x ) )

         co[0]  = kappa;
         co[1]  = mode.element[2];
```

```
        co[2]  = mode.element[3];
        co[3]  = mode.element[4];
        co[4]  = scale_factor;

   FUNCTIONS USED

      dcos.....................Lattice SSP cosine function
      dcosh....................Lattice SSP hyperbolic cosine function
      dsin.....................Lattice SSP sine function
      dsinh....................Lattice SSP hyperbolic sine function

   REFERENCES

      Harris, C.M. and Crede, C.V. (eds).  Shock and Vibration Handbook,
      2nd edition, McGraw-Hill, New York, pp. 7-13 through 7-15, 1976.

      Thomson, W.T.  "Theory of Vibration with Applications," Prentice-
      Hall, Inc. Englewood Cliffs, NJ, 1972.

   AUTHOR:   Rick Jones
   VERSION:  1.0
   DATE:     18 AUG 87

************************************************************************** */

double *co, x;
{
   double y;
   double dcos(), dcosh(), dsin(), dsinh();

   /* calculate third derivative of beam at x */
   y = co[4]*cube( co[0] )*( dsin( co[0]*x ) - co[1]*dcos( co[0]*x ) +
                     co[2]*dsinh( co[0]*x ) + co[3]*dcosh( co[0]*x ) );

   return ( y );
}



double ddphi( x, co )
/* ************************************************************************
   NAME

      ddphi....................second derivative of beam
                               characteristic equation with respect
                               to x.

   SYNOPSIS

      y = ddphi( x, co );      calculate second derivative of
                               beam characteristic equation with
                               respect to x

      double *co,              coefficients of characteristic equation
             x,                beam coordinate
             y;                curvature of beam at location x

   DESCRIPTION

      Calculate curvature of beam at location x.  Curvature has the
      following equation form

         ddphi(x) = scale_factor*co[0]^2*(      -cos( co[0]*x ) -
                                          co[1]*sin( co[0]*x ) +
                                          co[2]*cosh( co[0]*x ) +
                                          co[3]*sinh( co[0]*x ) )

         co[0]  = kappa;
         co[1]  = mode.element[2];
```

```
        co[2]  = mode.element[3];
        co[3]  = mode.element[4];
        co[4]  = scale_factor;

   FUNCTIONS USED

      dcos.....................Lattice SSP cosine function
      dcosh....................Lattice SSP hyperbolic cosine function
      dsin.....................Lattice SSP sine function
      dsinh....................Lattice SSP hyperbolic sine function

   REFERENCES

      Harris, C.M. and Crede, C.V. (eds).  Shock and Vibration Handbook,
      2nd edition, McGraw-Hill, New York, pp. 7-13 through 7-15, 1976.

      Thomson, W.T.  "Theory of Vibration with Applications," Prentice-
      Hall, Inc. Englewood Cliffs, NJ, 1972.

   AUTHOR:   Rick Jones
   VERSION:  1.0
   DATE:     18 AUG 87

************************************************************************** */

double *co, x;
{
   double y;
   double dcos(), dcosh(), dsin(), dsinh();

   /* calculate curvature of beam at x */
   y = co[4]*sqr( co[0] )*( -dcos( co[0]*x ) - co[1]*dsin( co[0]*x ) +
                     co[2]*dcosh( co[0]*x ) + co[3]*dsinh( co[0]*x ) );

   return ( y );
}



double ddphi2( x, co )
/* ************************************************************************
   NAME

      ddphi2.....................square of second derivative of beam
                                 characteristic equation with respect
                                 to x.

   SYNOPSIS

      y = ddphi2( x, co );       calculate square of second derivative of
                                    beam characteristic equation with
                                    respect to x

      double *co,                coefficients of characteristic equation
             x,                  beam coordinate
             y;                  curvature of beam at location x

   DESCRIPTION

      Calculate square of curvature of beam at location x.  Curvature has
      the following equation form

         ddphi(x) = scale_factor*co[0]^2*(      -cos( co[0]*x ) -
                                          co[1]*sin( co[0]*x ) +
                                          co[2]*cosh( co[0]*x ) +
                                          co[3]*sinh( co[0]*x ) )

         co[0]  = kappa;
```

```
        co[1]  = mode.element[2];
        co[2]  = mode.element[3];
        co[3]  = mode.element[4];
        co[4]  = scale_factor;

   FUNCTIONS USED

   REFERENCES

      Harris, C.M. and Crede, C.V. (eds).  Shock and Vibration Handbook,
      2nd edition, McGraw-Hill, New York, pp. 7-13 through 7-15, 1976.

      Thomson, W.T.  "Theory of Vibration with Applications," Prentice-
      Hall, Inc. Englewood Cliffs, NJ, 1972.

   AUTHOR:   Rick Jones
   VERSION:  1.0
   DATE:     18 AUG 87

************************************************************************** */

double *co, x;
{
   double ddphi();

   /* calculate square of curvature of beam at x */

   return ( sqr( ddphi( x, co ) ) );
}



double dphi( x, co )
/* ************************************************************************
   NAME

      dphi.....................first derivative of beam characteristic
                                  equation with respect to x.

   SYNOPSIS

      y = dphi( x, co );         calculate first derivative of beam
                                    characteristic equation with
                                    respect to x

      double *co,                coefficients of characteristic equation
             x,                  beam coordinate
             y;                  slope of beam at location x

   DESCRIPTION

      Calculate slope of beam at location x.  Curvature has the
      following equation form

         dphi(x) = scale_factor*co[0]*(      -sin( co[0]*x ) +
                                       co[1]*cos( co[0]*x ) +
                                       co[2]*sinh( co[0]*x ) +
                                       co[3]*cosh( co[0]*x ) )

         co[0]  = kappa;
         co[1]  = mode.element[2];
         co[2]  = mode.element[3];
         co[3]  = mode.element[4];
         co[4]  = scale_factor;

   FUNCTIONS USED

      dcos.....................Lattice SSP cosine function
```

```
      dcosh.....................Lattice SSP hyperbolic cosine function
      dsin......................Lattice SSP sine function
      dsinh.....................Lattice SSP hyperbolic sine function

   REFERENCES

      Harris, C.M. and Crede, C.V. (eds).  Shock and Vibration Handbook,
      2nd edition, McGraw-Hill, New York, pp. 7-13 through 7-15, 1976.

      Thomson, W.T.  "Theory of Vibration with Applications," Prentice-
      Hall, Inc. Englewood Cliffs, NJ, 1972.

   AUTHOR:   Rick Jones
   VERSION:  1.0
   DATE:     18 AUG 87

********************************************************************** */

double *co, x;
{
   double y;
   double dcos(), dcosh(), dsin(), dsinh();

   /* calculate slope of beam at x */
   y = co[4]*co[0]*( -dsin( co[0]*x ) + co[1]*dcos( co[0]*x ) +
                     co[2]*dsinh( co[0]*x ) + co[3]*dcosh( co[0]*x ) );

   return ( y );
}



/*ARGSUSED  parameter x is not used in this function */

double ezb_limit( x, co )
/* **********************************************************************
   NAME

      ezb_limit.................z coordinate lower limit of
                                  integration over the elastic range

   SYNOPSIS

      y = ezb_limit( x, co );    z coordinate lower limit of
                                    integration over the elastic beam
                                    material

      double *co,                user modifiable coefficients for
                                    defining lower limit
            x,                   value of x coordinate for application
                                    in setting lower limit
            y;                   lower limit of integration

   DESCRIPTION

      This function defines the lower limit of integration for the z
      coordinate of a beam.  The limit is specifically for the elastic
      range of material.  The function is called by multi_al, a routine
      that performs multiple numerical integration.

   FUNCTIONS USED

   REFERENCES

      Burden, R.L. and Faires, J.D.  "Numerical Analysis," third
      edition, Prindle, Weber and Schmidt, Boston, 1984, pp. 153-
      195.
```

```
   AUTHOR:   Rick Jones
   VERSION:  1.0
   DATE:     18 AUG 87

************************************************************************ */

double *co, x;
{
   /* the first element in the array of coefficients contains a constant
      that defines the lower limit for the function being integrated */

   return ( co[0] );

}



/*ARGSUSED  parameter x is not used in this function */

double eze_limit( x, co )
/* ************************************************************************
   NAME

      eze_limit.................z coordinate upper limit of
                                  integration over the elastic range

   SYNOPSIS

      y = ezb_limit( x, co );    z coordinate upper limit of
                                    integration over the elastic beam
                                    material

      double *co,                user modifiable coefficients for
                                    defining upper limit
             x,                  value of x coordinate for application
                                    in setting upper limit
             y;                  upper limit of integration

   DESCRIPTION

      This function defines the upper limit of integration for the z
      coordinate of a beam.  The limit is specifically for the elastic
      range of material.  The function is called by multi_al, a routine
      that performs multiple numerical integration.

   FUNCTIONS USED

   REFERENCES

      Burden, R.L. and Faires, J.D.  "Numerical Analysis," third
      edition, Prindle, Weber and Schmidt, Boston, 1984, pp. 153-
      195.

   AUTHOR:   Rick Jones
   VERSION:  1.0
   DATE:     18 AUG 87

************************************************************************ */

double *co, x;
{
   /* the second element in the array of coefficients contains a
      constant that defines the upper limit for the function being
      integrated */

   return ( co[1] );

}
```

```
int get_data( fp, input_int, input_real )
/* ************************************************************************
   NAME

      get_data.....................input data from file

   SYNOPSIS

      include <stdio.h>

      err = get_data( fp, input_int, input_real );  input material and
                                    program control constants

      FILE *fp;                   input file
      double *input_real;         pointer to array of real constants
      int err,                    error code:  0 - no error
                                               1 - error
          *input_int;             pointer to array of integer constants

   DESCRIPTION

      get_data accesses an open file and inputs the data associated with
      the two arrays.  Data is placed in the input file in the following
      format:

         input_real:

         a_0             = initial crack length (in).
         a_disl          = dislocation density coefficient (disl/in^2).
         a_final         = final crack length (in).
         alpha           = linear expansion coefficient (in/in/xF).
         b_crack         = material constant relating crack length to
                           torsional stiffness (lb-in).
         c               = Manson-Coffin ductility exponent.
         c_1             = internal damping coefficient.
         c_2             = internal damping coefficient (in/in).
         c_heat          = specific heat per unit volume (psi/xF)
         chi             = strain independent probability for the
                           remobilization of immobile dislocations.
         delta_ext       = damping ratio caused by external source
         e               = Young's modulus (psi).
         ei              = Young's modulus x moment of inertia (lb-in^2).
         n_max           = maximum strain in beam during damping data
                           collection (in/in).
         n_ult           = static plastic fracture value at 1/2 cycle
                           (in/in).
         g_check         = minimum crack growth before updating
                           eigenvector results (in).
         growth_rate     = crack growth rate constant based on
                           dislocation theory of crack growth
                           (in^7/lb^4-cycle).
         h               = beam height (in).
         k               = thermal conductivity (lb/sec-xF)
         k_knife_edge    = torsional stiffness at knife-edge support
                           (lb-in).
         l               = beam length
         l_exciter       = location of exciter relative to knife-edge
                           support (in).
         l_load          = location of load relative to knife-edge
                           support (in).
         lambda_0        = dislocatin density for n_p = 0 (disl/in^2).
         m_beam          = mass of beam per unit length (slug/inch).
         m_exciter       = mass of exciter and counterweight (slug).
         p               = fatigue load applied to beam (lb).
```

```
        e_yield         = yield stress (psi).
        slope_factor    = crack dependent constant relating beam slope
                          and damping.
        temperature     = ambient temperature of specimen (xF).
        toler           = tolerance for iteration algorithms.

        mode.element[0] thru [4] are initial guesses for the newton
        iterative solution to the nonlinear beam equation, and
        represent the following data

        element[0] - eigenvalue, kappa*l
        element[1] - resonant frequency, omega
        element[2] - B coefficient
        element[3] - C coefficient
        element[4] - D coefficient

        input_int:

        data_rate       = number of fatigue cycles between data output
        is_type_sif     = 0 for constant load
                          1 for constant stress intensity factor
        j               = initial cycle number
        m               = number of subintervals for integration
        maxum           = number of iteration cycles
        n               = number of subintervals for second integration

    FUNCTIONS USED

        fscanf.....................read from file

    REFERENCES

    AUTHOR:   Rick Jones
    VERSION:  1.0
    DATE:     19 AUG 87

************************************************************************** */

FILE *fp;
double *input_real;
int *input_int;
{
    int err, i;

    err = 0;                        /* initialize return code */

    /* input all real values, one per line */
    for ( i = 0; i < MAX_REAL; i++ )
        {
        if ( fscanf( fp, "%lf", ( input_real + i ) ) == 0 )
            {
            /* error in input */
            printf( "File error reading reals in get_data, i = %d\n", i );
            err = 1;                /* set error code */
            break;                  /* end for loop */
            }
        }

    /* input all integer values, one per line */
    if ( err == 0 )
        {
        for ( i = 0; i < MAX_INT; i++ )
            {
            if ( fscanf( fp, "%d", ( input_int + i ) ) == 0 )
                {
                /* error in input */
                printf( "File error reading integers in get_data, i = %d\n", i );
                err = 1;                /* set error code */
                break;                  /* end for loop */
```

```
            }
         }
      }

   /* return error code */
   return ( err );
}


void input_print( input_int, input_real )
/* ************************************************************************
   NAME

      input_print.............print input data to screen

   SYNOPSIS

      include <stdio.h>

      input_print( input_int, input_real );  print input material and
                                  program control constants to screen

      double *input_real;         pointer to array of real constants
      int *input_int;             pointer to array of integer constants

   DESCRIPTION

      This function takes the two input arrays and prints them on the
      the screen along with their descriptions.

         input_real:

         a_0             = initial crack length (in).
         a_disl          = dislocation density coefficient (disl/in^2).
         a_final         = final crack length (in).
         alpha           = linear expansion coefficient (in/in/xF).
         b_crack         = material constant relating crack length to
                           torsional stiffness (lb-in).
         c               = Manson-Coffin ductility exponent.
         c_1             = internal damping coefficient.
         c_2             = internal damping coefficient (in/in).
         c_heat          = specific heat per unit volume (psi/xF)
         chi             = strain independent probability for the
                           remobilization of immobile dislocations.
         delta_ext       = damping ratio caused by external source
         e               = Young's modulus (psi).
         ei              = Young's modulus x moment of inertia (lb-in^2).
         n_max           = maximum strain in beam during damping data
                           collection (in/in).
         n_ult           = static plastic fracture value at 1/2 cycle
                           (in/in).
         g_check         = minimum crack growth before updating
                           eigenvector results (in).
         growth_rate     = crack growth rate constant based on
                           dislocation theory of crack growth
                           (in^7/lb^4-cycle).
         h               = beam height (in).
         k               = thermal conductivity (lb/sec-xF)
         k_knife_edge    = torsional stiffness at knife-edge support
                           (lb-in).
         l               = beam length
         l_exciter       = location of exciter relative to knife-edge
                           support (in).
         l_load          = location of load relative to knife-edge
                           support (in).
         lambda_0        = dislocatin density for n_p = 0 (disl/in^2).
         m_beam          = mass of beam per unit length (slug/inch).
         m_exciter       = mass of exciter and counterweignt (slug).
```

```
        p               = fatigue load applied to beam (lb).
        e_yield         = yield stress (psi).
        slope_factor    = crack dependent constant relating beam slope
                          and damping.
        temperature     = ambient temperature of specimen (xF).
        toler           = tolerance for iteration algorithms.

        mode.element[0] thru [4] are initial guesses for the newton
        iterative solution to the nonlinear beam equation, and
        represent the following data

        element[0] - eigenvalue, kappa*l
        element[1] - resonant frequency, omega
        element[2] - B coefficient
        element[3] - C coefficient
        element[4] - D coefficient

        input_int:

        data_rate       = number of fatigue cycles between data output
        is_type_sif     = 0 for constant load
                          1 for constant stress intensity factor
        j               = initial cycle number
        m               = number of subintervals for integration
        maxum           = number of iteration cycles
        n               = number of subintervals for second integration

    FUNCTIONS USED

    REFERENCES

    AUTHOR:   Rick Jones
    VERSION:  1.0
    DATE:     19 AUG 87

************************************************************************** */

double *input_real;
int *input_int;
{
    /* print real input data to screen */
    printf( "initial crack length              %11.4le (in)\n", input_real[0] );
    printf( "dislocation density coefficient   %11.4le (disl/in^2)\n", input_real[1] );
    printf( "final crack length                %11.4le (in)\n", input_real[2] );
    printf( "linear expansion coefficient      %11.4le (in/in/xF)\n", input_real[3] );
    printf( "crack torsional stiffness slope   %11.4le (lb-in)\n", input_real[4] );
    printf( "Manson-Coffin ductility exponent  %11.4le \n", input_real[5] );
    printf( "internal damping coefficent 1     %11.4le \n", input_real[6] );
    printf( "internal damping coefficent 2     %11.4le (in/in)\n", input_real[7] );
    printf( "specific heat                     %11.4le (psi/xF)\n", input_real[8] );
    printf( "remobilization probability        %11.4le \n", input_real[9] );
    printf( "external damping ratio            %11.4le \n", input_real[10] );
    printf( "Young's modulus                   %11.4le (psi)\n", input_real[11] );
    printf( "modulus x Moment of Inertia       %11.4le (lb-in^2)\n", input_real[12] );
    printf( "damping cycle maximum strain      %11.4le (in/in)\n", input_real[13] );
    printf( "static plastic fracture value     %11.4le (in/in)\n", input_real[14] );
    printf( "eigenvalue update parameter       %11.4le (in)\n", input_real[15] );
    printf( "crack growth rate                 %11.4le (in^7/lb^4-cycle)\n", input_real[16] );
    printf( "beam height                       %11.4le (in)\n", input_real[17] );
    printf( "thermal conductivity              %11.4le (lb/sec-xF)\n", input_real[18] );
    printf( "knife-edge torsional stiffness    %11.4le (lb-in)\n", input_real[19] );
    printf( "beam length                       %11.4le (in)\n", input_real[20] );
    printf( "excitation location               %11.4le (in)\n", input_real[21] );
    printf( "initial dislocation density       %11.4le (disl/in^2)\n", input_real[22] );
    printf( "fatigue load location             %11.4le (in)\n", input_real[23] );
    printf( "beam mass per unit length         %11.4le (slug/in)\n", input_real[24] );
    printf( "exciter mass                      %11.4le (slug)\n", input_real[25] );
    printf( "fatigue load                      %11.4le (lb)\n", input_real[26] );
    printf( "yield stress                      %11.4le (psi)\n", input_real[27] );
```

```
   printf( "damping slope factor              %11.4le \n", input_real[28] );
   printf( "temperature                       %11.4le (xF)\n", input_real[29] );
   printf( "approximation tolerance           %11.4le \n", input_real[30] );
   printf( "initial guess of beam mode parameters\n" );
   printf( "   eigenvalue                     %11.4le \n", input_real[31] );
   printf( "   resonant frequency             %11.4le (rad/sec)\n", input_real[32] );
   printf( "   B coefficient                  %11.4le \n", input_real[33] );
   printf( "   C coefficient                  %11.4le \n", input_real[34] );
   printf( "   D coefficient                  %11.4le \n", input_real[35] );

   /* print integer input data to screen */
   printf( "sampling interval                 %5d       (cycle)\n", input_int[0] );

   /* report load type */
   if ( *( input_int + 1 ) == 0 )
      printf( "load type - constant load\n" );
   else
      printf( "load type - constant stress intensity factor\n" );
   printf( "initial cycle number              %5d       (cycle)\n", input_int[2] );
   printf( "subintervals for integration      %5d       (intervals)\n", input_int[3] );
   printf( "maximum iteration cycles          %5d       (cycle)\n", input_int[4] );
   printf( "subintervals on 2nd integration   %5d       (intervals)\n", input_int[5] );

   return;
}



double f( r )
/* ************************************************************************
   NAME

      f.........................empirical formula for pure bending
                                   stress intensity factor

   SYNOPSIS

      double f();

      y = f( r );                pure bending stress intensity factor
                                    empirical formula

      double r,                  ratio of crack length to section depth
             y;                  empirical formula for pure bending

   DESCRIPTION

      Calculate the empirical formula for pure bending

         f(a/h) = 1.122 - 1.4*(a/h) + 7.33*(a/h)^2 - 13.08*(a/h)^3 +
                  14*(a/h)^4

                  ( 0.2% for a/h < 0.6),
      or

         f(a/h) = sqrt(tan(p)/p)*
                               (.923 + .199*(1 - sin(p)))^4/cos(p),

      where p = c*a/(2*h) and r = a/h

                  ( 0.5% for any a/h).

   FUNCTIONS USED

      dcos.......................Lattice SSP cosine function
      dsin.......................Lattice SSP sine function
      dsqrt......................Lattice SSP square root function
      dtan.......................Lattice SSP tangent function
```

```
   REFERENCES

      Tada, H., Paris, P.C. and Irwin, G.R., "The Stress Analysis of
      Cracks Handbook," Del Research Corporation, Hellertown,
      Pennsylvania, 1973, pp 2.13-2.14.

   AUTHOR:   Rick Jones
   VERSION:  1.0
   DATE:     19 AUG 87

********************************************************************** */

double r;
{
   double p;
   double dcos(), dsin(), dsqrt(), dtan();

   /* select the formula */
   if ( r <= 0.6 )
      /* return polynomial calculation */
      return ( 1.122 - 1.4*r + 7.33*sqr( r ) - 13.08*cube( r ) + 14.*quad( r ) );
   else {
      /* return trigonometric calculation */
      p = .5*PI*r;
      return ( dsqrt( dtan( p )/p )*quad( .923 + .199*( 1. - dsin( p ) ) )/dcos( p ) );
   }

}



double ki( a, h, e )
/* **********************************************************************
   NAME

      ki.........................stress intensity factor for pure
                                    bending

   SYNOPSIS

      y = ki( a, h, e );          stress intensity factor for the case of
                                     pure bending

      double a,                   crack length
             h,                   section depth
             e,                   nominal stress
             y,                   stress intensity factor

   DESCRIPTION

      Begin by calculating the stress intensity factor using an
      empirical formula for pure bending

         f(a/h) = 1.122 - 1.4*(a/h) + 7.33*(a/h)^2 - 13.08*(a/h)^3 +
                  14*(a/h)^4

                  ( 0.2% for a/h < 0.6),
      or

         f(a/h) = sqrt(tan(psi)/psi)*
                               (.923 + .199*(1 - sin(psi)))^4/cos(psi),

      where psi = c*a/(2*h)

                  ( 0.5% for any a/h).

      y = e*sqrt(c*a)*f(a/h)   stress intensity factor

   FUNCTIONS USED
```

```
      dsqrt.....................Lattice SSP square root function

   REFERENCES

      Tada, H., Paris, P.C. and Irwin, G.R., "The Stress Analysis of
      Cracks Handbook," Del Research Corporation, Hellertown,
      Pennsylvania, 1973, pp 2.13-2.14.

   AUTHOR:   Rick Jones
   VERSION:  1.0
   DATE:     19 AUG 87

********************************************************************** */

double a, h, e;
{
   double f(), dsqrt();

   /* return the stress intensity factor */

   return ( e*dsqrt( PI*a )*f( a/h ) );

}



MATRIX modal( x, co, residuals )
/* **********************************************************************
   NAME

      modal.....................calculates residuals

   SYNOPSIS

      #include <numeric.h>

      residuals = modal( x, co, residuals );   calculate residuals of
                                                  nonlinear equations

      double *co;                pointer to array of nonlinear equation
                                    coefficients
      MATRIX residuals           vector containing equation errors based
                                    on equation coefficients and vector
                                    of guess values
             x;                  vector of guess values to solve
                                    nonlinear set of equations

   DESCRIPTION

      Contains user supplied equations to determine residuals in solving
      nonlinear system of equations in x.  This function is designed for
      use with newton(), the Newton-Raphson Iterative process for
      solving nonlinear sets of equations.

         co[0] = k_knife_edge;   knife-edge stiffness
         co[1] = k_crack;        crack stiffness
         co[2] = l;              beam length
         co[3] = m_beam;         beam mass per unit length
         co[4] = m_exciter;      mass of exciter
         co[5] = ei;             modulus and moment of inertia
         co[6] = l_exciter;      position of exciter relative to knife-
                                    edge
         co[7] = (double) m;     number of subdivisions for integration

   FUNCTIONS USED
      coeff_red.................reduce characteristic oefficients
      dcos......................Lattice SSP cosine function
```

```
      dcosh.....................Lattice SSP hyperbolic cosine function
      ddphi2....................square of the second derivative of the
                                  characteristic equation
      dsin......................Lattice SSP sine function
      dsinh.....................Lattice SSP hyperbolic sine function
      mat_assign................assign matrix parameters to variable
      mat_delete................delete matrix storage space
      phi2......................square of the characteristic equation
      simpson...................numerical integration using Simpson's rule

********************************************************************** */

double *co;
MATRIX residuals, x;
{
   D_SUPPLD h_fun, ddh_fun;
   double ch_ei, c_ei, eigen, gen_mass, gen_stiff;
   double sh_ei, s_ei, stiff_c, stiff_ke;
   double phi_data[5];
   double ddphi2(), phi2();
   double dcos(), dcosh(), dsin(), dsinh();
   int i;
   MATRIX a, coeff;
   MATRIX coeff_red(), mat_assign(), mat_delete();

   /* user supplied equations for beam analysis */

   eigen         = x.element[0]*co[2];       /* eigenvalue * length        */
   ch_ei         = dcosh( eigen );
   c_ei          = dcos( eigen );
   sh_ei         = dsinh( eigen );
   s_ei          = dsin( eigen );
   stiff_c       = co[1]/( x.element[0]*co[5] );  /* characteristic stiffness
                                                     at crack               */
   stiff_ke      = co[0]/( x.element[0]*co[5] );  /* characteristic stiffness
                                                     at boundary            */

   h_fun.funct   = phi2;          /* beam characteristic equation          */
   h_fun.coeff   = phi_data;      /* eigenvector data                      */

   ddh_fun.funct = ddphi2;          /* second derivative of beam characteristic
                                       equation                            */
   ddh_fun.coeff = phi_data;      /* eigenvector data                      */

   /* characteristic equation coefficients */
   phi_data[0]  = x.element[0];
   phi_data[1]  = x.element[2];
   phi_data[2]  = x.element[3];
   phi_data[3]  = x.element[4];
   phi_data[4]  = 1.;             /* use scale factor of 1                 */

   /* create a matrix */
   a            = mat_assign( 4, 4, NULL );

   /* fill a matrix */
   a.element[ 0] = 1.;
   a.element[ 1] = 1.;
   a.element[ 2] = -( c_ei + stiff_c*s_ei );
   a.element[ 3] = s_ei;
   a.element[ 4] = 0.;
   a.element[ 5] = stiff_ke;
   a.element[ 6] = -s_ei + stiff_c*c_ei;
   a.element[ 7] = -c_ei;
   a.element[ 8] = 1.;
   a.element[ 9] = -1.;
   a.element[10] = ch_ei + stiff_c*sh_ei;
   a.element[11] = sh_ei;
   a.element[12] = 0.;
   a.element[13] = stiff_ke;
```

```
   a.element[14] = sh_ei + stiff_c*ch_ei;
   a.element[15] = ch_ei;

   /* determinate of a should be 0, first residual is det(a) */
   residuals.element[0] = mat_determ( a );

   /* create a vector to hold coefficients */
   coeff        = mat_assign( 4, 1, NULL );

   /* fill coefficients in terms of coeff[0] */
   coeff        = coeff_red( a, coeff );

   /* calculate residuals for mode shape coefficents */
   for ( i = 1; i <= 3; ++i )
      residuals.element[i+1] = coeff.element[i] - x.element[i+1];

   /* beam mass */
   gen_mass     = co[3]*simpson( 0., co[2], (int) co[7], h_fun ) +
                        co[4]*phi2( co[6], phi_data );

   /* beam stiffness */
   gen_stiff    = co[5]*simpson( 0., co[2], (int) co[7], ddh_fun );

   /* residual for frequency */
   residuals.element[1] = sqr( x.element[1] )*gen_mass - gen_stiff;

   /* release storage */
   a        = mat_delete( a );
   coeff    = mat_delete( coeff );

   return( residuals );
}



double n2_theta_h( x, z, co )
/* ************************************************************************
   NAME

      n2_theta_h.................beam strain squared multiplied by
                                 internal damping ratio

   SYNOPSIS

      y = n2_theta_h( x, z, co );   beam strain squared times internal
                                    damping ratio

      double *co,                expression coefficients
             x,                  length coordinate of beam
             y,                  result
             z;                  height coordinate of beam

   DESCRIPTION

      Calculate beam strain squared multiplied by internal damping ratio
      at any x, z coordinate of a beam.  The result is computed from the
      following equation

         y = n(x,z)^2*c_1*(c_2/n(x,z))^2*ei1(c_2/n(x,z)),

      where c_1 and c_2 are material constants.  n() is the beam strain
      and ei1() is the exponential integral function.

         co[0]  = c_1;              internal damping coefficient
         co[1]  = c_2;              internal damping coefficient
         co[2]  = kappa;            eigenvalue
         co[3]  = mode.element[2];  phi(x) coefficient B
         co[4]  = mode.element[3];  phi(x) coefficient C
         co[5]  = mode.element[4];  phi(x) coefficient D
```

```
        co[6]  = phi_data[4];        amplitude scale factor

   FUNCTIONS USED

      ei1.....................Lattice SSP exponential integral
                              function
      strain..................beam strain

   REFERENCES

      Harris, C.M. and Crede, C.V. (eds).  Shock and Vibration Handbook,
      2nd edition, McGraw-Hill, New York, pp. 7-13 through 7-15, 1976.

      Thomson, W.T.  "Theory of Vibration with Applications," Prentice-
      Hall, Inc. Englewood Cliffs, NJ, 1972.

      Povolo, F.  "On the Granato-Lucke Expression for the Amplitude-
      Dependent Damping," Scripta Metallurgica, v 9, pp 865-872, 1975.

   AUTHOR:   Rick Jones
   VERSION:  1.0
   DATE:     23 AUG 87

********************************************************************** */

double *co, x, z;
{
   double ratio;
   double ei1(), strain();
   int irc;

   /* initialize error code */
   irc = 0;

   /* test input to exponential integral function */
   if ( z )                     /* z coordinate must be nonzero */
      ratio = abs( co[1]/strain( x, z, &co[2] ) );
   else
      return( 0. );

   if ( ratio > 669. )          /* test for underflow */
      return ( 0. );
   else
      /* return result - ignore first two coefficients when providing
         pointer to strain function */
      return( co[0]*sqr( co[1] )*ei1( ratio, &irc ) );
}



double phi( x, co )
/* **********************************************************************
   NAME

      phi.....................beam characteristic equation

   SYNOPSIS

      y = phi( x, co );         calculate displacement from
                                   beam characteristic equation

      double *co,               coefficients of characteristic equation
             x,                 beam coordinate
             y;                 displacement of beam at location x

   DESCRIPTION
```

```
   Calculate displacement of beam at location x.  Displacement has
   the following equation form

      phi(x) = scale_factor*( cos( co[0]*x ) + co[1]*sin( co[0]*x ) +
                  co[2]*cosh( co[0]*x ) + co[3]*sinh( co[0]*x ) )

      co[0]  = kappa;
      co[1]  = mode.element[2];
      co[2]  = mode.element[3];
      co[3]  = mode.element[4];
      co[4]  = scale_factor;

   FUNCTIONS USED

      dcos.....................Lattice SSP cosine function
      dcosh....................Lattice SSP hyperbolic cosine function
      dsin.....................Lattice SSP sine function
      dsinh....................Lattice SSP hyperbolic sine function

   REFERENCES

      Harris, C.M. and Crede, C.V. (eds).  Shock and Vibration Handbook,
      2nd edition, McGraw-Hill, New York, pp. 7-13 through 7-15, 1976.

      Thomson, W.T.  "Theory of Vibration with Applications," Prentice-
      Hall, Inc. Englewood Cliffs, NJ, 1972.

   AUTHOR:   Rick Jones
   VERSION:  1.0
   DATE:     18 AUG 87

************************************************************************ */

double *co, x;
{
   double y;
   double dcos(), dcosh(), dsin(), dsinh();

   /* calculate displacement of beam at x */
   y = co[4]*( dcos( co[0]*x ) + co[1]*dsin( co[0]*x ) +
                  co[2]*dcosh( co[0]*x ) + co[3]*dsinh( co[0]*x ) );

   return ( y );
}



double phi2( x, co )
/* ************************************ ***************************
   NAME

      phi2.....................square of beam characteristic equation

   SYNOPSIS

      y = phi2( x, co );         calculate square of displacement from
                                    beam characteristic equation

      double *co,                coefficients of characteristic equation
             x,                  beam coordinate
             y;                  displacement of beam at location x

   DESCRIPTION

      Calculate square of displacement of beam at location x.  Displacement
      has the following equation form

         phi(x) = scale_factor*( cos( co[0]*x ) + co[1]*sin( co[0]*x ) +
                     co[2]*cosh( co[0]*x ) + co[3]*sinh( co[0]*x ) )
```

```
        co[0]  = kappa;
        co[1]  = mode.element[2];
        co[2]  = mode.element[3];
        co[3]  = mode.element[4];
        co[4]  = scale_factor;

   FUNCTIONS USED

      phi.....................beam characteristic equation

   REFERENCES

      Harris, C.M. and Crede, C.V. (eds).  Shock and Vibration Handbook,
      2nd edition, McGraw-Hill, New York, pp. 7-13 through 7-15, 1976.

      Thomson, W.T.  "Theory of Vibration with Applications," Prentice-
      Hall, Inc. Englewood Cliffs, NJ, 1972.

   AUTHOR:   Rick Jones
   VERSION:  1.0
   DATE:     18 AUG 87

************************************************************************** */

double *co, x;
{
   double phi();

   /* calculate square of displacement of beam at x */

   return ( sqr( phi( x, co ) ) );
}



/*ARGSUSED  parameter x is not used in this function */

double pzb_limit( x, co )
/* **************************************************************************
   NAME

      pzb_limit.................z coordinate lower limit of
                                  integration over the plastic range

   SYNOPSIS

      y = pzb_limit( x, co );    z coordinate lower limit of
                                   integration over the plastic beam
                                   material

      double *co,                user modifiable coefficients for
                                   defining lower limit
             x,                  value of x coordinate for application
                                   in setting lower limit
             y;                  lower limit of integration

   DESCRIPTION

      This function defines the lower limit of integration for the z
      coordinate of a beam.  The limit is specifically for the plastic
      range of material.  The function is called by multi_al, a routine
      that performs multiple numerical integration.

   FUNCTIONS USED

   REFERENCES
```

```
      Burden, R.L. and Faires, J.D.  "Numerical Analysis," third
      edition, Prindle, Weber and Schmidt, Boston, 1984, pp. 153-
      195.

   AUTHOR:   Rick Jones
   VERSION:  1.0
   DATE:     18 AUG 87

********************************************************************** */

double *co, x;
{
   /* the first element in the array of coefficients contains a constant
      that defines the lower limit for the function being integrated */

   return ( co[0] );

}



/*ARGSUSED  parameter x is not used in this function */

double pze_limit( x, co )
/* **********************************************************************
   NAME

      pze_limit.................z coordinate upper limit of
                                  integration over the plastic range

   SYNOPSIS

      y = pzb_limit( x, co );    z coordinate upper limit of
                                    integration over the plastic beam
                                    material

      double *co,                user modifiable coefficients for
                                    defining upper limit
             x,                  value of x coordinate for application
                                    in setting upper limit
             y;                  upper limit of integration

   DESCRIPTION

      This function defines the upper limit of integration for the z
      coordinate of a beam.  The limit is specifically for the plastic
      range of material.  The function is called by multi_al, a routine
      that performs multiple numerical integration.

   FUNCTIONS USED

   REFERENCES

      Burden, R.L. and Faires, J.D.  "Numerical Analysis," third
      edition, Prindle, Weber and Schmidt, Boston, 1984, pp. 153-
      195.

   AUTHOR:   Rick Jones
   VERSION:  1.0
   DATE:     18 AUG 87

********************************************************************** */

double *co, x;
{
   /* the second element in the array of coefficients contains a
      constant that defines the upper limit for the function being
      integrated */
```

```
   return ( co[1] );

}


/* ************************************************************************
   NAME

      p2??.....................partial derivative functions

   SYNOPSIS

      y = p2??( x, co );         partial deriviative of second equation

      double *co,                pointer to array of coefficients
             x,                  location on beam
             y;                  partial derivative

   DESCRIPTION

      These functions are partial derivatives of beam generalize mass
      and stiffness with respect to the eigenvalue and the beam
      characteristic equation coefficients:

         p2k.....................partial of generalized stiffness with
                                    respect to the eigenvalue
         p2kb....................partial of generalized stiffness with
                                    respect to the B coefficient
         p2kc....................partial of generalized stiffness with
                                    respect to the C coefficient
         p2kd....................partial of generalized stiffness with
                                    respect to the D coefficient
         p2m.....................partial of generalized mass with
                                    respect to the eigenvalue
         p2mb....................partial of generalized mass with
                                    respect to the B coefficient
         p2mc....................partial of generalized mass with
                                    respect to the C coefficient
         p2md....................partial of generalized mass with
                                    respect to the D coefficient


         co[0]  = kappa;
         co[1]  = mode.element[2];
         co[2]  = mode.element[3];
         co[3]  = mode.element[4];
         co[4]  = scale_factor;

   FUNCTIONS USED

      dcos.....................Lattice SSP cosine function
      dcosh....................Lattice SSP hyperbolic cosine function
      dsin.....................Lattice SSP sine function
      dsinh....................Lattice SSP hyperbolic sine function
      dphi.....................derivative of characteristic equation
                                 with respect to length coordinate
      ddphi....................second derivative of characteristic
                                 equation with respect to length
                                 coordinate
      dddphi...................third derivative of characteristic
                                 equation with respect to length
                                 coordinate
      phi......................beam characteristic equation

   REFERENCES

      Burden, R.L. and Faires, J.D.  "Numerical Analysis," third
```

```
      edition, Prindle, Weber and Schmidt, Boston, 1984, pp. 153-
      195.

      Harris, C.M. and Crede, C.V. (eds).  Shock and Vibration Handbook,
      2nd edition, McGraw-Hill, New York, pp. 7-13 through 7-15, 1976.

      Thomson, W.T.  "Theory of Vibration with Applications," Prentice-
      Hall, Inc. Englewood Cliffs, NJ, 1972.

   AUTHOR:   Rick Jones
   VERSION:  1.0
   DATE:     25 AUG 87

********************************************************************** */



double p2k( x, co)
double *co, x;
{
   double ddphi(), dddphi();

   /* partial derivative of generalized stiffness with respect to
      eigenvalue */
   return( 2.*x*ddphi( x, co )*dddphi( x, co )/co[0] );

}



double p2kb( x, co)
double *co, x;
{
   double ddphi(), dsin();

   /* partial derivative of generalized stiffness with respect to
      coefficient B */
   return ( -2.*sqr( co[0] )*ddphi( x, co )*dsin( co[0]*x ) );

}



double p2kc( x, co)
double *co, x;
{
   double ddphi(), dcosh();

   /* partial derivative of generalized stiffness with respect to
      coefficient C */
   return ( 2.*sqr( co[0] )*ddphi( x, co )*dcosh( co[0]*x ) );

}



double p2kd( x, co)
double *co, x;
{
   double ddphi(), dsinh();

   /* partial derivative of generalized stiffness with respect to
      coefficient D */
   return ( 2.*sqr( co[0] )*ddphi( x, co )*dsinh( co[0]*x ) );

}
```

```
double p2ma( x, co)
double *co, x;
{
   double dphi(), phi();

   /* partial derivative of generalized mass with respect to eigenvalue */
   return ( 2.*x*phi( x, co )*dphi( x, co )/co[0] );
}



double p2mb( x, co)
double *co, x;
{
   double dsin(), phi();

   /* partial derivative of generalized mass with respect to
      coefficient B */
   return ( 2.*phi( x, co )*dsin( co[0]*x ) );

}



double p2mc( x, co)
double *co, x;
{
   double dcosh(), phi();

   /* partial derivative of generalized mass with respect to
      coefficient C */
   return ( 2.*phi( x, co )*dcosh( co[0]*x ) );

}



double p2md( x, co)
double *co, x;
{
   double dsinh(), phi();

   /* partial derivative of generalized mass with respect to
      coefficient D */
   return ( 2.*phi( x, co )*dsinh( co[0]*x ) );

}



double strain( x, z, co )
/* ************************************************************************
   NAME

      strain.....................,beam strain

   SYNOPSIS

      y = strain( x, z, co );    compute beam strain

      double *co,                coefficients used in strain term
             x,                  x coordinate of beam
             y,                  beam strain
             z;                  z coordinate of beam

   DESCRIPTION
```

```
      Compute strain at beam coordinates given at x and z.
      The strain is computed from the following formula

               n(x,z) = z*phi"(x)

         co[0]  = kappa;
         co[1]  = mode.element[2];
         co[2]  = mode.element[3];
         co[3]  = mode.element[4];
         co[4]  = scale_factor;

   FUNCTIONS USED

      ddphi.....................curvature of beam at location x

   REFERENCES

      Harris, C.M. and Crede, C.V. (eds).  Shock and Vibration Handbook,
      2nd edition, McGraw-Hill, New York, pp. 7-13 through 7-15, 1976.

      Thomson, W.T.  "Theory of Vibration with Applications," Prentice-
      Hall, Inc. Englewood Cliffs, NJ, 1972.

   AUTHOR:   Rick Jones
   VERSION:  1.0
   DATE:     20 AUG 87

************************************************************************** */

double *co, x, z;
{
   double ddphi();

   /* compute and return the beam strain at location x, z. */

   return( z*ddphi( x, co ) );

}



double strain2( x, z, co )
/* ************************************************************************
   NAME

      strain2...................square of beam strain

   SYNOPSIS

      y = strain2( x, z, co );   compute square of beam strain

      double *co,                coefficients used in strain term
             x,                  x coordinate of beam
             y,                  square of beam strain
             z;                  z coordinate of beam

   DESCRIPTION

      Compute and square strain at beam coordinates given at x and z.
      The strain is computed from the following formula

               strain(x,z) = z*phi"(x)

         co[0]  = kappa;
         co[1]  = mode.element[2];
         co[2]  = mode.element[3];
         co[3]  = mode.element[4];
         co[4]  = scale_factor;
```

```
   FUNCTIONS USED

      strain.....................strain of beam at location x, z

   REFERENCES

      Harris, C.M. and Crede, C.V. (eds).  Shock and Vibration Handbook,
      2nd edition, McGraw-Hill, New York, pp. 7-13 through 7-15, 1976.

      Thomson, W.T.  "Theory of Vibration with Applications," Prentice-
      Hall, Inc. Englewood Cliffs, NJ, 1972.

   AUTHOR:   Rick Jones
   VERSION:  1.0
   DATE:     20 AUG 87

************************************************************************** */

double *co, x, z;
{
   double strain();

   /* compute and return the squared beam strain at location x, z. */

   return( sqr( strain( x, z, co ) ) );

}
```

Appendix E

INTERNAL DAMPING TEST RESULTS

Results of the internal damping test are presented, together with a discussion of damping measurement errors. Two types of internal damping were observed: amplitude- and frequency-dependent damping.

DAMPING ERRORS AND CORRECTIONS

Two primary sources of error were uncovered while collecting the symmetric cantilever beam damping data. The first error involves the range of data collected. Low levels of strain and acceleration are imposed by the limits of the Lücke-Granato model (Ref 34, 44), requiring sensitive transducers to accurately depict the low input levels. In addition, measurements are taken in the first three flexural modes of the 6- and 8-inch beam specimens; thus, imposing a large frequency span requirement on accelerometer performance. Table E-1 lists the range of input data collected during the damping tests.

Table E-1. Range of Accelerations and Strains for Cantilever Beam Damping Tests

Parameter	Range
Strain	10 to 100 (microstrain)
Acceleration	1 to 300 (in./sec^2)
Frequency	60 to 2000 (Hz)

The second area of error lies in the wires connecting the strain gages to their amplifiers. These wires, vibrating with the beam specimen, burden the system with external damping that must be quantified in order to extract the internal damping values from the total damping quantity. Quantification of the external damping due to strain gage wiring is accomplished by removing one set of wires at a time and computing the resulting change in damping. Figure E-1 shows the strain gage arrangement and indicates the order in which the wires are removed. Designating the damping states with zero, one, two, three and four sets of wires removed as Δ^0, Δ^1, Δ^2, Δ^3, and Δ^4, respectively, indicates a damping state, Δ^4, for which no measurements may be taken. Δ^4 is estimated from Δ^3 by subtracting the change in damping when the third set of wires is removed, that is, $\Delta^3 - (\Delta^2 - \Delta^3)$ or:

$$\Delta^4 = 2\Delta^3 - \Delta^2 \qquad \text{(E-1)}$$

This estimate assumes that the removal of the fourth set of wires affects the damping exactly as the removal of the third set of wires. This assumption is reasonable in light of the symmetric location of the third and fourth strain gages.

To determine the external damping decrement, the frequency-dependent decrement, Δ_I, calculated from Equation 37, is subtracted from Δ^4 of Equation E-1. The external damping decrement is determined for a beam specimen at the three fundamental modes and an average is taken. The expression for the external damping:

$$\Delta_{ext} = \frac{1}{3} \sum_{i}^{3} (\Delta^4{}_i - \Delta_{Ii}) \qquad \text{(E-2)}$$

where $\Delta^4{}_i$ and Δ_{Ii} are the results of Equation E-1 and Equation 37 in the main text of this report for the i^{th} mode, respectively. Figure 26 shows the effect of Equation E-2 on the frequency-dependent damping decrement for the first three modes of two symmetric cantilever beams, one 6 inches and the other 8 inches long. Figure 26 also shows Zener's Theory super-

imposed on the experimental data to demonstrate the error in using Equation E-2. The maximum errors for the first, second, and third modes occurred for 6-inch beam specimens and were 9, 36, and 100 percent, respectively. In each case, the damping ratio error was on the order of 6×10^{-6}.

STRAIN-AMPLITUDE DEPENDENT DAMPING DECREMENT

Calculation of the frequency-dependent and external damping decrements reduces Equation F-22 in Appendix F to solving for the average strain-amplitude dependent damping decrement, $\bar{\Delta}_H$. In Equation F-17, $\bar{\Delta}_H$ is calculated by the integration of $\varepsilon^2 \Delta_H(\varepsilon)$, where $\Delta_H(\varepsilon)$ is given by (Ref 44):

$$\Delta_H(\varepsilon) = C_1 (C_2/\varepsilon)^2 E_1(C_2/\varepsilon) \qquad \text{(E-3)}$$

where C_1 and C_2 are material constants and E_1 represents the exponential integral function of the first order.

Figure 14 in the main text of this report presents damping and strain data collected from symmetric cantilever beam tests. In Figure 14, the damping and strain data are scaled by estimates of the material constants C_1 and C_2, respectively. These estimates are based on numerical integration of $\varepsilon^2 \Delta_H(\varepsilon)$ with $\Delta_H(\varepsilon)$ from Equation E-3 and strain expressed in the form of Equation F-24 in Appendix F. A least squares fit was used to obtain the best fit of the data to the table generated by numerical integration. An algorithm based on Neville's Iterated Interpolation was used to obtain damping values lying between tabulated quantities. Converting all strain measurements to maximum beam strain resulted in a minimum measurable damping ratio of 6×10^{-6} in a strain range of 10 to 20 microstrain. Estimates of material constants are $C_1 = 54 \times 10^{-3}$ and $C_2 = 144 \times 10^{-6}$.

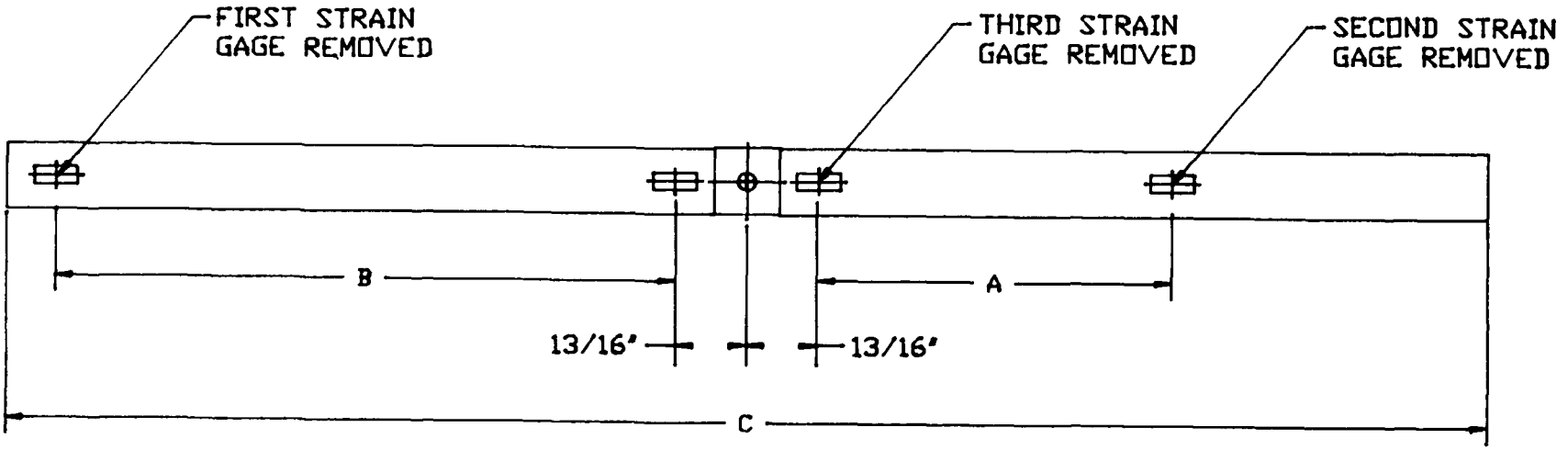

TOP VIEW

	MARK	
	1	2
A	4"	3"
B	7"	5"
C	17.00 ± .01	13.00 ± .01

Figure E-1. Cantilever beam strain gate locations.

Appendix F

DERIVATION OF SYMMETRIC CANTILEVER BEAM MODEL

INTRODUCTION

The purpose of this appendix is to develop the equations and terms required to analyze the internal damping test results. An equation of motion with its mass and stiffness terms is presented. The damping ratio emerges in a form directly applicable to the internal damping test approach and data reduction. Specific damping capacity is defined and the experimental results in terms of amplitude- and frequency-dependent damping are expressed together with external sources of damping.

EQUATION OF MOTION

The differential equation of motion for the symmetric cantilever beam model is (Ref 72):

$$[EIw''(x,t)]'' + c(x)\dot{w}(x,t) + m(x)[\ddot{w}_b(t) + \ddot{w}(x,t)] = 0 \qquad \text{(F-1)}$$

where w is the beam displacement in the z direction and I is the beam moment of inertia. Equation F-1 is rearranged to distinguish the forcing function:

$$[EIw''(x,t)]'' + c(x)\dot{w}(x,t) + m(x)\ddot{w}(x,t) = -m(x)\ddot{w}_b(t) \qquad \text{(F-2)}$$

Thus, the forcing function is expressed as an inertial force per unit length $-m(x)\ddot{w}_b(t)$. Assuming a solution in the form:

$$w(x,t) = \sum_i B_i \, q_i(t) \, \phi_i(x) \qquad \text{(F-3)}$$

where B_i is an amplitude-scaling factor, q_i is a generalized coordinate, and ϕ_i is a characteristic shape function. The equation for the generalized coordinate q_i becomes (Ref 76):

$$\ddot{q}_i + 2\zeta_i \omega_i \dot{q}_i + \omega_i^2 q_i = -\ddot{w}_b(t) \, \frac{m(x)}{M_i} \int_0^1 \phi_i(x) \, dx \qquad \text{(F-4)}$$

where $\zeta_i = C_i/C_{ci}$, $C_{ci} = 2(M_i K_i)^{1/2}$, $\omega_i = (K_i/M_i)^{1/2}$

and

$$C_i = \int_0^1 \phi_i^2(x) c(x) \, dx \qquad \text{(F-5)}$$

$$K_i = \int_0^1 EI[\phi_i''(x)]^2 \, dx \qquad \text{(F-6)}$$

$$M_i = \int_0^1 \phi_i^2(x) m(x) \, dx$$

From beam theory (Ref 77), the moment in a beam vibrating in the i^{th} mode, M(x), is calculated by:

$$M(x) = EI \, B_i \, \phi_i''(x) \qquad \text{(F-7)}$$

where the second derivative of the characteristic shape function with respect to x, $\phi_i''(x)$, describes the curvature in the vibrating beam. Combining Equation F-7 with the bending moment-bending strain relationship (Ref 77) produces an expression for the amplitude-scaling factor in terms of a measured strain:

$$B_i = \frac{2\,\varepsilon(x_o)}{h\kappa_i^{\,2}\,\phi_i''(x_o)} \qquad \text{(F-8)}$$

where $\varepsilon(x_o)$ is a measured strain at location x_o and κ_i is the eigenvalue of the i^{th} mode.

DAMPING RATIO

The acceleration expression, on the right-hand side of Equation F-4, may be replaced by a solitary parameter, $\ddot{z}_i(t)$, where:

$$\ddot{z}_i(t) = -\ddot{w}_b(t)\,\frac{m(x)}{M_i}\int_0^1 \phi_i(x)\,dx \qquad \text{(F-9)}$$

Assuming sinusoidal motion with $w_b(t) = W_b \sin \omega t$ for the vibrating beam, it follows $z_i(t) = Z_i \sin \omega t$ and $\ddot{z}_i = -z_i\,\omega^2$ from which Equation F-4 may be rewritten:

$$\ddot{q}_i + 2\zeta_i\omega_i\dot{q}_i + \omega_i^{\,2}q_i = Z_i\,\omega^2 \sin \omega t \qquad \text{(F-10)}$$

The steady-state solution $q_i = B_i \sin(\omega t - \theta)$ is then available from inspection to be:

$$B_i = \frac{Z_i(\omega/\omega_i)^2}{\{[1 - (\omega/\omega_i)^2]^2 + [2\zeta_i(\omega/\omega_i)]^2\}^{1/2}} \qquad \text{(F-11)}$$

where ω_i is the resonant frequency of the beam and Z_i is defined by:

$$Z_i = W_b(t)\,\frac{m(x)}{M_i}\int_0^1 \phi_i(x)\,dx$$

When the beam is driven at its resonance frequency, that is, $\omega = \omega_i$, Equation F-11 reduces to:

$$B_i = \frac{Z_i}{2\zeta_i} \tag{F-12}$$

Rearranging Equation F-12 to solve for the damping ratio, ζ_i, results in:

$$\zeta_i = \frac{Z_i}{2B_i} \tag{F-13}$$

Determination of the damping ratio, ζ_i, for Equation F-2 is accomplished by vibrating the beam at its resonant frequency, ω_i, while measuring the base acceleration, $\ddot{w}_b$, and the strain at some known location on the beam, $\varepsilon(x_o)$. Equation F-8 uses $\varepsilon(x_o)$ to solve for B_i and Equation F-9 requires $\ddot{w}_b$ and ω_i to solve for Z_i. Using Equation F-13 with B_i and Z_i will determine the damping ratio.

SPECIFIC DAMPING CAPACITY

For a material, the ratio of energy dissipated per cycle, W_d, to the peak potential energy per cycle, U, is defined as the specific damping capacity, Δ,

$$\Delta = \frac{W_d}{U} \tag{F-14}$$

As developed by Shimanuki and Doi (Ref 43), the average specific damping capacity of a material, subject to internal friction, is expressed using a volume element:

$$\bar{\Delta} = \frac{\int \Delta w \, dV}{2\int w \, dV} \tag{F-15}$$

where Δw and w are the energy dissipated and the peak potential energy per cycle in a volume element, respectively. Shimanuki and Doi assume that Δw is a function of dislocation damping in the form of Δ_H, the strain amplitude-dependent decrement and Δ_I, the frequency-dependent decrement. Substituting for Δw and w in Equation F-15:

$$\bar{\Delta} = \bar{\Delta}_H + \Delta_I \tag{F-16}$$

where

$$\bar{\Delta}_H = \frac{\int \varepsilon^2 \Delta_H(\varepsilon)\, dV}{\int \varepsilon^2\, dV} \tag{F-17}$$

and $w = \varepsilon^2$.

In analyzing the specific damping capacity for the dynamic model described in Equation F-2 an assumption must be made about c(x). As presented in Equation F-16, the average specific damping capacity consists of two terms: $\bar{\Delta}_H$ which is strain-amplitude dependent, and Δ_I which is frequency dependent. Thus, neither term is proportional to velocity and c(x) must be treated as an equivalent expression of viscous damping, c_{eq} (Ref 72). From Equation F-2,

$$W_d = \oint c_{eq}\, \dot{w}\, dw \tag{F-18}$$

Expanding w from Equation F-3, Equation F-18 becomes:

$$W_{di} = c_{eq} \int_0^1 \phi_i^2(x)\, dx \oint \dot{q}_i^2(t)\, dt$$

From Equation F-5:

$$C_{eqi} = c_{eq} \int_0^1 \phi_i^2(x)\, dx$$

with the resul that:

$$W_{di} = C_{eqi} \oint \dot{q}_i^2(t)\, dt$$

Assuming steady-state harmonic displacement and velocity,

$$W_{di} = B_i^2 \pi \omega C_{eqi} \qquad \text{(F-19)}$$

From Thompson (Ref 72), $\omega C_{eqi} = 2\zeta_i K_i$, which when substituted into Equation F-19 produces the final expression for W_{di}:

$$W_{di} = 2B_i^2 \pi \zeta_i K_i$$

The peak potential energy per cycle in the i^{th} mode is given by:

$$U_i = 1/2 B_i^2 K_i$$

Substituting for W_d and U in Equation F-14, the average specific damping capacity for the beam is:

$$\bar{\Delta} = 4\pi\zeta_i \qquad \text{(F-20)}$$

Equating Equations F-16 and F-20:

$$\bar{\Delta}_H + \Delta_I = 4\pi\zeta_i \qquad \text{(F-21)}$$

Equation F-21 assumes no external damping influences the damping ratio. This assumption is not an accurate reflection of a "real-world" system where attachment points and connections are subject to slippage and friction. Therefore some external damping must be included in the

system. This external damping is represented by Δ_{ext}. Before the specific damping capacity can be determined, Δ_{ext} must be estimated. Modifying Equation F-21 to reflect the inclusion of external damping:

$$\bar{\Delta}_H + \Delta_I = 4\pi\zeta_i - \Delta_{ext} \qquad \text{(F-22)}$$

Characteristic shape functions for a cantilever beam are well-defined, with authors using various formats for identical expressions (Ref 72, 78). This paper will borrow the format of Harris and Crede (Ref 78) to symbolize the shape function for a cantilever beam:

$$\phi_i(x) = (\cos \kappa_i x - \cosh \kappa_i x) + R_i(\sin \kappa_i x - \sinh \kappa_i x) \qquad \text{(F-23)}$$

where R_i is a ratio of nonzero constants. Table F-1 displays values of $\kappa_i l$ and R_i for the first three modes of vibration. Differentiating Equation F-23 twice with respect to x produces the beam curvature:

$$\phi_i''(x) = -\kappa_i^2[(\cos \kappa_i x + \cosh \kappa_i x) + R_i(\sin \kappa_i x + \sinh \kappa_i x)] \qquad \text{(F-24)}$$

Equation F-24 is used in conjunction with Equation F-8 to compute the amplitude scaling factor, B_i, from experimental data, $\varepsilon(x_o)$.

Table F-1. $\kappa_i l$ and R_i for First Three Modes of a Cantilever Beam

Mode, i	Eigenvalue, $\kappa_i l$	Ratio, R_i
1	1.8751	-0.7341
2	4.6941	-1.0185
3	7.8548	-0.9992

Appendix G

DERIVATION OF FOUR-POINT BEAM FATIGUE MODEL

INTRODUCTION

This appendix parallels the procedure of Appendix F in the derivation of a model with which to analyze the results of the four-point beam fatigue tests. An expression for the knife edges supporting the fatigue specimen is derived and the boundary conditions are determined. The equation of motion and mass and stiffness terms are presented, and the damping term is derived. Finally, an empirical expression for the damping observed in 4340 steel beam fatigue specimens is provided.

KNIFE-EDGE SUPPORT MODEL

Support for the four-point beam is a clamped knife-edge pair (see Figure 10 in the main text). The knife-edge pair, while allowing some rotation, does impose a moment, M_{ke}. Visual observation of the knife edges during fatigue loading indicates the beam rotates about the more rigidly mounted knife edge of the pair. This situation introduces some axial loading to the beam that must be accounted for when analyzing the beam under fatigue load. However, as the strains, and therefore the rotations, are small for the load applied during damping data acquisition, it is assumed the point of rotation lies along the center of the beam and the axial loading is negligible. The error associated with this assumption is on the order of 10^{-7} given a maximum strain of 100 micro-strain in a simple-supported beam.

BOUNDARY CONDITIONS

The moment imposed by the knife-edge support is computed from:

$$M_{ke} = k_{ke}\, w'(0) \qquad \text{(G-1)}$$

where $w'(0)$ is the beam rotation at the knife-edge support. As:

$$M_{ke} = EIw''(0)$$

where $w''(0)$ is the beam curvature at the knife-edge support, Equation G-1 provides a boundary condition in the form:

$$EIw''(0) = k_{ke}\, w'(0)$$

The moment imposed by a crack at the beam midpoint is computed from (Ref 79):

$$M_c = k_c(a)\, w'(1/2) \qquad \text{(G-2)}$$

where M_c is the imposed moment and $w'(1/2)$ is the beam rotation at its midpoint. The moment is expressed as a function of the curvature at the beam midpoint, $w''(1/2)$,

$$M_c = EIw''(1/2) \qquad \text{(G-3)}$$

Equation G-2 and G-3 provide a second boundary condition:

$$EIw''(1/2) = k_c(a)\, w'(1/2)$$

The two remaining boundary conditions are based on a beam with a simple support at one endpoint and guided at the other. These boundary conditions are given by:

$$w(0) = 0$$

and

$$w'''(1/2) = 0$$

where $w(0)$ is the displacement at the knife-edge support and $w'''(1/2)$ is the third derivative of the beam displacement with respect to x at the beam midpoint.

EQUATION OF MOTION

The equation of motion for the four-point beam is given by:

$$[EIw''(x,t)]'' + c(x)\dot{w}(x,t) + m(x)\ddot{w}(x,t) + m_{ex}\ddot{w}(l_{ex},t) = F_{ex}(l_{ex},t) \quad \text{(G-4)}$$

Employment of Equation F-3 in transforming Equation G-4 produces an equation of motion in generalized coordinates:

$$\ddot{q}_i + 2\zeta_i\omega_i\dot{q}_i + \omega_i^2 q_i = \frac{1}{M_i}\int_0^1 \phi_i(x)\, F_{ex}(l_{ex},t)\, dx \quad \text{(G-5)}$$

Equations F-5 and F-6 apply to Equation G-5; however, the generalized mass expression has been altered due to the mass of the exciter. The generalized mass is expressed as:

$$M_i = \int_0^1 \phi_i^2(x)m(x)\, dx + \phi_i^2(l_{ex})m_{ex}$$

The unit impulse or delta function, $\delta(x-\xi)$ (Ref 72), models a point load at the location $\xi = l_{ex}$. Assuming $F_{ex}(l_{ex},t)$ is harmonic, the forcing function is separated into two components, one x and the other t dependent.

With this assumption, the forcing function becomes $f_{ex}\delta(x-l_{ex})\sin \omega t$, where f_{ex} is the amplitude scaling factor. Using this expression, integration in Equation G-5 becomes trivial, with the result:

$$\ddot{q}_i + 2\zeta_i\omega_i\dot{q}_i + \omega_i^2 q_i = \frac{f_{ex}}{M_i}\phi_i(l_{ex}) \sin \omega t \qquad \text{(G-6)}$$

SPECIFIC DAMPING CAPACITY

Treating the right-hand side of Equation G-6 as the parameter $\ddot{z}_i(t)$, that is,

$$\ddot{z}_i(t) = \frac{f_{ex}}{M_i}\phi_i(l_{ex}) \sin \omega t \qquad \text{(G-7)}$$

the relationship between displacement and specific damping capacity is established as demonstrated in Appendix F. From Equation G-7, it follows $z_i(t) = Z_i \sin \omega t$ where $\ddot{z}_i = -z_i\,\omega^2$ and:

$$Z_i = \frac{f_{ex}}{M}\phi_i(l_{ex}) \qquad \text{(G-8)}$$

Substitution of Z_i into Equation G-6 produces Equation F-10 of Appendix F. Thus, the four-point beam specimen will have its specific damping capacity determined in a manner similar to that applied to the symmetric cantilever beam damping specimen.

Results from the 4340 steel beam fatigue tests do not conform to the dislocation damping based model. This appendix develops a second damping mechanism, based on crack surface rotation, that adequately models and explains the observed damping phenomena. This new mechanism produces an empirical expression that is used in the four-point beam fatigue model.

EMPIRICAL DAMPING EXPRESSION

With the results of the 4340 steel beam fatigue test suggesting a strong relationship between the crack length and damping, the decision was made to review previous work to reconcile the proposed constitutive relationship with experimental data. Previous work with 1018 steel beams (Ref 73) included similar fatigue tests. These tests were performed under constant load. The softer 1018 steel forms a large plastic zone with the increasing stress intensity function associated with a constant load. This large plastic zone does not allow the crack surfaces to touch as the beam vibrates to collect damping data.

Figures 16 through 18 in the main text show a crack growth rate per cycle that is proportional to the stress intensity factor raised to the fourth power. In equation form, this relation is expressed by:

$$\frac{da}{dN} = \alpha_c K_I^4 \qquad \text{(G-9)}$$

where α_c is a material dependent constant, N is the fatigue cycle number, and K_I is the stress intensity factor. Equation G-9 is consistent with the dislocation theory of crack growth as described by Frost, Marsh, and Pook (Ref 60). Rearranging Equation G-9 and integrating over one cycle produces:

$$\int_{a_{j-1}}^{a_j} \frac{da}{K_I^4(a)} = \alpha_c \qquad \text{(G-10)}$$

where the crack growth in one cycle is calculated from:

$$\Delta a_j = a_j - a_{j-1}$$

In Equation G-10, K_I is assumed to be a function of the crack length. The expression for K_I is taken from Equation 31 in the main text.

Numerical integration is required to solve the integrand when this complex term is substituted for K_I. From the Experimental Approach section in the main text of this report, σ is defined by:

$$\sigma = \frac{6M}{h^2}$$

where M is given by:

$$M = \frac{1}{2} \; l_a P - M_{ke} \qquad \text{(G-11)}$$

In Equation G-11, l_a is the distance from the knife-edge support to the applied load, P, and M_{ke} is the moment created by the knife-edge.

The natural frequency of the fatigue specimen, as the crack propagates, is computed from the ratio of Equations F-6 and F-16 with adjustments to k_c to simulate the crack growth. The relationship between k_c and the crack length, a, using least squares analysis is:

$$k_c = b_c \; (h/a)^3 \qquad \text{(G-12)}$$

where b_c is a material-dependent constant (see Figure G-1). For the 4340 steel beam specimens, $b_c = 2.45$. This relationship, for the three beam specimens analyzed, resembles the moment of inertia expression in its usage of beam height (Ref 77).

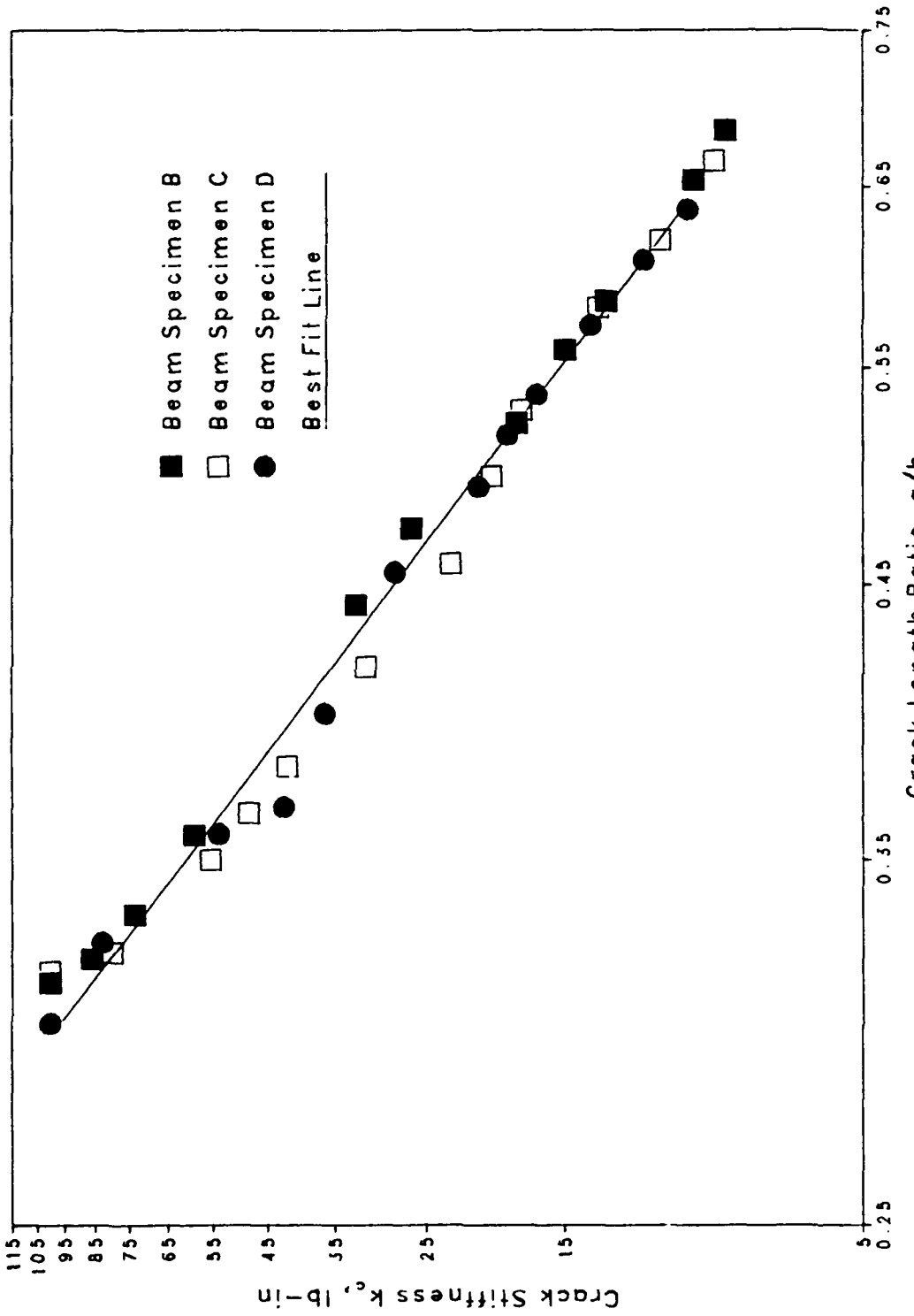

Figure G-1. Crack stiffness versus crack length ratio.

DISTRIBUTION LIST

ADVANCED TECHNOLOGY, INC / Ops Cen Mgr (Bednar), Camarillo, CA
AF / 438 ABG/DEE (Wilson), McGuire AFB, NJ
AF / AFIT/DET (Hudson), Wright-Patterson AFB, OH
AF HQ / ESD/AVMS, Hanscom AFB, MA
AF HQ / ESD/DEE, Hanscom AFB, MA
AFB / HQ MAC/DEEE, Scott AFB, IL
AFESC / TIC Lib, Tyndall AFB, FL
AFIT / DET, Wright-Patterson AFB, OH
AMERICAN CONCRETE / Lib, Detroit, MI
ARMY / HQDA (DAEN-ZCM), Washington, DC
ARMY / R&D Lab, STRNC-UE, Natick, MA
ARMY CECOM R&D TECH LIBRARY / ASNC-ELC-I-T, Ft Monmouth, NJ
ARMY CERL / CECER-EME (Hayes), Champaign, IL
ARMY CERL / Lib, Champaign, IL
ARMY EHA / HSHB-EW, Aberdeen Proving Ground, MD
ARMY ENGRG DIST / CENPS-ED-SD, Seattle, WA
ARMY ENGRG DIST / Lib, Seattle, WA
ARMY ENGRG DIST / LMVCO-A/Bentley, Vicksburg, MS
ARMY ENGRG DIST / Phila, Lib, Philadelphia, PA
ARMY ENGRG DIV / CEHND-ED-CS, Huntsville, AL
ARMY ENGRG DIV / ED-SY (Loyd), Huntsville, AL
ARMY ENGRG DIV / HNDED-SY, Huntsville, AL
ARMY EWES / GP-EC (Webster), Vicksburg, MS
ARMY EWES / Lib, Vicksburg, MS
ARMY EWES / WESCD-P (Melby), Vicksburg, MS
ARMY EWES / WESCV-Z (Whalin), Vicksburg, MS
ARMY EWES / WESGP, Vicksburg, MS
ARMY MISSILE R&D CMD / Ch, Docs, Sci Info Ctr, Redstone Arsenal, AL
ARMY MMRC / DRXMR-SM (Lenoe), Watertown, MA
ATLANTIC RICHFIELD CO / RE Smith, Dallas, TX
BATTELLE / D. Frink, Columbus, OH
BECHTEL CIVIL, INC / K. Mark, San Francisco, CA
BETHLEHEM STEEL CO / Engrg Dept, Bethlehem, PA
BRITISH EMBASSY / Sci & Tech Dept (Wilkins), Washington, DC
BROWN & ROOT / Ward, Houston, TX
CAL STATE UNIV / C.V. Chelapati, Long Beach, CA
CANADA / Viateur De Champlain. Matane, Quebec
CASE WESTERN RESERVE UNIV / CE Dept (Perdikaris), Cleveland, OH
CATHOLIC UNIV / CE Dept (Kim) Washington, DC
CHEVRON OIL FLD RSCH CO / Strickland, La Habra, CA
CHILDS ENGRG CORP / K.M. Childs, Jr., Medfield, MA
CITY OF LIVERMORE / Dackins, PE, Livermore, CA
CLARENCE R JONES / Augusta, GA
CLARKSON COLL OF TECH / CE Dept, Potsdam, NY
CNA / Tech Lib, Alexandria, VA
COGUARD R&D CEN / Lib, Groton, CT
COLLINS ENGRG, INC / M Garlich, Chicago, IL
COLORADO STATE UNIV / CE Dept (Criswell), Ft. Collins, CO
COMDT COGUARD / Lib, Washington, DC
CONRAD ASSOC / Luisoni, Van Nuys, CA

CONSOER TOWNSEND & ASSOC / Schramm, Chicago, IL
CONSTRUCTION TECH LABS, INC / G. Corley, Skokie, IL
CORNELL UNIV / Civil & Environ Engrg, Ithaca, NY
CORNELL UNIV / Lib, Ithaca, NY
DAMES & MOORE / Lib, Los Angeles, CA
DAVY DRAVO / Wright, Pittsburg, PA
DILLINGHAM CONSTR CORP / (HD&C), F McHale, Honolulu, HI
DIRSSP / Tech Lib, Washington, DC
DOE / Wind/Ocean Tech Div, Port Tobacco, MD
DTIC / Alexandria, VA
DTRCEN / Code 172, Bethesda, MD
DTRCEN / Code 4111, Bethesda, MD
EARL & WRIGHT CONSULTING ENGRGS / Jensen, San Francisco, CA
EDWARD K NODA & ASSOC / Honolulu, HI
ESCO SCIENTIFIC PRODUCTS (ASIA) / PTE LTD, , Singapore
EVALUATION ASSOC, INC / MA Fedele, King of Prussia, PA
FAA / Code APM-740 (Tomita), Washington, DC
FLORIDA ATLANTIC UNIV / Ocean Engrg Dept (Su), Boca Raton, FL
FLORIDA INST OF TECH / CE Dept (Kalajian), Melbourne, FL
GEORGIA INST OF TECH / CE Schl (Kahn), Atlanta, GA
GEORGIA INST OF TECH / CE Schl (Swanger), Atlanta, GA
GEORGIA INST OF TECH / CE Schl (Zuruck), Atlanta, GA
GIDEP / OIC, Corona, CA
GRUMMAN AEROSPACE CORP / Tech Info Ctr, Bethpage, NY
HALEY & ALDRICH, INC. / T.C. Dunn, Cambridge, MA
HARTFORD STEAM BOILER INSP & INS CO / Spinelli, Hartford, CT
HAYNES & ASSOC / H. Haynes, PE, Oakland, CA
HIRSCH & CO / L Hirsch, San Diego, CA
HJ DEGENKOLB ASSOC / W. Murdough, San Francisco, CA
HUGHES AIRCRAFT CO / Tech Doc Cen, El Segundo, CA
INST OF MARINE SCIENCES / Lib, Port Aransas, TX
INTL MARITIME, INC / D. Walsh, San Pedro, CA
IRE-ITTD / Input Proc Dir (R. Danford), Eagan, MN
JAMES ISHIHARA / OES/PHS/DHHS, Seattle, WA
JOHN HOPKINS UNIV / CE Dept, Jones, Baltimore, MD
JOHN J MC MULLEN ASSOC / Arlington, VA
LAWRENCE LIVERMORE NATL LAB / FJ Tokarz, Livermore, CA
LAWRENCE LIVERMORE NATL LAB / Plant Engrg Lib (L-654), Livermore, CA
LEHIGH UNIV / Linderman Library, Bethlehem, PA
LEO A DALY CO / Honolulu, HI
LIBRARY OF CONGRESS / Sci & Tech Div, Wasnington, DC
LIN OFFSHORE ENGRG / P. Chow, San Francisco, CA
LINDA HALL LIBRARY / Doc Dept, Kansas City, MO
LONG BEACH PORT / Engrg Dir (Allen), Long Beach, CA
MARATHON OIL CO / Gamble, Houston, TX
MARITECH ENGRG / Donoghue, Austin, TX
MC CLELLAND ENGRS, INC / Lib, Houston, TX
MICHIGAN TECH UNIV / CO Dept (Haas), Houghton, MI
MIT / Engrg Lib, Cambridge, MA
MIT / Lib, Tech Reports, Cambridge, MA
MOBIL R&D Corp / Offshore Engrg Lib, Dallas, TX
MT DAVISSON / CE, Savoy, IL
NATL ACADEMY OF SCIENCES / NRC, Naval Studies Bd, Washington, DC

NAVAIRENGCEN / Code 1822, Lakehurst, NJ
NAVAL WAR COLLEGE / Code 24, Newport, RI
NAVCOASTSYSCEN / Tech Lib, Panama City, FL
NAVEODTECHCEN / Tech Lib, Indian Head, MD
NAVFACENGCOM / Code 03, Alexandria, VA
NAVFACENGCOM / Code 03T (Essoglou), Alexandria, VA
NAVFACENGCOM / Code 09M124 (Lib), Alexandria, VA
NAVSCOLCECOFF / Code C35, Port Hueneme, CA
NEW ZEALAND CONCRETE RSCH ASSN / Lib, Porirua,
NRL / Code 2511, Wasnington, DC
NRL / Code 4670, Washington, DC
NUHN & ASSOC / A.C. Nuhn, Wayzata, NM
OREGON STATE UNIV / CE Dept (Hicks), Corvallis, OR
PACIFIC MARINE TECH / M. Wagner, Duvall, WA
PENNSYLVANIA STATE UNIV / Gotolski, University Park, PA
PENNSYLVANIA STATE UNIV / Rsch Lab, State College, PA
PILE BUCK, INC / Smoot, Jupiter, FL
PMB ENGRG / Lundberg, San Francisco, CA
PORTLAND CEMENT ASSOC / AE Fiorato, Skokie, IL
PORTLAND STATE UNIV / Engrg Dept (Migliori), Portland, OR
PRESNELL ASSOC, INC / DG Presnell, Jr, Louisville, KY
PURDUE UNIV / CE Scol (Leonards), West Lafayette, IN
PURDUE UNIV / Engrg Lib, West Lafayette, IN
SAN DIEGO STATE UNIV / CE Dept (Krishnamoorthy), San Diego, CA
SANDIA LABS / Lib, Livermore, CA
SARGENT & HERKES, INC / JP Pierce, Jr, New Orleans, LA
SAUDI ARABIA / King Saud Univ, ,
SEATECH CORP / Peroni, Miami, FL
SEATTLE PORT / W Ritchie, Seattle, WA
SEATTLE UNIV / CE Dept (Schwaegler), Seattle, WA
SHELL OIL CO / E. Doyle, Houston, TX
SIMPSON, GUMPERTZ & HEGER, INC / Hill, Arlington, MA
SOUTHWEST RSCH INST / Energetic Sys Dept (Esparza), San Antonio, TX
SOUTHWEST RSCH INST / King, San Antonio, TX
SOUTHWEST RSCH INST / M. Polcyn, San Antonio, TX
SOUTHWEST RSCH INST / Marchand, San Antonio, TX
STATE UNIV OF NEW YORK / CE Dept, Buffalo, NY
STATE UNIV OF NEW YORK / CE Dept, Buffalo, NY
TEXAS A&M UNIV / CE Dept (Machemehl), College Station, TX
TEXAS A&M UNIV / CE Dept (Niedzwecki), College Station, TX
TEXAS A&M UNIV / Ocean Engr Proj, College Station, TX
TRW INC / Crawford, Redondo Beach, CA
TRW INC / Dai, San Bernardino, CA
TRW INC / Engr Lib, Cleveland, OH
TRW INC / Rodgers, Redondo Beach, CA
TUDOR ENGRG CO / Ellegood, Phoenix, AZ
UNIV OF CALIFORNIA / CE Dept (Fenves), Berkeley, CA
UNIV OF CALIFORNIA / CE Dept (Fourney), Los Angeles, CA
UNIV OF CALIFORNIA / CE Dept (Gerwick), Berkeley, CA
UNIV OF CALIFORNIA / CE Dept (Taylor), Davis, CA
UNIV OF CALIFORNIA / CE Dept (Williamson), Berkeley, CA
UNIV OF CALIFORNIA / Naval Archt Dept, Berkeley, CA
UNIV OF HARTFORD / CE Dept (Keshawarz), West Hartford, CT

UNIV OF HAWAII / CE Dept (Chiu), Honolulu, HI
UNIV OF HAWAII / Manoa, Lib, Honolulu, HI
UNIV OF HAWAII / Ocean Engrg Dept (Ertekin), Honolulu, HI
UNIV OF ILLINOIS / Lib, Urbana, IL
UNIV OF ILLINOIS / Metz Ref Rm, Urbana, IL
UNIV OF MICHIGAN / CE Dept (Richart), Ann Arbor, MI
UNIV OF NEBRASKA / Director, Lincoln, NE
UNIV OF NEW MEXICO / HL Schreyer, Albuquerque, NM
UNIV OF NEW MEXICO / NMERI (Bean), Albuquerque, NM
UNIV OF NEW MEXICO / NMERI (Falk), Albuquerque, NM
UNIV OF NEW MEXICO / NMERI (Leigh), Albuquerque, NM
UNIV OF PENNSYLVANIA / Dept of Arch, Philadephia, PA
UNIV OF RHODE ISLAND / CE Dept (Kovacs), Kingston, RI
UNIV OF RHODE ISLAND / CE Dept, Kingston, RI
UNIV OF TEXAS / CE Dept (Thompson), Austin, TX
UNIV OF TEXAS / Construction Industry Inst, Austin, TX
UNIV OF TEXAS / ECJ 4.8 (Breen), Austin, TX
UNIV OF WASHINGTON / CE Dept (Mattock), Seattle, WA
UNIV OF WISCONSIN / Great Lakes Studies Cen, Milwaukee, WI
USDA / Ext Serv, T. Maher, Washington, DC
USDA / For Svc Reg 8, (Bowers), Atlanta, GA
USDA / For Svc, Reg Bridge Engr, Aloha, OR
USDA / Forest Svc, Washington, DC
USNA / Ch, Mech Engrg Dept (C Wu), Annapolis, MD
USNA / Ocean Engrg Dept, Annapolis, MD
VSE / Ocean Engrg Gp (Murton), Alexandria, VA
VULCAN IRON WORKS / Warrington, Cleveland, TN
WESTINGHOUSE ELECTRIC CORP / Lib, Pittsburg, PA
WISS, JANNEY, ELSTNER, & ASSOC / DW Pfeifer, Northbrook, IL
WISWELL, INC. / Wiswell, Southport, CT
WOODWARD-CLYDE CONSULTANTS / R. Cross, Oakland, CA

INSTRUCTIONS

The Naval Civil Engineering Laboratory has revised its primary distribution lists. The bottom of the label on the reverse side has several numbers listed. These numbers correspond to numbers assigned to the list of Subject Categories. Numbers on the label corresponding to those on the list indicate the subject category and type of documents you are presently receiving. If you are satisfied, throw this card away (or file it for later reference).

If you want to change what you are presently receiving:

- Delete - mark off number on bottom of label.
- Add - circle number on list.
- Remove my name from all your lists - check box on list.
- Change my address - line out incorrect line and write in correction **(DO NOT REMOVE LABEL).**
- Number of copies should be entered after the title of the subject categories you select.

Fold on line below and drop in the mail.

Note: Numbers on label but not listed on questionnaire are for NCEL use only, please ignore them.

Fold on line and staple.

DEPARTMENT OF THE NAVY

Naval Civil Engineering Laboratory
Port Hueneme, CA 93043-5003

Official Business
Penalty for Private Use, $300

NO POSTAGE
NECESSARY
IF MAILED
IN THE
UNITED STATES

BUSINESS REPLY CARD

FIRST CLASS PERMIT NO. 69

POSTAGE WILL BE PAID BY ADDRESSE

Commanding Officer
Code L34
Naval Civil Engineering Laboratory
Port Hueneme, California 93043-5003

DISTRIBUTION QUESTIONNAIRE

The Naval Civil Engineering Laboratory is revising its Primary distribution lists.

SUBJECT CATEGORIES

1 SHORE FACILITIES
2 Construction methods and materials (including corrosion control, coatings)
3 Waterfront structures (maintenance/deterioration control)
4 Utilities (including power conditioning)
5 Explosives safety
6 Aviation Engineering Test Facilities
7 Fire prevention and control
8 Antenna technology
9 Structural analysis and design (including numerical and computer techniques)
10 Protective construction (inciuding hardened shelters, shock and vibration studies)
11 Soil/rock mechanics
14 Airfields and pavements

15 ADVANCED BASE AND AMPHIBIOUS FACILITIES
16 Base facilities (including shelters, power generation, water supplies)
17 Expedient roads/airfields/bridges
18 Amphibious operations (including breakwaters, wave forces)
19 Over-the-Beach operations (including containerization, materiel transfer, lighterage and cranes)
20 POL storage, transfer and distribution

28 ENERGY/POWER GENERATION
29 Thermal conservation (thermal engineering of buildings, HVAC systems, energy loss measurement, power generation)
30 Controls and electrical conservation (electrical systems, energy monitoring and control systems)
31 Fuel flexibility (liquid fuels, coal utilization, energy from solid waste)
32 Alternate energy source (geothermal power, photovoltaic power systems, solar systems, wind systems, energy storage systems)
33 Site data and systems integration (energy resource data, energy consumption data, integrating energy systems)
34 ENVIRONMENTAL PROTECTION
35 Solid waste management
36 Hazardous/toxic materials management
37 Waste water management and sanitary engineering
38 Oil pollution removal and recovery
39 Air pollution

44 OCEAN ENGINEERING
45 Seafloor soils and foundations
46 Seafloor construction systems and operations (including diver and manipulator tools)
47 Undersea structures and materials
48 Anchors and moorings
49 Undersea power systems, electromechanical cables, and connectors
50 Pressure vessel facilities
51 Physical environment (including site surveying)
52 Ocean-based concrete structures
54 Undersea cable dynamics

TYPES OF DOCUMENTS

85 Techdata Sheets 86 Technical Reports and Technical Notes
83 Table of Contents & Index to TDS
82 NCEL Guides& Abstracts
91 Physical Security

☐ None-remove my name

NCEL DOCUMENT EVALUATION

You are number one with us; how do we rate with you?

We at NCEL want to provide you our customer the best possible reports but we need your help. Therefore, I ask you to please take the time from your busy schedule to fill out this questionnaire. Your response will assist us in providing the best reports possible for our users. I wish to thank you in advance for your assistance. I assure you that the information you provide will help us to be more responsive to your future needs.

R. N. STORER, Ph.D, P.E.
Technical Director

DOCUMENT NO. _____ TITLE OF DOCUMENT: _____

_____

Date: _____ Respondent Organization : _____

Name: _____ Activity Code: _____
Phone: _____ Grade/Rank: _____

Category (*please check*):

Sponsor _____ User _____ Proponent _____ Other (*Specify*) _____

Please answer on your behalf only; not on your organization's. Please check (*use an X*) only the block that most closely describes your attitude or feeling toward that statement:

SA Strongly Agree A Agree O Neutral D Disagree SD Strongly Disagree

---

	SA	A	N	D	SD
1. The technical quality of the report is comparable to most of my other sources of technical information.	( )	( )	( )	( )	( )
2. The report will make significant improvements in the cost and or performance of my operation.	( )	( )	( )	( )	( )
3. The report acknowledges related work accomplished by others.	( )	( )	( )	( )	( )
4. The report is well formatted.	( )	( )	( )	( )	( )
5. The report is clearly written.	( )	( )	( )	( )	( )
6. The conclusions and recommendations are clear and directly supported by the contents of the report.	( )	( )	( )	( )	( )
7. The graphics, tables, and photographs are well done.	( )	( )	( )	( )	( )

Do you wish to continue getting NCEL reports? ☐ YES ☐ NO

Please add any comments (e.g., in what ways can we improve the quality of our reports?) on the back of this form.

Comments:

Please fold on line and staple

DEPARTMENT OF THE NAVY

Naval Civil Engineering Laboratory
Port Hueneme, CA 93043-5003

Official Business
Penalty for Private Use $300

Code L03B
NAVAL CIVIL ENGINEERING LABORATORY
PORT HUENEME, CA 93043-5003